

List of Abstracts

1.1 Saturation-Dependence of Non-Fickian Transport in Porous Media	13
VAHID NIASAR	
1.2 Interactions between tidal flows and convection	14
CRAIG DUGUID [†] , ADRIAN BARKER & CHRIS JONES	
1.3 Modelling dynamic stall of a pitching airfoil in large-scale freestream turbulence	15
THANKGOD BOYE [†] & ZHENG-TONG XIE	
1.4 Regime transitions and energetics of sustained stratified shear flows	17
ADRIEN LEFAUVE, JAMIE PARTRIDGE & PAUL LINDEN	
1.5 The construction and evolution of an inviscid background state for Earth's magnetic field	19
COLIN M. HARDY [†] , PHILIP W. LIVERMORE, AND JITSE NIESEN	
1.6 Shape of a recoiling liquid filament [Was: Capillary retraction of an axisymmetric liquid ligament]	20
F. P. CONTÒ ^{†1} , J. F. MARÍN ² , L. GORDILLO ² , J. R. CASTREJON-PITA ¹ & A. A. CASTREJON-PITA ³	
1.7 An investigation into the trigger of wake bimodality behind square-back bluff bodies using LES	22
FARON HESSE [†]	
1.8 Surface Roughness Effects in Finite-Rate Reacting Hypersonic Boundary Layers	23
ATHANASIOS MARGARITIS ^{†1} , TARANEH SAYADI ² , OLAF MARXEN ³ & PETER J. SCHMID ¹	
1.9 Multifunctional Adsorbent Structures for use as Emergency Respirators	25
JONATHAN BARNARD [†] , Y. M. JOHN CHEW & SEMALI PERERA	
1.10 A New Method of Microbubble Production for Dissolved Air Flotation	27
BERT SWART [†] , JANNIS WENK & Y. M. JOHN CHEW	
1.11 Boundary layer control of rotating convection in the Earth's core	29
ROBERT S. LONG [†] , JON E. MOUND, CHRISTOPHER J. DAVIES & STEVE M. TOBIAS	
1.12 A theoretical study of the invariant sets and transient dynamics of a finite air bubble in a perturbed Hele-shaw	30
J. S. KEELER, A. THOMPSON, A. HAZEL & A. JUEL	

1.13 CFD Modelling of Alginate Production: A First Approach to Dynamic Rheology and Its Impact on Stirred and Aerated Bioprocesses	31
CONSTANZA SADINO-RIQUELME ^{†1} , JOSÉ RIVAS ² , DAVID JEISON ³ , ROBERT E. HAYES ¹ & ANDRÉS DONOSO-BRAVO ^{2,4}	
1.14 Numerical investigation of impinging synthetic jet for cooling of electronic devices [Retracted]	33
1.15 Experimental measurements in transitional partially-filled pipe flows using stereoscopic particle image velocimetry	34
THOMAS O. THORNHILL, HENRY C. H. NG & DAVID J. C. DENNIS	
1.16 On Entrainment and Mixing Characteristics of Round Variable-Density Jets [Retracted]	35
1.17 Confinement effects for 3D advection-diffusion boundary layers in U-shape and V-shape channel flows	36
JULIEN R. LANDEL ¹ , MERLIN A. ETZOLD ² & STUART B. DALZIEL ²	
1.18 Extending Generalised Taylor Dispersion theory for the population-level model of a suspension of micro-swimmers	37
LLOYD FUNG [†] & YONGYUN HWANG	
1.19 A customized immersed boundary method for turbulent flows with moving objects: application to vertical axis tidal turbines	38
ATHANASIOS E. GIANNENAS [†] & SYLVAIN LAIZET	
1.20 An adaptive lattice Boltzmann solver with complex sub-grid scale turbulence models	39
CHRISTOS GKOUDESNES [†] & RALF DEITERDING	
1.21 Active vs. passive bundling of prokaryotic flagella	40
ALEXANDER CHAMOLLY [†] & ERIC LAUGA	
1.22 Relative importance of dispersive and Reynolds stresses in turbulent channel flow over irregular Gaussian roughness	41
THOMAS O. JELLY ^{1,2} & ANGELA BUSSE ¹	
1.23 Defending against lava flows	42
EDWARD HINTON ^{†1} , ANDREW HOGG ² & HERBERT HUPPERT ³	
1.24 Capillary adhesion on rough surfaces: When is splitting droplets beneficial?	43
MATTHEW BUTLER [†] & DOMINIC VELLA	
1.25 Modelling bubble propagation in elasto-rigid Hele-Shaw channels	44
JOÃO V. FONTANA [†] , ANNE JUEL & ANDREW L. HAZEL	
1.26 Scale-resolving simulations of three-dimensional gravity currents beyond the Boussinesq limit	45
PAUL BARTHOLOMEW & SYLVAIN LAIZET	

1.27 Analysis of the Boundary Layer Vortex Sheet for Surging and Rotating Bodies of Finite Thickness	46
P. GEHLERT [†] & H. BABINSKY	
1.28 A novel CFD Methodology for Prediction of Direct Laser Metal Deposition	47
ALESSIO BASSO	
1.29 Flow Regimes of Stratified Particle-Laden Plumes [Poster]	48
JONATHAN BARNARD [†]	
1.30 Drag Reduction and Net-Energy Saving in a Turbulent Boundary Layer Using Bayesian Optimisation and Wall Blowing	49
O. A. MAHFOZE ^{†1} , A. MOODY ² , A. WYNN ¹ , R. D. WHALLEY ² & S. LAIZET ¹	
1.31 LES-based investigation of the angle of attack-dependence of flow past a cactus-shaped cylinder with four ribs	50
OLEKSANDR ZHDANOV [†] & ANGELA BUSSE	
1.32 The late-time evolution of an isolated symmetrically unstable front [Poster]	51
AARON WIENKERS [†] & JOHN R. TAYLOR	
1.33 A Lattice Boltzmann Method in Generalized Curvilinear Coordinates	52
J. A. REYES BARRAZA & R. DEITERDING	
1.34 Shear-thinning fluids can be slippery! Non-identifiability of parameters for the Bird-Cross-Carreau-Yasuda family of models when applied to blood rheology	53
DAVID J. SMITH ¹ , MEURIG T. GALLAGHER ¹ , RICHARD A. J. WAIN ^{1,2} , SONIA DARI ¹ & JUSTIN P. WHITTY ²	
1.35 Asymptotic dynamics of high dynamic range stratified turbulence	54
G. D. PORTWOOD ^{1,2} , S. M. DE BRUYN KOPS ² & C. P. CAULFIELD ^{3,4}	
1.36 Numerical simulations of wall cooling performance and associated effects on transition in hypersonic flows with injection from porous surfaces	55
ADRIANO CERMINARA, RALF DEITERDING & NEIL SANDHAM	
1.37 Evaluating turbine wake steering techniques using scale-resolving simulations	57
GEORGIOS DESKOS, SYLVAIN LAIZET & RAFAEL PALACIOS	
1.38 Negating gust effects by actively pitching a wing	58
IGNACIO ANDREU ANGULO [†]	

1.39 Nematic Liquid Crystal Flow During the Manufacture of Liquid Crystal Devices	59
JOSEPH R. L. COUSINS [†] , S. K. WILSON & N. J. MOTTRAM	
1.40 Jetting Behaviour in the Presence of Surfactants in Inkjet Printing	60
EVANGELIA ANTONOPOULOU [†] , OLIVER G. HARLEN, MARK A. WALKLEY & NIKIL KAPUR	
1.41 Experimental modelling of infectious aerosols from people with cystic fibrosis	61
JESSICA PROCTOR [†]	
1.42 Evolution of hydroacoustic waves in deep oceanic waters with generalised sound-speed profiles	62
S. MICHELE & E. RENZI	
1.43 A microfluidic assay to study the migration behaviour of marine bacteria in viscosity gradients	63
SASI KIRAN PASUPULETI, OSCAR GUADAYOL & STUART HUMPHRIES	
1.44 Modelling flows in thermochemical nonequilibrium adaptive and mapped meshes	64
CHAY W. C. ATKINS & RALF DEITERDING	
1.45 A Fluid Dynamics Model of Kidney Morphogenesis	66
VLADIMIR ZUBKOV	
1.46 Rivulet Flow Down an Inclined Permeable Membrane	67
A. S. ALSHAIKHI [†] , M. GRINFELD & S. K. WILSON	
1.47 Time-frequency analysis for wakes of accelerating ships	68
RAVINDRA PETHIYAGODA	
1.48 Hele-Shaw flows in doubly connected domains	69
SCOTT McCUE, LIAM MORROW, MICHAEL JACKSON, MICHAEL DALLASTON & TIMOTHY MORONEY	
1.49 Coalescence of Droplets with Dissimilar Surface Tension	70
THOMAS C. SYKES ^{†1} , ALFONSO A. CASTREJÓN-PITA ² , J. RAFAEL CASTREJÓN-PITA ³ , MARK C. T. WILSON ¹ , DAVID HARBOTTLE ¹ , ZINEDINE KHATIR ¹ & HARVEY M. THOMPSON ¹	
1.50 Efficient Implementation of Elastohydrodynamic Integral Operators for Stokesian Filaments	71
ATTICUS L. HALL-McNAIR ^{†1} , MEURIG T. GALLAGHER ¹ , THOMAS D. MONTENEGRO-JOHNSON ¹ , HERMES GADÉLHA ² & DAVID J. SMITH ¹	
1.51 Determining how the microstructure of the Endothelial Glycocalyx Layer affects its bulk fluid-dynamical properties	72
T. C. LEE , V. SURESH & R. J. CLARKE	

1.52 Effect of vapour pressure on the performance of a Leidenfrost engine	73
PRASHANT AGRAWAL ¹ , GARY G. WELLS ¹ , RODRIGO LEDESMA-AGUILAR ¹ , GLEN MCHALE ¹ , ANTHONY BUCHOUX ² , KHELLIL SEFIANE ² , ADAM STOKES ² , ANTHONY J. WALTON ² & JONATHAN G. TERRY ²	
1.53 Flow physics and sensitivity to RANS modelling assumptions of a multiple normal shock wave boundary layer interactions	74
KIRIL BOYCHEV [†] , G. N. BARAKOS & R. STEIJL	
1.54 Effect of Ambient Pressure Oscillation on the Primary Break-up of Jet Spray	76
ZHEN ZHANG ^{1,2} & DONG-HYUK SHIN ¹	
1.55 Experimental simulation of the Vortex Ring State	77
D. PICKLES, R. GREEN & A. BUSSE	
1.56 Robust Optimisation of Microfluidic Flow Systems [Poster]	78
FOTEINI ZAGKLAVARA [†]	
1.57 Droplet Mobility on the Flexible Slips (F-Slips) [Poster]	79
MUMTAHINA RAHMAN [†] , GLEN MCHALE, RODRIGO LEDESMA-AGUILAR & GARY G. WELLS	
1.58 On the aerodynamics of the gliding seeds of Javan cucumber	81
DANIELE CERTINI [†] , C. CUMMINS, E. MASTROPAOLO, N. NAKAYAMA & I. M. VIOLA	
1.59 Self-propelled droplet transport on liquid surfaces	82
G. LAUNAY ¹ , M. S. SADULLAH ² , G. MCHALE ¹ , R. LEDESMA-AGUILAR ¹ , H. KUSUMAATMAJA ² & G. G. WELLS ¹	
1.60 High-Order Relativistic Hydrodynamic Simulations using Rotated- Hybrid Riemann Solvers of the Kelvin–Helmholtz Instability and High Mach Number Flows	84
JAMIE TOWNSEND [†] , LÁSZLÓ KÖNÖZSY & KARL W. JENKINS	
1.61 The effect of heat transfer on boundary layer kinetic energy dis- sipation	85
LACHLAN JARDINE ^{†1} , ANDREW WHEELER ¹ , ROB MILLER ¹ & BUDIMIR ROSIC ²	
1.62 Spontaneous Synchronization of Beating Cilia: An Experimental Proof Using Vision-Based Control	86
MOHAMED ELSHALAKANI [†] & CHRISTOPH H. BRÜCKER	
1.63 A Lattice-Boltzmann Model of Electrocapillarity	87
ÉLFEGO RUIZ-GUTIÉRREZ, GLEN MCHALE & RODRIGO LEDESMA-AGUILAR	
1.64 The role of protein concentration on the rheology of synovial fluid when modelling elastohydrodynamic lubrication of joint prostheses	89
L. NISSIM [†] , H. BUTT, L. GAO, C. MYANT & R. HEWSON	

1.65 Experimental study of atmospheric stratification and urban flow and dispersion	91
DAVIDE MARUCCI & MATTEO CARPENTIERI	
1.66 FAST, NEAREST and flagellar regulation	92
M. T. GALLAGHER ^{1,2} , G. CUPPLES ^{1,2} , J. C. KIRKMAN-BROWN ² & D. J. SMITH ^{1,2}	
1.67 Bifurcation analysis of evaporating droplets on smooth surfaces	93
MICHAEL EWETOLA [†] & MARC PRADAS	
1.68 Finite Element Modelling of Microswimmers with Applications in Reproductive Biology	94
CARA V. NEAL [†] , DAVID J. SMITH, MEURIG T. GALLAGHER & THOMAS D. MONTENEGRO-JOHNSON	
1.69 Applying the Goldilocks Principle to predict coral habitat engi- neering	95
KONSTANTINOS GEORGIOULAS [†]	
1.70 Low-order Prediction and Modelling of Intermittent Flow Sepa- ration and Reattachment in Unsteady 2D Flows	96
DESANGA FERNANDO & KIRAN RAMESH	
1.71 Is climate change increasing atmospheric turbulence?	97
PAUL D. WILLIAMS	
1.72 Numerical simulations of grid-turbulence, and dissipation mod- elling in large-eddy simulations.	98
RORY HETHERINGTON [†]	
1.73 Contact line dynamics and hysteresis measurements on social sur- faces	99
HERNAN BARRIO-ZHANG [†] , ÉLFEGO RUIZ-GUTIÉRREZ, GARY G. WELLS & RODRIGO LEDESMA-AGUILAR	
1.74 A computational model to predict the onset of secondary flows of blood in a cone and plate rheometer	100
NATHANIEL KELLY [†] , DANIEL JELLIFFE, HARINDERJIT GILL, KATHARINE FRASER & ANDREW COOKSON	
1.75 Large eddy simulations of plumes in a stratified room	101
CAROLANNE VOURIOT [†]	
1.76 Sedimentation of tephra from stratified plumes	102
DANIEL WARD [†]	
1.77 Elasticity suppresses fluidisation of yield-stress material under vibrations	103
ASHISH GARG [†] , MATTHIAS HEIL & ANNE JUEL	

1.78 Parallel-in-time integration of Dynamo Simulations	104
ANDREW CLARKE [†]	
1.79 Multiphase plumes in a stratified ambient	105
NICOLA MINGOTTI & ANDREW W. WOODS	
1.80 Predicting orientation of suspensions of elongated particles in three-dimensional thin channel flow	106
G. CUPPLES ¹ , D. J. SMITH ¹ , M. HICKS ² & R. J. DYSON ¹	
1.81 DNS of a turbulent rotating jet	107
SAMUEL D. DUNSTAN [†] & YONGMANN M. CHUNG	
1.82 The impact of shark skin denticles on the turbulent flat plate boundary layer	110
CHARLIE LLOYD ^{†1} , JEFFREY PEAKALL ¹ , ALAN BURNS ¹ , GARETH KEEVIL ¹ & ROBERT DORRELL ²	
1.83 Structural and physical determinants of solute transport in com- plex microvascular networks	111
ALEXANDER ERLICH ¹ , PHILIP PEARCE ² , GARETH NYE ³ , PAUL BROWNBILL ³ , ROMINA PLITMAN MAYO ⁴ , OLIVER JENSEN ¹ & IGOR CHERNYAVSKY ^{1,3}	
1.84 The Dynamics of Anisotropic Ice in Simple Configurations	112
DANIEL RICHARDS [†] , SAM PEGLER, SANDRA PIAZOLO & OLIVER HARLEN	
1.85 Supersonic wind tunnels: Effects of nozzle geometry	113
KSHITIJ SABNIS [†] & HOLGER BABINSKY	
1.86 On the Lift Augmentation Mechanism of an Asymmetrically Pitch- ing Foil	114
SHŪJI ŌTOMO ^{†1} , KAREN MULLENERS ² , KIRAN RAMESH ³ & IGNAZIO MARIA VIOLA ¹	
1.87 Evaporation-driven transport through soft hydrogels	115
MERLIN A. ETZOLD, M. GRAE WORSTER, & PAUL F. LINDEN	
1.88 Aerodynamic Optimisation of Supersonic Aerofoils Based on Deep Neural Networks	116
AARON FERIA-ALANIS [†] & ANTONIOS F. ANTONIADIS	
1.89 Adjoint-based optimal control of an inkjet waveform	118
PETR KUNGURTSEV [†] & MATTHEW P. JUNIPER	
1.90 On the formation of hydraulic jump for low- and high-viscosity liquids	119
ROGER E. KHAYAT & YUNPENG WANG	
1.91 Vesicle transport and cytoplasmic streaming in the pollen tube	120
R. J. DYSON ¹ , J. TYRRELL ¹ , Y. CHEBLI ² , D. J. SMITH ¹ & A. GEITMANN ²	

1.92 Computational Aerodynamic Solutions of Hovering Rotors by High-Order Schemes on Unstructured Grids	121
PAULO A. S. F. SILVA [†] , FRANCESCO RICCI, PANAGIOTIS TSOUTSANIS, KARL W. JENKINS & ANTONIOS F. ANTONIADIS	
1.93 Simulation of turbulent flows with Nek5000	124
DANIEL FENTON [†]	
1.94 Drag reduction by anisotropic permeable substrates – analysis and DNS	125
GARAZI GÓMEZ-DE-SEGURA [†] & RICARDO GARCÍA-MAYORAL	
1.95 Particle-laden gravity currents	127
MARTIN C. LIPPERT [†] & ANDREW W. WOODS	
1.96 Sound generation by entropy perturbations passing through cross-sectional area changes	128
DONG YANG, JUAN GUZMÁN & AIMEE S. MORGANS	
1.97 Shape sensitivity analysis of thermoacoustic instability in an annular combustor using an adjoint Helmholtz solver	129
STEFANO FALCO [†]	
1.98 High density ratio lattice Boltzmann simulations [Retracted] . . .	130
1.99 On dispersion in heterogeneous porous rocks	131
NEERAJA BHAMIDIPATI [†] & ANDREW W. WOODS	
1.100 Internal gravity waves, shear, and mixing in forced stratified turbulence	132
CHRISTOPHER J. HOWLAND [†] , JOHN R. TAYLOR & COLM-CILLE P. CAULFIELD	
1.101 A unified approach to the study of turbulence over smooth and drag-reducing surfaces	133
JOSEPH I. IBRAHIM [†] & RICARDO GARCÍA-MAYORAL	
1.102 On analytical solutions for the mean wind profile in an urban canopy	134
OMDUTH COCEAL	
1.103 The effect of rotor wakes on compressor flow field within the multistage machines	135
PAWEL J. PRZYTARSKI [†] & ANDREW P. S. WHEELER	
1.104 Detour induced by the piston effect in double-diffusive convection of near-critical fluids	136
ZHAN-CHAO HU [†] & XIN-RONG ZHANG	
1.105 Turbulence in the Body of Gravity Currents	137
CAROLINE MARSHALL [†]	

1.106 A new approach to modelling polydisperse sprays with phase exchange based on the Fully Lagrangian Approach	138
OYUNA RYBDYLOVA, YUAN LI & TIMUR ZARIPOV	
1.107 Aerosol generation from liquid droplet impact on solid surfaces [Poster]	139
ISLAM SALEM [†]	
1.108 Quantifying the effect of morphological features of river channels on discharge relations	140
DUNCAN LIVESEY [†]	
1.109 Fluid dynamics of single/multiple droplets onto a substrate with a topographical feature	141
K. H. A. AL-GHAITHI [†] , M. C. T. WILSON, O. G. HARLEN & N. KAPUR	
1.110 Pulse propagation in quasi-laminar gravity currents [Retracted]	143
1.111 Energy cascade in a homogeneous swarm of bubbles rising in a vertical channel	144
BRUNO FRAGA ¹ , CHRIS C. K. LAI ² , WAI HONG RONALD CHAN ³ & MICHAEL DODD ³	
1.112 Numerical Simulation of a Bubble Swarm: Void Fraction and Bubble Size Analysis	145
ERNESTO RAMA NOVO & BRUÑO FRAGA	
1.113 Development and verification a green approach towards isolating essential oils from <i>Rosmarinus officinalis</i> using ultrasound-assisted supercritical CO ₂	146
MING-CHI WEI ¹ , SHOW-JEN HONG ² , DA-HSIANG WEI ² , PEI-HUI LIN ³ & YU-CHIAO YANG ^{2,4}	
1.114 Production of essential oil from <i>Lavandula angustifolia</i> through a green procedure and its theoretical solubility consideration . . .	147
YU-CHIAO YANG ^{1,2} , SHOW-JEN HONG ¹ , DA-HSIANG WEI ¹ , PEI-HUI LIN ³ & MING-CHI WEI ⁴	
1.115 A Droplet Mop	148
JOSH SACZEK ¹ , GUANQI WANG ¹ , VLADIMIR ZIVKOVIC ¹ , BEN XU ² & STEVEN WANG ¹	
1.116 Feedback stabilization of a Plane Couette Flow Exact Coherent Structure	149
GEOFFROY C. P. CLAISSE [†] & ATI S. SHARMA	
1.117 Coherent patterns and bypass laminar turbulent transition in boundary layers	152
JOSEPH OLOO [†] & VICTOR SHRIRA	

1.118 A dam-break driven by a moving source: a simple model for a powder snow avalanche	153
JOHN BILLINGHAM	
1.119 Large-eddy simulation of enhanced mixing for water treatment applications	154
BOYANG CHEN [†] & BRUÑO FRAGA	
1.120 Droplet Retention and Shedding on Slippery Substrates	155
B. V. ORME [†] , G. MCHALE, R. LEDESMA-AGUILAR & G. G. WELLS	
1.121 A multicompartment SIS stochastic model with zonal ventilation for the spread of nosocomial infections: detection, outbreak management and infection control	156
MARTÍN LÓPEZ-GARCÍA, MARCO-FELIPE KING & CATHERINE J. NOAKES	
1.122 Evaluating CFD against a zonal ventilation model for predicting airborne pathogen transfer under different hospital ward ventilation configurations	157
ROSIE JONES [†] , MARCO-FELIPE KING, MARTÍN LÓPEZ-GARCÍA & CATHERINE J. NOAKES	
1.123 Dune-Dune Repulsion	158
K. A. BACIK ^{†1} , C. P. CAULFIELD ^{2,1} , S. LOVETT ³ & N. M. VRIEND ^{1,2}	
1.124 Nonlinear feedback control of the bi-modal flow behind a three-dimensional blunt bluff body	159
D. AHMED [†] & A. S. MORGANS	
1.125 Influence of moving ground use on the unsteady wake of a small-scale commercial road vehicle	160
ALEKSANDRA ANNA REJNIAK [†] & ALVIN GATTO	
1.126 Exit dynamics of a 2D cylinder from the water	161
INTESAAF ASHRAF, ANOUCHKA LILOT AND STÉPHANE DORBOLO	
1.127 Coarse grained models for reactive flows in porous media: homogenisation and numerical simulations	163
FEDERICO MUNICCHI & MATTEO ICARDI	
1.128 Three-dimensional numerical simulations of a thin film falling vertically down the inner surface of a rotating cylinder	164
USMAAN FAROOQ ^{†1} , JASON STAFFORD ² , CAMILLE PETIT ¹ & OMAR K. MATAR ¹	
1.129 Numerical Study of the Wave Kinetic Equation for Drift Wave/Zonal Flow Interactions	165
KRISTOFFER SMEDT [†]	
1.130 Influence of stack chimneys on the displacement ventilation of an enclosed geometry	166
DANIEL FIUZA DOSIL [†]	

1.131 Shaping supersonic contoured nozzles for cold spraying metallic particles	167
ALDO RONA & LUIZA F. ZAVALAN [†]	
1.132 Impact of surfactants on inertia-induced undulations on the surface of capillary bubbles	168
A. BATCHVAROV ¹ , M. MAGNINI ² , L. KAHOUADJI ¹ , R. V. CRASTER ³ & O. K. MATAR ¹	
1.133 DNS for the dynamics of 3D surfactant-laden bursting bubbles .	169
R. CONSTANTE-AMORES [†] , L. KAHOUADJ, A. BATCHVAROV & O. K. MATAR	
1.134 From walking to shooting modes in droplet vibrations	170
L. KAHOUADJI, O. K. MATAR & R. V. CRASTER	
1.135 Implementation and verification of CFD model for crude-oil fouling	171
GABRIEL F. N. GONÇALVES ^{†1} , MIRCO MAGNINI ² & OMAR K. MATAR ¹	
1.136 Turbulent flows over sparse canopies	172
AKSHATH SHARMA [†] & RICARDO GARCÍA-MAYORAL	
1.137 CFD Based Optimisation of Swirl Inducing Multi-Nozzle Annular Jet Pump	173
ANDREW MORRALL	
1.138 Flow-induced symmetry breaking in growing bacterial biofilms .	174
PHILIP PEARCE	
1.139 SPT: Slender Phoretic Theory of Chemically Active Filaments .	175
PANAYIOTA KATSAMBA ¹ , SÉBASTIEN MICHELIN ² & THOMAS D. MONTENEGRO-JOHNSON ¹	
1.140 Recasting Navier-Stokes Equations	176
S. KOKOU DADZIE & M. H. LAKSHMINARAYANA REDDY	
1.141 Variability of stochastically forced zonal jets	177
LAURA COPE [†]	
1.142 Potential flows through periodic domains with multiple objects per period	178
PETER J. BADDOO [†] & LORNA J. AYTON	

2.1 Methods for investigating dissolution in surfactant solutions	179
RACHEL HENDRIKSE [†]	
2.2 Accurate Lattice Boltzmann Simulations of Gas Permeability through Nanoporous Media	180
DIAN FAN, ANH PHAN & ALBERTO STRIOLO	
2.3 Predicting Spray Impact on and Carry-Over from Complex Shaped Surfaces	181
LIAM GRAY [†]	

2.4 Fluid Transport Correlations in Partially Filled Pipes for Nuclear Decommissioning	182
CHRISTOPHER CUNLIFFE [†] & DAVID DENNIS	
2.5 Massively Parallelized Models of Fluid-Solid Multiphase Flow . . .	183
DAMILOLA ADEKANYE [†]	
2.6 The Zhang–Viñals Equations for Pattern Forming Problems	184
REECE COYLE [†]	
2.7 Folding and necking of layered viscous structures	185
OLIVIA GOULDEN [†]	
2.8 Turbulence modelling in astrophysical turbulent mixing layers . .	186
JONATHAN DAVID FINN [†]	
2.9 Conventional and cryogenic coolants for machining applications . .	187
ELEANOR HARVEY	
2.10 Direct Numerical Simulation of an Oldroyd-B filament thinning .	188
KONSTANTINOS ZINELIS [†] , RICARDO CONSTANTE, LACHLAN MASON & OMAR MATAR	
2.11 Utilisation of instrumented particles for the study of incipient entrainment	189
KHALDOON ALOBAIDI [†] , ATHANASIOS ALEXAKIS & MANOUSOS VALYRAKIS	
2.12 Hydrological Representations of Extreme Precipitation in East Africa under Climate Change using a Convection-Permitting Model	190
CLAIRE WEST [†]	
2.13 Modelling the motion of the vitreous humour: A boundary inte- gral approach	191
LAURA BEVIS [†]	
2.14 Power spectrum and machine learning analysis applied to dried blood droplets [Talk]	192
L. HAMADEH, S. IMRAN, M. BENCSIK, G. SHARPE, M. JOHNSON & D. J. FAIRHURST	
2.15 Flow analysis and fouling behaviour in 3-D printed wavy-patterned membranes [Talk]	193
SAEED MAZINANI, ABOUTHER AL-SHIMMERY, Y. M. JOHN CHEW & DAVIDE MATTIA	
2.16 How Long To Reach Similarity? [Talk]	194
HERBERT HUPPERT, THOMASINA BALL & JOSEPH WEBBER	

1 Talks

1.1 Saturation-Dependence of Non-Fickian Transport in Porous Media

VAHID NIASAR

School of Chemical Engineering and Analytical Science,
University of Manchester

Solute transport in two-phase flow through porous media is an important topic for many industrial and natural processes such as nutrient transport in partially-saturated soils in agriculture, transport of chemicals in oil reservoirs for enhanced oil recovery, or in soil remediation. Modeling multiphase flow and transport in different applications is essential to improve the design and operational condition. Hence, the predictive capabilities of such models need to be improved. To evaluate the assumptions embedded in one of the most commonly used theories, referred to as the mobile-immobile theory, we have performed pore-scale simulations and experiments of these physical processes. By upscaling the simulation, microfluidic and 4D microCT imaging results, we directly estimated the transport properties and compared them with the inverse modelling results using the mobile-immobile theory. There is a significant discrepancy between the directly and indirectly estimated results that imply the potential shortcomings in the mobile-immobile theory. Moreover, it has been discussed that potentially the two-phase relative permeability data can be used as a proxy to estimate the stagnant (immobile) saturation that will link two-phase Darcy theory with the transport models.

References:

1. NK Karadimitriou, V Joekar-Niasar, M Babaei, CA Shore, Critical Role of the Immobile Zone in Non-Fickian Two-Phase Transport: A New Paradigm, 2016, *Environmental Science & Technology* 50 (8), 4384-4392
2. NK Karadimitriou, V Joekar-Niasar, OG Brizuela, Hydro-dynamic Solute Transport under Two-Phase Flow Conditions, 2017, *Scientific Reports*, doi:10.1038/s41598-017-06748-1
3. R Aziz, V Joekar-Niasar, P Martinez-Ferrer, Pore-scale insights into transport and mixing in steady-state two-phase flow in porous media, 2018, *International Journal of Multiphase Flow* 109, 51-62
4. Sharul Hasan, Vahid Joekar-Niasar, Nikolaos K. Karadimitriou, Muhammad Sahimi, Saturation-dependence of non-Fickian transport in porous media, *Water Resources Research*, 2019, accepted

1.2 Interactions between tidal flows and convection

CRAIG DUGUID[†], ADRIAN BARKER & CHRIS JONES

University of Leeds

Tidal interactions are important in driving spin and orbital evolution in various astrophysical systems such as hot Jupiters, close binary stars and planetary satellites. The fluid dynamical mechanisms responsible for tidal dissipation in giant planets and stars remain poorly understood. One key mechanism is the interaction between tidal flows and turbulent convection. This is thought to act as an effective viscosity in damping large-scale tidal flows, but there exists a long-standing controversy over the efficiency of this mechanism in the limit of large tidal frequencies (which is the relevant regime in many astrophysical applications).

We explore the interaction between tidal flows and convection as a mechanism for tidal dissipation using hydrodynamical simulations. Our approach is to study the interaction between an oscillatory background shear flow, which represents a large-scale tidal flow, and the convecting fluid inside a small patch of a star or planet. We simulate Rayleigh-Bénard convection in this Cartesian model and explore how the effective viscosity of the turbulence depends on the tidal (shear) frequency.

We will present the results from our simulations to determine the effective viscosity, and its dependence on the tidal frequency in both laminar and weakly turbulent regimes. We will also present our extension to the theoretical framework of Ogilvie and Lesur (2012), so that it applies to Rayleigh-Bénard convection, which we will use to interpret and explain some of our results. We will focus on the scaling of the effective viscosity with tidal frequency in the limit of large tidal frequencies. We will also demonstrate, using both analytical theory and numerical simulations, that negative effective viscosities are possible in this system (corroborating a tentative finding in Ogilvie & Lesur, 2012). The astrophysical implications of our results will be briefly discussed.

1.3 Modelling dynamic stall of a pitching airfoil in large-scale freestream turbulence

THANKGOD BOYE[†] & ZHENG-TONG XIE

Aerodynamics and Flight Mechanics group (AFM),
University of Southampton

The aspect of dynamic stall associated with large-scale freestream turbulence effect is not well understood particularly in flow over a pitching aerofoil. Substantial understanding of the effect of large-scale freestream turbulence is crucial for pitching airfoil because of the need for innovative aerodynamic design of modern large wind turbine blades. Although considerable experimental and numerical work of laminar inflow have been done to investigate aerodynamic characteristics on the dynamic stall phenomena of an aerofoil, Gandhi et al. [1] reported that there are a few experimental studies of the effect of the freestream turbulence on a pitching aerofoil and even fewer numerical studies, perhaps due to the complexity of the methods involved to develop and implement the incoming turbulence inflow conditions in experiments and numerical simulations. Researchers who have studied turbulence effects on the dynamic stall of an aerofoil focus on the effect of high turbulent intensity and small integral length-scales [2-3]. They found that an increase of the turbulent intensity resulted in an increase of the lift coefficient, but little research particularly on the effect of large integral length-scales has been conducted.

Turbulence integral length-scales in the atmospheric boundary layer are typically much greater than the aerofoil chord length. The effects of the large-scales turbulence on the aerodynamic characteristics of aerofoil are of greater importance than the effects of the high turbulence intensity [4]. Mahmoodilari et al. [5] identified that an increase in integral length-scale adversely affects the lift. Ravi et al. [6-7] revealed that the integral length-scale and turbulent intensity had opposing influence on the lift coefficient, and an increase in integral length-scale rendered an increase in lift. Harbst et al. [8] reported that an increase in integral length-scale enhances the probability of occurrence of short separation bubbles close to the leading edge of the aerofoil. Therefore it is not clear whether the incoming large eddies improve performance of the aerodynamic forces of a pitching aerofoil. The advanced numerical modelling methods such as large-eddy simulation (LES) are promising to simulate complex unsteady flow and to capture crucial flow physics of large-scale turbulence interactions with a pitching aerofoil.

In this paper, we aim to investigate the effect of large integral length-scales on a pitching NACA 0012 aerofoil at a moderate Reynolds number $Re = 1.35 \times 10^5$ based on the chord length and the freestream velocity. A turbulence inflow condition method for LES is employed for the study. At the inlet large integral length-scale greater than the chord length are used for modelling the energetic large-eddies impact-

ing on the pitching aerofoil at various reduced frequencies $k_{\text{red}} = 0.1, 0.15$ and 0.2 . Preliminary results of baseline simulations show good agreement with experimental and numerical data in [3]. The lift, drag and moment coefficients and corresponding flow-field of the large-scale turbulence structures will be presented. We are more focused on revealing the effects of the large integral length-scales on the dynamic stall of the pitching aerofoil. The data and knowledge derived from this study will contribute to enhancing innovative aerodynamic design of modern large wind turbine blade that operates within the atmospheric boundary layer.

References:

1. A. Gandhi, B. Brandon and Y. Peet. Effect of reduced frequency on dynamic stall of a pitching airfoil in turbulent wake, AIAA SciForum, AIAA Aerospace Sciences Meeting, 55: 1-15, 2017.
2. X. Amandolese and E. Szechenyi. Experimental study of the effect of turbulence on a section model blade oscillating in stall. *Wind Energy*, 7(4):267-282, 2004.
3. Y. Kim and Z. T. Xie. Modelling the effect of freestream turbulence on dynamic stall of wind turbine blade. *Comp. fluids*, 129:53-66, 2016.
4. J. Stack. Test in the variable density wind tunnel to investigate the effect of scales and turbulence on airfoil characteristics. Technical notes National advisory committee for aeronautics, 364:1-15 1931.
5. M. Mahmoodilari. The effect of turbulence flow on wind turbine loading and performance. Ph.D. Thesis, University of Manchester, 2012.
6. S. Ravi, S. Watkins, J. Watmuff, K. Massey, P. Peterson and M. Marino. Influence of large-scale freestream turbulence on the performance of thin airfoi. *AIAA Journal*, 50:2448-2459, 2012.
7. S. Ravi, S. Watkins, J. Watmuff and A. Fisher. Transient Loads occurring over a thin airfoil subjected to large-scale freestream turbulence. *AIAA journal*, 51(6):1473-1485, 2013.
8. S. L. Harbst, C. J. Kahler and R. Hain. Influence of large-scale freestream turbulence on an SD7003 airfoil at low Reynolds numbers. AIAA, Aviation Forum Applied aerodynamics conference, 1-13, 2018.

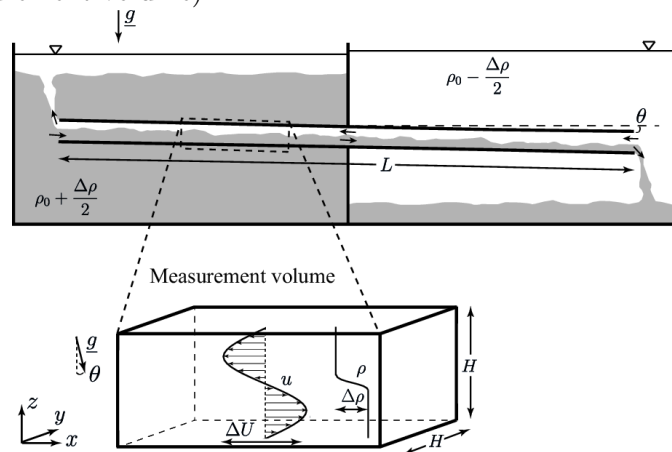
1.4 Regime transitions and energetics of sustained stratified shear flows

ADRIEN LEFAUVE, JAMIE PARTRIDGE & PAUL LINDEN

Department of Applied Mathematics and Theoretical Physics,
University of Cambridge

Problem: We describe the long-term dynamics of sustained stratified shear flows in the laboratory. The Stratified Inclined Duct (SID) experiment sets up a two-layer exchange flow in an inclined duct connecting two reservoirs containing salt solutions of different densities (figure 1). This flow is primarily characterised by two non-dimensional parameters: the tilt angle of the duct with respect to the horizontal, θ (a few degrees at most), and the Reynolds number Re , an input parameter based on the density difference $\Delta\rho$ driving the flow. The flow can be sustained with constant forcing over arbitrarily long times and exhibits a wealth of dynamical behaviours representative of geophysically-relevant sustained stratified shear flows. Varying θ and Re leads to four qualitatively different regimes: laminar flow; mostly laminar flow with finite-amplitude, travelling Holmboe waves; spatio-temporally intermittent turbulence with substantial interfacial mixing; and sustained, vigorous interfacial turbulence [1]. In this paper, We seek to explain the scaling of the transitions between flow regimes in the two-dimensional plane of input parameters (θ, Re) .

Figure 1: The Stratified Inclined Duct (SID) experimental setup (showing the measurement volume).



Approach: We improve upon previous studies of this problem by providing a firm physical basis and non-dimensional scaling laws that are mutually consistent and in good agreement with the empirical transition curves we inferred from 360 experiments spanning $\theta \in [-1^\circ, 6^\circ]$ and $Re \in [300, 5000]$. To do so, we employ state-of-the-art simul-

taneous volumetric measurements of the density field and the three-component velocity field, and analyse these experimental data using time- and volume-averaged potential and kinetic energy budgets.

Results: We show that regime transitions are caused by an increase in the non-dimensional time- and volume-averaged kinetic energy dissipation within the duct, which scales with θRe at high enough angles. As the power input scaling with θRe is increased above zero, the two-dimensional, parallel-flow dissipation (power output) increases to close the budget through an increase in the magnitude of the exchange flow, incidentally triggering Holmboe waves above a certain threshold in interfacial shear. However, once the hydraulic limit of two-layer exchange flows is reached, two-dimensional dissipation plateaus and three-dimensional dissipation at small scales (turbulence) takes over, first intermittently, and then steadily, in order to close the budget and follow the θRe scaling.

Implications: This general understanding of regime transitions and energetics in the SID experiment may serve as a basis for the study of more complex sustained stratified shear flows found in the natural environment.

References:

1. C. R. Meyer & P. F. Linden. Stratified shear flow: experiments in an inclined duct. *J. Fluid Mech.*, **753**:242–253, 2014

1.5 The construction and evolution of an inviscid background state for Earth's magnetic field

COLIN M. HARDY[†], PHILIP W. LIVERMORE, AND JITSE NIESEN
University of Leeds

Vigorous, rotationally constrained, buoyant convection of the molten iron within the Earth's outer core is responsible for the sustaining the Earth's magnetic field through the mechanism known as the geodynamo. The fluid motion driving the geodynamo is governed by the MHD equations, and significantly, rotational forces are dominant over inertial and viscous forces, which in terms of dimensionless numbers means that the Ekman and Rossby numbers are very small. The extreme nature of these values leads to a problem for numerical simulations, since it means that they are required to resolve a large contrast of both spatial and temporal scales, making it too computationally expensive to be feasible for the correct parameter regime.

There is an alternative approach proposed by Taylor in 1963, of an inertia-free and viscosity-free model as the asymptotic limit of Earth's dynamo. In this theoretical limit of a magnetostrophic balance, a certain necessary condition, now well known as Taylor's constraint, must hold. This provides a restriction on the magnetic field structure inside the core. We combine this constraint with geomagnetic observations at the core-mantle boundary, to construct a model for the large scale background field within Earth's core, which is consistent with both. We then numerically evolve a suite of these fields subject to a small but finite viscosity and carry out an investigation of their stability. We search for stable, self-consistent fields which continue to approximately obey Taylor's constraint over time and report the dependence on the value of the Ekman number.

1.6 Shape of a recoiling liquid filament [Was: Capillary retraction of an axisymmetric liquid ligament]

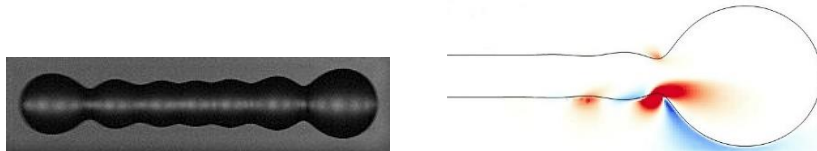
F. P. CONTÒ¹, J. F. MARÍN², L. GORDILLO²,
J. R. CASTREJON-PITA¹ & A. A. CASTREJON-PITA³

¹School of Engineering and Materials Science, Queen Mary
University of London

²Departamento de Física, Universidad de Santiago de Chile

³Department of Engineering Science, University of Oxford

We study the capillary retraction of a Newtonian semi-infinite liquid filament through analytical methods. We derive a long-time asymptotic-state expansion for the filament profile using a one-dimensional free-surface slender cylindrical flow model based on the three-dimensional axisymmetric Navier-Stokes equations. The analysis identifies three distinct length and time scale regions in the retraction domain: a steady filament section, a growing spherical blob, and an intermediate matching zone. We show that liquid filaments naturally develop travelling capillary waves along their surface and a neck behind the blob. We analytically prove that the wavelength of the capillary waves is approximately 3.63 times the filament's radius at the inviscid limit. Additionally, the waves' asymptotic wavelength, decay length, and the minimum neck size are analysed in terms of the Ohnesorge number. Finally, our findings are compared with previous results from the literature and numerical simulations in Basilisk obtaining a good agreement. This analysis provides a full picture of the recoiling process going beyond the classic result of the velocity of retraction found by Taylor and Culick.



Acknowledgements: F.P.C. and L.G. acknowledge FONDECYT 11170700; J.F.M. was partially funded by USA1899 - Vridei 041931YZ-PAP Universidad de Santiago de Chile; F.P.C., J.R.C.P. and A.A.C.P. thank the Royal Society and UK Engineering and Physical Science Research Council for the financial support.

References

1. Wang F., Contò F.P., Naz N., Castrejón-Pita J.R., Castrejón-Pita A.A., Bailey C.G., Wang W., Feng J.J. and Sui Y., 'A fate-alternating transitional regime in contracting liquid filaments', *Journal of Fluid Mechanics*, **2019**, 860, pp.640-653.
2. Gordillo L., Agbaglah G., Duchemin L. and Josserand C., 'Asymptotic behavior of a retracting two-dimensional fluid sheet', *Physics of Fluids*, **2011**, 23(12), p.122101.

3. Eggers J. and Dupont T.F., 'Drop formation in a one-dimensional approximation of the Navier– Stokes equation', *Journal of fluid mechanics*, **1994**, 262, pp.205-221.

1.7 An investigation into the trigger of wake bimodality behind squareback bluff bodies using LES

FARON HESSE[†]

Imperial College, London

A large eddy simulation (LES) study of the mechanism responsible for triggering bluff body wake bimodality is provided. Bimodality is a three-dimensional drag enhancing phenomenon in the turbulent flow regime that occurs over large and random time-scales. A $Re_H = 33000$ flow past the squareback Ahmed body is investigated using both true LES and wall-modelled LES (WMLES) coupled to grids of varying near-body resolution. It is found that only true LES with a fine near-body grid is capable of resolving horizontal wake bimodality, the Ahmed body's preferred direction for off-center wake motion. By comparing the resolved turbulence levels in the upstream turbulent boundary layer, it becomes clear that true LES predicts a significantly higher RMS value for the streamwise direction in the buffer layer, where most turbulence energy production occurs, indicating that particularly flow fluctuations in the streamwise direction are responsible for providing the stochasticity needed to force a bimodal event. Meanwhile, although WMLES does not resolve a bimodal event, it has been shown to collectively explore both of the wake's bimodal states through two simulations that use a moderately different near-wall spacing, illustrating WMLES's known grid sensitivity. This study represents a crucial step in understanding the origin of and, therefore, suppressing wake bimodality.

1.8 Surface Roughness Effects in Finite-Rate Reacting Hypersonic Boundary Layers

ATHANASIOS MARGARITIS^{†1}, TARANEH SAYADI², OLAF MARXEN³
& PETER J. SCHMID¹

¹Imperial College London

²Sorbonne University

³University of Surrey

Hypersonic flow has been found to be significantly influenced by finite-rate thermochemical effects. These effects often have an order-one influence on macroscopic quantities of interest, such as laminar-turbulent transition and heat transfer. Therefore, they have to be taken into account to achieve accurate predictions and effective flow control. Finite-rate chemistry models are highly parametrised and their effect on important output quantities is usually not quantifiable.

Even though the thermochemistry of reacting gases in free space has been previously investigated, the interaction of flow with solid boundaries at high speeds is fundamentally unexplored. The inclusion of an approximate finite-rate gas chemistry model at hypersonic speeds generates significant uncertainty in the fluid system, whose effect on the macroscopic quantities of interest is not trivial to identify; even less obvious is the sensitivity of such reacting flow in the presence of surface roughness.

These two aspects of hypersonic flow are addressed in this research, using a mathematical framework to assess the sensitivity of output flow quantities to input model parameters related to finite-rate chemistry or surface roughness. Using adjoint techniques we are able to identify critical model parameters that require particular accuracy to ensure physically observable output quantities. The objective and tools are formulated in general conditions to ensure adaptability to practical flows; validation of the tools is done in generic flat-plate boundary layer configurations to isolate the influence of each effect.

Finite-rate chemistry models relevant to atmospheric entry are implemented in a compressible Navier-Stokes solver. Non-equilibrium effects are investigated. The effect of localised wall roughness arrays on the flow is also explored, by means of a novel approach. Sensitivity analysis is carried out for the separate and the combined effect of the uncertainty of the chemistry and roughness parameters.

References:

1. M. Fosas de Pando, D. Sipp, and P. J. Schmid, *Efficient evaluation of the direct and adjoint linearized dynamics from compressible flow solvers*, Journal of Computational Physics, 231 (2012), pp. 7739–7755.
2. O. Marxen, G. Iaccarino, and T. E. Magin, *Direct numerical simulations of hypersonic boundary-layer transition with finite-rate chemistry*, Journal of Fluid Mechanics, 755 (2014), pp. 35–49.

3. S. Nagarajan, S. K. Lele, and J. H. Ferziger, *A robust high-order compact method for large eddy simulation*, Journal of Computational Physics, 191 (2003), pp. 392–419.
4. T. Sayadi, C. W. Hamman, and P. Moin, *Direct numerical simulation of complete h-type and k-type transitions with implications for the dynamics of turbulent boundary layers*, Journal of Fluid Mechanics, 724 (2013), pp. 480–509.
5. P. J. Schmid, M. Fosas de Pando, and N. Peake, *Stability analysis for n-periodic arrays of fluid systems*, Physical Review Fluids, 2 (2017), pp. 7739–7755.

1.9 Multifunctional Adsorbent Structures for use as Emergency Respirators

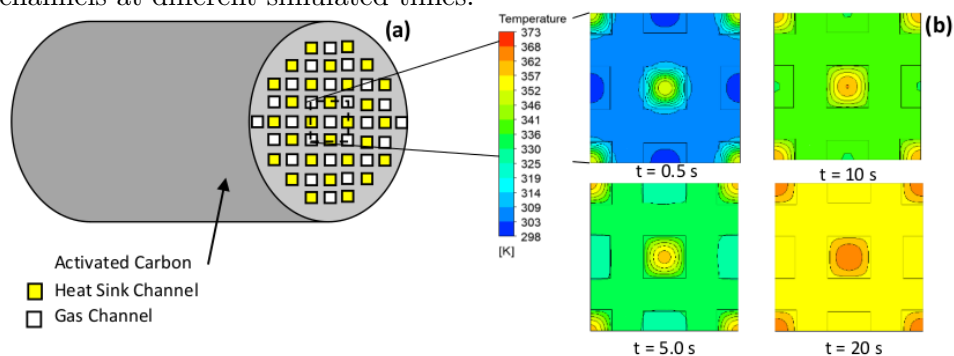
JONATHAN BARNARD[†], Y. M. JOHN CHEW & SEMALI PERERA

University of Bath

Fire toxicity still remains the predominant cause of fatality in building fires, accounting for 62% of deaths [1]. The combination of toxicants, irritants, hypoxic conditions and heat makes escaping a building fire extremely difficult, with each passing second reducing the chance of survival. The aim of this research is to design and fabricate a multifunctional device that is capable of adsorbing/reacting a wide variety of asphyxiant and irritant gases whilst removing the heat from the hot environment. The structure will ultimately be incorporated into a simple protective hood that is portable and lightweight.

The initial proposed design is an activated carbon monolithic adsorbent structure with multiple gas adsorption and heat absorption channels (Figure 2). The low pressure drop structure will provide: (i) the required volumetric adsorption capacity, (ii) a solid framework to enable metal impregnation for chemisorption, and catalytic oxidation of CO and (iii) a heat absorbing material distributed across some of the monolithic channels to remove the environmental heat and heats of adsorption and reaction. The heat sink channels would contain a shape stable phase change material (SS-PCM), utilising the latent heat to maximise heat absorption whilst not compromising the mechanical stability of the adsorbent monolith walls. These materials undergo no visible phase change, ensuring an inherently level of safety by preventing the SS-PCM escaping through the adsorbent walls.

Figure 2: Proposed monolith design (a), including adsorption and heat sink channels and inlet temperature profile contour plots (b) for a sample of channels at different simulated times.



This work presents numerical studies to elucidate the transport processes within the monolith. This will be required to optimise the

spatial arrangement, channel shape and ratio of adsorption to heat sink channels. These variables are intrinsically linked to the adsorption and heat absorbing performance of the structures. Where, incorrect distribution of heat sink channels would increase inhalation temperature and too few adsorption channels would reduce hazardous component uptake, as adsorbate/adsorbent contact area is reduced.

References:

1. Home Office. "Fire Statistics: Fatalities from fires by cause of death". 2018.

1.10 A New Method of Microbubble Production for Dissolved Air Flotation

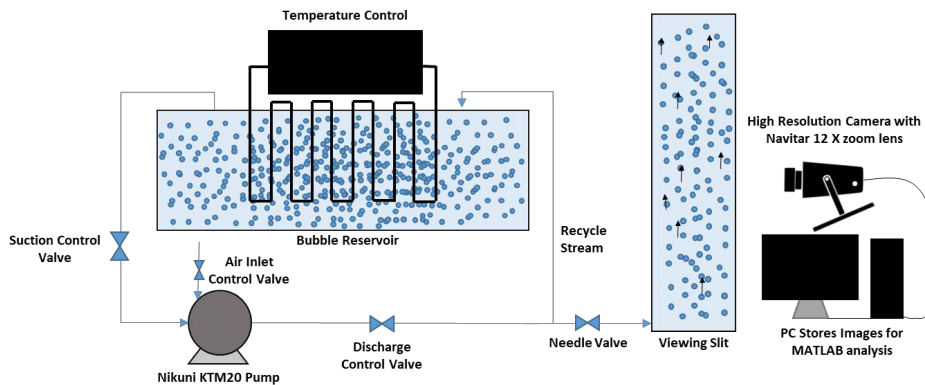
BERT SWART[†], JANNIS WENK & Y. M. JOHN CHEW

University of Bath

The production of microbubbles (MBs) with $10 - 100\mu\text{m}$ in diameter [1] for use in the Dissolved Air Flotation (DAF) process has been employed to remove solids in wastewater treatment for decades. The small size of the bubbles results in slow rise velocities, leading to long residence times and small forces of inertia, hence maximising particle attachment to bubbles. Traditionally the MBs in DAF are produced by saturating water with air at high pressure, followed by pressure drop which results in the nucleation of MBs. This pressurisation step is by far the most energy intensive step in the DAF process [2].

The purpose of this research is to investigate the use of a regenerative turbine pump which harnesses frictional, axial and centrifugal forces to create vortexes and areas of low pressure in which air shears and becomes entrained in the liquid in the form of MB's, with the aim to understand bubble dynamics and demonstrate the potential reduction in energy intensity by retro-fitting such MB generators into existing DAF units. This work focused on the characterisation of the MBs produced with a *Nikuni KTM20N* pump under different operating conditions. The bubble size distribution, rise velocity and effect of surfactants were evaluated.

Figure 3: Experimental setup used to investigate bubble size distribution and rise velocity.



Images of bubbles flowing in a viewing slit were captured by a high-resolution camera. MATLAB was used to analyse and identify the bubble size and trajectory. Bubble imaging shows that MBs were spherical and sizes ranged between 70 and 150 microns. The rise velocities on average matching the prediction from Stoke's Law within

12%. Current on-going work includes design and constructing a lab-scale DAF unit to investigate bubble-particle interactions and removal efficiency.

References:

J. K. Edzwald, "Principles and applications of dissolved air flotation," *Water Sci. Technol.*, vol. 31, no. 3-4, 1995.

J. K. Edzwald, *Water Quality & Treatment*, 6th ed. 2011.

1.11 Boundary layer control of rotating convection in the Earth's core

ROBERT S. LONG[†], JON E. MOUND, CHRISTOPHER J. DAVIES &
STEVE M. TOBIAS

University of Leeds

Convection is present in natural systems across many areas of astro- and geophysical fluid dynamics including planetary atmospheres, Earth's liquid metal outer core, and even plasma in the Sun. The dynamics within Earth's liquid iron outer core are so extreme that even state of the art physical and numerical experiments cannot match the relevant parameter values. Our models have parameters representing the strength of rotation (Ekman number, E) and buoyancy (Rayleigh number, Ra) many orders of magnitude different from those of the Earth's core. Recent work has used systematic studies of Ekman-Rayleigh space to show that different dynamical regimes exist which ultimately behave as being either rotationally constrained, or free from rotational effects. The transition between these two regimes is linked to processes in the thin regions close to the boundaries; the thermal boundary layers. An important issue in the study of convective fluid dynamics is then to determine the temperature distribution within a very thin layer in the vicinity of the heated bounding walls, i. e., the thermal boundary layers.

The classical methods for defining the edge of the thermal boundary layer originated in studies of non-rotating convection which exhibits a well-mixed isothermal fluid bulk and the net heat transport is dictated by processes in the thermal boundary layers. In contrast rotating convection is able to maintain persistent interior temperature gradients. We present an evaluation of the traditional methods using simulations of rotating convection in a spherical shell. We show how interior temperature gradients and fixed-flux thermal boundary conditions can compromise the classical definitions. We suggest an alternative definition which identifies the edge of the thermal boundary layer by the location at which the advective and diffusive contributions of the heat transport crossover (this is analogous to the treatment of the viscous boundary layer). Using this new definition we explicitly highlight the intimate link between the boundary layers and global heat transport in rotating convection systems.

1.12 A theoretical study of the invariant sets and transient dynamics of a finite air bubble in a perturbed Hele-shaw

J. S. KEELER, A. THOMPSON, A. HAZEL & A. JUEL

University of Manchester

Pressure-driven pattern formation of a closed finite air bubble propagating through a rectangular Hele-Shaw cell with a non-uniform cross-section is considered. Recent experimental work at the Manchester Centre of Nonlinear Dynamics (MCND) has revealed that the transient dynamics of a single bubble will become increasingly disordered as the extraction rate of the fluid is increased. This disorder is characterised by an increasing number of tips forming before the bubble breaks-up into two or more distinct bubbles. Here, we present theoretical results for higher flow rates where there is increased sensitivity to noise in the system. We reveal a rich bifurcation structure with a number of interesting features, including the existence of a bi-stable region, periodic solutions and non-unique asymmetric states. We perform a weakly nonlinear stability analysis which provides an approximation to the location, size and stability of the invariant fixed points and limit cycles and these are compared favourably with the fully nonlinear numerical simulations where a non-trivial dependence on the initial phase of the perturbation can lead to a number of different modes of transient behaviour, including the topological break-up of the bubble. Finally these theoretical results are compared to recent experiments at the MCND.

1.13 CFD Modelling of Alginate Production: A First Approach to Dynamic Rheology and Its Impact on Stirred and Aerated Bioprocesses

CONSTANZA SADINO-RIQUELME^{†1}, JOSÉ RIVAS², DAVID JEISON³,
ROBERT E. HAYES¹ & ANDRÉS DONOSO-BRAVO^{2,4}

¹Department of Chemical and Materials Engineering, University of Alberta, 9211 - 116 Street NW, Edmonton, AB, Canada

²Departamento de Ingeniería Química y Ambiental, Universidad Federico Santa María, Avenida Vicuña Mackenna 3939, Santiago, Chile

³Escuela de Ingeniería Bioquímica, Pontificia Universidad Católica de Valparaíso, Avenida Brasil 2085, Valparaíso, Chile

⁴CETAQUA, Los Pozos 7340, Las Condes, Chile

Mathematical modelling using Computational Fluid Dynamic (CFD) has been applied to study different bioprocesses, such as the baker's yeast production [1], biohydrogen formation [2], synthesis of cellulose [3] and anaerobic digestion in different reactor configurations [4]. Although these studies have enhanced the knowledge of relevant issues in the bioprocess field, the rheological changes caused by the bioprocess itself have been widely overlooked.

Based on these findings, the overall goal of the project is to implement a CFD model to represent the alginate production including the dynamic rheological changes caused by the alginate accumulation in a batch culture. Alginate is a polysaccharide that can be secreted by bacteria such as *Azotobacter vinelandii* and is used as gelling agent in several industries. Batch mode production of alginate was selected as the case study because the apparent viscosity of the culture medium changes gradually as the alginate is secreted, which impairs the mass transfer of substrate and oxygen inside the reactor medium [5].

For the project's first stage, several abiotic system were studied, experimentally, to mimic the rheological behaviour of a real culture medium at different stages of the alginate production, using Newtonian (water and PEG) and non-Newtonian (Xanthan gum) fluids in a dual impeller baffled bioreactor (4 L). Different CFD models were evaluated to find which one fits best the fluid dynamics of the tank for the different rheological stages under mixed (400 rpm) and aerated (1vvm) and non-aerated conditions. The torque and power drawn were experimentally monitored in each case to validate the CFD models. The validated models could be useful to study aeration or mixing strategies which improve the oxygen mass transfer at different stages of the alginate production process.

References:

1. McClure, D. D., Kavanagh, J. M., Fletcher, D. F., & Barton, G. W. (2016). Characterizing bubble column bioreactor performance using computational fluid dynamics. *Chemical Engineering Science*, 144, 58–74.

2. Srirugsa, T., Prasertsan, S., Theppaya, T., Leevijit, T., & Prasertsan, P. (2017). Comparative study of Rushton and paddle turbines performance for biohydrogen production from palm oil mill effluent in a continuous stirred tank reactor under thermophilic condition. *Chemical Engineering Science*, 174, 354–364.
3. Bach, C., Yang, J., Larsson, H., Stocks, S. M., Gernaey, K. V., Albaek, M. O., & Krühne, U. (2017). Evaluation of mixing and mass transfer in a stirred pilot scale bioreactor utilizing CFD. *Chemical Engineering Science*, 171, 19–26.
4. Sadino-Riquelme, C., Hayes, R. E., Jeison, D., & Donoso-Bravo, A. (2018). Computational fluid dynamic (CFD) modelling in anaerobic digestion: General application and recent advances. *Critical Reviews in Environmental Science and Technology*, 48 (1), 39–76.
5. Diaz-Barrera, A., & Soto, E. (2010). Biotechnological uses of *Azotobacter vinelandii*: Current state, limits and prospects. *African Journal of Biotechnology*, 9(33), 5240–5250.

**1.14 Numerical investigation of impinging synthetic jet for cooling of
electronic devices [Retracted]**

1.15 Experimental measurements in transitional partially-filled pipe flows using stereoscopic particle image velocimetry

THOMAS O. THORNHILL, HENRY C. H. NG & DAVID J. C. DENNIS
School of Engineering, University of Liverpool

Stereoscopic particle image velocimetry (S-PIV) has been used to obtain velocity measurements in transitional pipe flow in a partially-filled pipe. Transition has been studied both numerically and experimentally in detail for the full pipe arrangement, but not for partially-filled pipes despite the fact that there are many applications for running a pipe partially full. The very large scale pipe flow facility in the University of Liverpool will operate under partially full conditions from laminar to fully turbulent Reynolds numbers and measurements were taken over a range of flow depths (50% to 80% full pipe). S-PIV was used to measure the instantaneous three component velocity field on the pipe cross-section and using Taylor's hypothesis a 3D flow field was reconstructed, allowing an in-depth analysis of transitional flow in partially-filled pipes and the turbulent structures within the flow. The Reynolds number defined using the hydraulic diameter (Re_H) is plotted against the turbulent kinetic energy (TKE) for flows with different fill depths, showing the critical Re_H (Re_H at which transition first occurs). The critical Re_H is shown to increase as the flow depth of the pipe decreases, with a full pipe transitioning at lower Reynolds numbers than a 50% full pipe. An equivalent Reynolds number (Re_{EQ}) has been used to allow a direct comparison between full pipe flow and partially-filled pipe flow. Re_{EQ} is defined using the equivalent diameter as the length scale (D_{EQ}), which is the diameter a full pipe would have to be to have the same flow cross-sectional area as a partially-filled pipe. It was found that by using this definition all critical Re_{EQ} values collapse close to the full pipe case. Turbulent structures within the transitional flow regime have also been captured at each flow depth for a range of transitional Reynolds numbers.

**1.16 On Entrainment and Mixing Characteristics of Round
Variable-Density Jets [Retracted]**

1.17 Confinement effects for 3D advection-diffusion boundary layers in U-shape and V-shape channel flowsJULIEN R. LANDEL¹, MERLIN A. ETZOLD² & STUART B. DALZIEL²¹School of Mathematics, University of Manchester²Department of Applied Mathematics and Theoretical Physics,
University of Cambridge

This problem is motivated by the advective transport of diffusive passive scalars in narrow channels with U-shape or V-shape walls. One application is the decontamination of confined spaces such as gaps, cracks and folds. When hazardous liquids are spilled over material surfaces, such as building surfaces, grounds or equipment, a portion can be driven into the sub-surface features by gravity, capillary forces or the initial momentum at impact. In this study, we present modelling results showing the impact of geometrical confinement for the decontamination of a drop lodged inside U-shape or V-shape channels. We model the mass transfer at the interface of the drop and the decontaminant flow using advective-diffusive boundary layer techniques. The effect of advection on the mass transfer is characterised by a Sherwood number, Sh , which depends on the Péclet number, Pe , rescaled with the aspect ratio of the drop dimensions. Solving the full three-dimensional problem numerically, we show that the contributions of the cross-channel fluctuation flux on the Sherwood number are generally small. Thus, we solve the simplified cross-channel averaged advection-diffusion equation using boundary layer analysis and similarity solutions for some of the asymptotic regimes, as well as using two-dimensional numerical simulations. Depending on the ratio of the boundary layer thickness and the channel width, we find different regimes: $Sh \sim Pe^{\frac{1}{2}}$ for thick boundary layers in U-shape channels, and $Sh \sim Pe^{\frac{1}{3}}$ for thin boundary layers in both U-shape and V-shape channels. For thick boundary layers in V-shape channels, we find a more complex dependence of the Sherwood number with the Péclet number, which also depends on the channel opening angle. For both geometries, vertical confinement imposes $Sh \sim Pe$, as can be shown by simple scaling arguments. Our asymptotic predictions are in good agreement with the numerical simulations. We discuss implications of our results for practical decontamination purposes.

1.18 Extending Generalised Taylor Dispersion theory for the population-level model of a suspension of micro-swimmers

LLOYD FUNG[†] & YONGYUN HWANG

Imperial College London

A suspension of motile micro-swimmers can generate flow pattern with a length scale orders of magnitude higher than the swimmer's size due to the coupling of their negative buoyancy and different kinds of taxes (e. g., gyrotaxis, phototaxis, chemotaxis). While the detailed mechanism on how the swimmer 'swims' and perform taxes can be resolved in the Stokesian environment, the resulting fluid pattern (e. g., Bioconvection) usually exists in higher Reynolds number regimes and is often non-linear.

To fully resolve the non-linear phenomenon across scales with a large number of swimmers, a coarse-grained approach is necessary to simplify the description of the suspension into a population-level advection-diffusion-typed equation for the swimmer's density in the fluid. The Generalised Taylor Dispersion theory first developed by Brenner (1980, *PhysicoChemical Hydro.* 1:91-123) was shown to be a good and accurate model (Croze *et. al.*, 2017, *J. Fluid Mech.* 816:481-506) for gyrotactic swimmers, but the model is restrictive in applicability. In particular, the theory is only strictly valid when the local velocity gradient tensor has only imaginary eigenvalues, i.e. the flow is not strain-dominant (Bearon *et. al.*, 2011, *J. Fluid Mech.* 680:602-635).

This talk will be about extending the generalised Taylor's dispersion theory to overcome the current limitation. In particular, I will focus on the development of a novel description for diffusivity in flowing suspensions of gyrotactic microorganisms. The development of a mathematically rigorous model of diffusivity is a key step toward accurate modelling of swimmer population in more generalised non-linear flow environments.

1.19 A customized immersed boundary method for turbulent flows with moving objects: application to vertical axis tidal turbinesATHANASIOS E. GIANNENAS[†] & SYLVAIN LAIZET

Department of Aeronautics, Imperial College London

Performing high-fidelity simulations of multiple moving objects in a fluid remains a major challenge due to the great computational cost associated with the reconstruction of a body-fitted mesh to map the moving objects. Immersed Boundary Methods (IBMs) provide an appealing alternative as the boundary interface of the object is represented on a fixed and structured Eulerian mesh by imposing no-slip or Neumann boundary conditions via an additional forcing term in the Navier-Stokes equations.

A new Alternating Direction Forcing IBM (ADF-IBM) for multiple moving objects is presented. The appropriate boundary condition at the fluid/object interface and a continuous velocity field are ensured by reconstructing an artificial velocity inside the object via one-dimensional cubic spline interpolations. By removing the velocity discontinuities which exist in sharp interface IBMs, spurious numerical errors can be reduced by an order of magnitude.

The proposed ADF-IBM is implemented in the high-order flow solver `Incompact3d` which is based on a Cartesian mesh and implicit finite-difference schemes. It is compatible with a 2D domain decomposition approach, allowing simulations on supercomputers with a large number of mesh-nodes. For validation purposes, simulations of the flow around a moving cylinder at $Re = 40$ are performed and compared with a reference solution obtained with spectral methods. An excellent agreement is found, with a significant reduction in the L_2 velocity norm by comparison to the conventional IBM with no reconstruction (i.e. with a discontinuity on the velocity field).

To demonstrate the capabilities of the ADF-IBM, scale-resolving simulations of vertical axis tidal turbines (VATTs) are performed for a wide range of chord-based Reynolds numbers ($Re_c = 100$ to $Re_c = 73,600$). Hydrodynamic and power coefficients are compared with results obtained with body-fitted and diffusive interface IBMs. The focus of this study is on the blade-vortex interaction phenomenon and the effect of the tip-speed ratio on the dynamic stall.

1.20 An adaptive lattice Boltzmann solver with complex sub-grid scale turbulence models

CHRISTOS GKOUDESNES[†] & RALF DEITERDING

School of Engineering, University of Southampton

The standard discretisation of the Lattice Boltzmann Method (LBM) based on finite differences imposes the use of Cartesian grids. This restriction leads inevitably to expensive simulations for complex geometries and high Reynolds number flows. A solution to this problem is the use of Adaptive Mesh Refinement (AMR) techniques. To this course, an LBM solver has been integrated into the in-house AMROC (AMR in Object-oriented C++) framework [1] that provides the capability of a block-structured AMR method. The collision term is modelled based on a single relaxation time, while the *D3Q19* model is used for the discretisation of the phase space. Moreover, a variety of Large Eddy Simulation (LES) models have been incorporated, namely the constant Smagorinsky and recently the dynamic Smagorinsky and WALE models. The application of the LES models is achieved through an effective relaxation time estimated locally per cell. To further improve the performance, a wall model has been currently implemented. A campaign of test cases has been launched for the verification of the new components. Initially, forced and decaying homogeneous isotropic turbulence in a periodic box have been simulated and a comparison between direct numerical simulation and the available LES models has been carried out. A model spectrum has been employed as a benchmark. Furthermore, the test case of a 3D bi-periodic channel flow was chosen to verify the implementation of the wall function and its integration with the LES models and the AMR algorithm. Finally, a square cylinder will be simulated to validate the solver against external flows with wakes behind obstacles, a typical situation for engineering applications.

References:

1. Deiterding, R. Block-Structured Adaptive Mesh Refinement - Theory, Implementation and Application. *ESAIM: Proc.* **34**, pp. 97–150, (2011).

1.21 Active vs. passive bundling of prokaryotic flagella

ALEXANDER CHAMOLLY[†] & ERIC LAUGA

Department of Applied Mathematics and Theoretical Physics,
University of Cambridge

A lot of recent research activity has addressed the swimming dynamics of single prokaryotic cells, in particular flagellated bacteria. These cells propel through viscous fluid by rotating helical flagellar filaments. In particular, *peritrichous* bacteria, such as the oft-studied *E. coli*, have multiple flagella distributed essentially randomly on the surface of the cell body. During forward locomotion, their flagellar filaments form a helical bundle located in the cell's wake where all filaments rotate in synchrony. The exact dynamics of the bundle formation are complex, and most hitherto proposed models aiming for a detailed and complete description have involved an interplay between a number of physical effects including long-range hydrodynamic interactions, elastic restoring forces and short-range steric interactions while respecting the overall force and torque balance between flagella and the cell body. In this study we aim to understand what fundamental physical mechanism triggers bundle formation in the first place. We distinguish between active bundling, induced by hydrodynamic interaction of the flexible flagella with each other (as studied in [1],[2]), and *passive* bundling, triggered by advection of fluid around a moving cell body (as studied in [3]). We propose a minimal analytical model that involves only the essential hydrodynamics of flagellar propulsion and show that it is able to predict the formation of bundling, as well as the relative strength of both effects.

References:

1. Kim, M, Bird, J.C, Van Parys, A.J, Breuer, K.S, Powers, T.R, *A macroscopic scale model of bacterial flagellar bundling*, PNAS, 100(26), 15481-15485, 2003
2. Man, Y, Page, W, Poole, R, Lauga, E, *Bundling of elastic filaments induced by hydrodynamic interactions*, Physical Review Fluids, 2, 123101, 2017
3. Riley, E.E, Das, D, Lauga, E, *Swimming of peritrichous bacteria is enabled by an elastohydrodynamic instability*, Scientific Reports, 8, 10728, 2018

1.22 Relative importance of dispersive and Reynolds stresses in turbulent channel flow over irregular Gaussian roughness

THOMAS O. JELLY^{1,2} & ANGELA BUSSE¹

¹School of Engineering, University of Glasgow

²Department of Mechanical Engineering, University of Melbourne

Practical fluid mechanics problems often involve turbulent flow past irregular rough surfaces. Examples include the flow past eroded turbine vanes and bio-fouled ship hulls, as well as naturally-occurring rough-wall flows such as rivers and streams. Surface roughness affects near-wall turbulence as the viscous length scale of the flow and the characteristic roughness height become commensurate. As a result, if the physical height of the roughness topography is held fixed, then stronger roughness effects tend to occur at higher Reynolds numbers.

In this study, direct numerical simulations (DNS) of fully-developed turbulent channel flow with irregular rough walls have been performed at four separate friction Reynolds numbers, yielding data in both the transitionally- and fully-rough regime. The same roughness topography, which was synthesised with an irregular near-Gaussian height distribution, is used in each simulation. Particular attention is directed towards the wall-normal variation of flow statistics in the near-roughness region and the fluid-occupied region beneath the crests – a region where experimental data can be very challenging to obtain.

The principal aim of this study is to understand how the relative importance of “form-induced” and “turbulence-induced” stresses vary as a function of the friction Reynolds number. To this end, the instantaneous DNS data was double-averaged (DA) – by applying time-then-space averaging in the fluid-occupied region – in order to recover the components of the dispersive and Reynolds stress tensors. By analysing the DA stresses, we quantify the relative magnitude of “form-induced” dispersive stresses and Reynolds stresses (and their spatial gradients). The results indicate that significant levels of dispersive stress are confined to the region below the roughness crests, i.e. within the roughness canopy itself. In addition, we explore the possibility of predicting the levels of streamwise dispersive stress using a phenomenologically-inspired closure model originally proposed in the context of turbulent flow past idealised vegetation canopies.

1.23 Defending against lava flows

EDWARD HINTON¹, ANDREW HOGG² & HERBERT HUPPERT³

¹BP Institute, University of Cambridge

²School of Mathematics, University of Bristol

³Department of Applied Mathematics and Theoretical Geophysics,
University of Cambridge

Attempts to divert lava flows away from buildings by constructing earthen barriers have had limited success. Motivated by this problem, we study the gravitationally-driven flow of viscous fluid as it migrates down a slope and interacts with a topographical mound. Lubrication theory is used to derive the governing equation for the thickness of the steady flow that develops at late times. We investigate the steady flow through numerical integration of the governing equation and asymptotic analysis. In the simplest case of an axisymmetric mound, the problem is controlled by the angle of inclination of the slope and three length scales: two describing the mound and the third is the thickness of the flow far upstream of the mound. In the regime of oncoming flow that is shallow relative to the extent of the mound, the flow surmounts smaller mounds but for larger mounds there is a dry zone, in which there is no fluid, enclosing the top of the mound. We identify a dimensionless parameter, M , which quantifies the ratio of the typical gradient of the mound to the angle of the inclined plane to the horizontal. The onset of dry zones corresponds to M exceeding a critical value that is a function of the axisymmetric shape. We determine this critical value and study the ponding of fluid that occurs upstream of the mound when it is exceeded. In particular, we find how far up the mound fluid flows and establish an upper limit on the stress that is exerted on the mound.

1.24 Capillary adhesion on rough surfaces: When is splitting droplets beneficial?MATTHEW BUTLER[†] & DOMINIC VELLA

Mathematical Institute, University of Oxford

A fluid droplet can adhere two solids together by the action of surface tension at its free surface: a tension-like force acting at the three-phase contact line and a suction pressure force acting over the droplet footprint area can both act to pull the solids together. It is believed that these capillary forces can (at least partially) explain how insects are able to adhere strongly to a wide variety of substrates, and there is evidence that a large number of small droplets may be present under insect footpads. Motivated by this, one may ask: given a fixed volume of fluid, is it better to have many small droplets or just one large droplet? Previous attempts to address this question have considered two flat, rigid, parallel plates; in this case, splitting the fluid into many droplets was found to give at best only a mild improvement in the adhesion force. We consider the additional effect of surface roughness, and how this could affect the enhancement of adhesion by splitting droplets. We show that droplets on the scale of the substrate roughness can exploit the local geometry in such a way as to increase the capillary force exerted on the solids; in this scenario splitting droplets can result in significantly enhanced adhesion over the comparative case of a single droplet sandwiched between smooth, flat plates. We also discuss the shear force that results from roughness.

1.25 Modelling bubble propagation in elasto-rigid Hele-Shaw channelsJOÃO V. FONTANA[†], ANNE JUEL & ANDREW L. HAZEL

University of Manchester

We study a model of pulmonary airway reopening where air is driven at constant volume flux into a liquid-filled Hele-Shaw channel, with an upper compliant boundary. An equivalent rigid channel supports a stable, steadily propagating air finger and a variety of unstable solutions. In the compliant channel, however, initial collapse of the channel introduces additional cross-sectional depth gradients. The induced normal and transverse depth variations alter the finger morphology and promote a variety of instabilities from tip-splitting to small-scale fingering on the curved front. In an experimental study, Ducloué et al. (2017) [1] showed stable and unstable modes of propagation for different initial levels of collapse of the compliant boundary. We simulate numerically a depth-averaged model for the system using the open-source, finite-element library, oomph-lib, in order to explore underlying mechanisms and the relative importance of the elastic, capillary and viscous effects. The model exhibits a complex solution structure and qualitatively similar instabilities to those observed experimentally in [1]. The solution structure is related to that found in a rigid Hele-Shaw channel but here the solution branches interact due to the fluid-structure interaction introduced by the compliant boundary. Using the flow rate, the capillary number and the initial level of collapse as control parameters we achieved excellent quantitative agreement with experiments 1 for the bubble pressure, finger width and morphology. We also performed time-dependent simulations and the stability analysis of our steady solutions.

References:

1. L. Ducloué, A. L. Hazel, A. B. Thompson and A. Juel, *J. Fluid Mech.* **819**, 121-146, 2017

1.26 Scale-resolving simulations of three-dimensional gravity currents beyond the Boussinesq limit

PAUL BARTHOLOMEW & SYLVAIN LAIZET

Department of Aeronautics, Imperial College London

Gravity currents are flows driven by the horizontal pressure gradient arising from different density fluids in a gravity field. They are frequently found in nature for example at river deltas sediment or salinity may drive gravity currents and are often destructive with avalanches and pyroclastic flows being examples. A better understanding of the physics of gravity currents is therefore vital to be able to predict and assess their risk.

The Boussinesq approximation is often employed to simulate gravity currents. This allows an existing incompressible flow solver to be readily used by incorporation of a concentration field giving the buoyancy term, however it is inherently limiting in the density differences that may be studied – typically on the order of less than 1%. In addition, simulations are frequently two-dimensional – seemingly a reasonable assumption based on the predominantly two-dimensional nature of the flow.

In this talk we will present our results from studying gravity currents beyond the Boussinesq limit using the open-source high-order CFD framework `Xcompact3d`. This builds upon previous work to implement a variable density solver for the Low Mach Number approximation and enables the simulation of density ratios for which the Boussinesq approximation no longer applies. Simulations in two- and three-dimensions show that over longer times the two-dimensional results under predict the distance travelled by the gravity current. We also find an inverse effect of density ratio with the difference between two- and three-dimensional results being most pronounced for simulations in or near the Boussinesq limit.

1.27 Analysis of the Boundary Layer Vortex Sheet for Surging and Rotating Bodies of Finite Thickness

P. GEHLERT[†] & H. BABINSKY

Department of Engineering, University of Cambridge

Creating low order models to predict unsteady low Reynolds number aerodynamic forces hinges on predicting the shed vorticity correctly. In the case of large separations leading and trailing edge vortices form which dominate the force response and therefore, need to be captured accurately. Modeling the respective unsteady flow fields hence necessitates the correct prediction of the position of separation as well as the corresponding strength of shed vorticity. This is investigated on various translating and rotating bodies with 2D planar particle image velocimetry (PIV) of the complete flow field. The boundary layer is interrogated to understand the physics involved in the creation of boundary layer vorticity. This found that prior to separation, the experimentally recovered flux of the boundary layer vortex sheet matches well to that predicted by potential flow theory. This result is a definitive indication, that by using the correct methodology, it is possible to accurately capture key features of the boundary layer even when this is under resolved. This can occur when the experiment requires large portions of the flow field to be captured. Further analysis of the boundary layer vortex sheet flux at the point of separation led to accurate estimations of the strength of shed vorticity. The impact of this is that the strength of the shed circulation can be determined by acquiring flow field data of the boundary layer at the point of separation, together with the body kinematics. Measurements of the remaining flow field are not required. This is a significant step towards the development of low order models. Further to this, the techniques developed here can be used to remove any errors associated with three-dimensional flow in 2D planar PIV set-ups when trying to compute the amount of shed vorticity or problems with vorticity leaving the field of view.

1.28 A novel CFD Methodology for Prediction of Direct Laser Metal Deposition

ALESSIO BASSO

Numerical Modelling and Optimisation, Integrity Management
Group, TWI Ltd, Middlesbrough

Direct energy deposition (or laser metal deposition – LMD) is an open-architecture metal additive manufacturing technique that enables high precision, thin-wall components to be produced. The main advantages of LMD are the use of a relatively low-power heat source as well as better process control and tolerance monitoring due to the accurate delivery of metal powder and precise control of the processing head. Understanding of the multiple physical phenomena involved in LMD, e.g. particle turbulent flow interaction, thermal interaction between metal particles and laser heat source, particle melting and thermal interaction between particles and between particles and molten pool on the work surface, is of paramount importance to predict the solidification front and material microstructure of the component being manufactured.

In the present work, a coaxial-nozzle configuration for the jet of metal particles is taken in consideration at different laser power inputs, particle jet velocities and operating conditions. A commercial package software for CFD simulation (ANSYS Fluent v19.2) is used to build the numerical model, which includes: a) the Discrete Particle Model (DPM) – to track the trajectory of solid metal particles ejected from the nozzle; b) the Solidification/Melting Model to predict the thermal interaction between solid particles, turbulent flow and laser heat source; c) the Volume of Fluid (VOF) Model to track solid particle shapes while melting and impinging on the molten pool formed on the bottom working surface.

The numerical CFD model proposed in this work is validated against experimental measurements from previous work and current literature, in an attempt to accurately calibrate numerical parameters and conditions from real LMD processes.

1.29 Flow Regimes of Stratified Particle-Laden Plumes [Poster]JONATHAN BARNARD[†]Department of Chemical Engineering and Biotechnology,
University of Cambridge

The dynamics of stratified particle-laden forced plumes were investigated by injecting fresh water laden with ballotini particles into an environment with a linear density gradient. The plume dynamics were observed under varying source particle loading, characterised by the ratio of particle and interstitial fluid buoyancy flux, ω ; and ambient stratification strength, characterised by buoyancy frequency, N . Upon release into the tank, the plume rises to a maximum height as predicted by single-phase plume theory, before collapsing and spreading as a particle-laden intrusion at the height of neutral buoyancy. The particles within the intrusion settle into the environment and due to plume entrainment, are dragged towards the plume creating a sedimenting veil. A portion of the particles within this veil are subsequently re-entrained into the plume which significantly influences plume dynamics. For all plumes where $\omega > 0$, the maximum height can be seen to decrease until a steady state height is achieved. This maximum height disappears below the intrusion for $\omega > 0.2$ and minor convection is seen in the sedimenting veil. When $\omega > 0.3$, a regime change is observed as the interstitial plume fluid and particles separate at the maximum plume height. The separated fluid continues to rise until reaching a new neutral buoyancy height and below, a particle-rich fountain appears. Without the presence of interstitial fluid, the particles no longer spread radially in the environment, but instead settle at the plume margins inducing significant convection in the environment. At even greater particle loadings ($\omega > 0.5$), a portion of plume fluid is dragged into the ambient convection cylinder and upon depositing the heavy particles, the buoyant fluid rises and spreads as a secondary intrusion between the initial spreading height and the tank floor. Such behaviour is similar to what is observed in nature when considering the development of pyroclastic flows and co-ignimbrite plumes.

1.30 Drag Reduction and Net-Energy Saving in a Turbulent Boundary Layer Using Bayesian Optimisation and Wall Blowing

O. A. MAHFOZE^{†1}, A. MOODY², A. WYNN¹, R. D. WHALLEY² &
S. LAIZET¹

¹Department of Aeronautics, Imperial College London

²School of Engineering, Newcastle University

Skin-friction drag reduction is a topic of great interest due to its importance in many engineering applications. Yet despite many decades of extensive research, a practical and affordable method for reducing the turbulent skin-friction drag force in air flows is yet to be found and implemented in real-world applications. It is well known that low-amplitude wall-normal blowing applied at the wall of a turbulent boundary layer (TBL) can significantly reduce the skin-friction drag. However, the power consumption of wall-normal blowing devices can be very high, resulting in energy losses for the system. In the present study, a Bayesian optimisation framework is combined with scale-resolving simulations of a TBL to obtain the optimal parameters of a wall-normal blowing strategy in order to achieve not only skin-friction drag reduction but more importantly net-energy saving for the system. Numerically, the wall-normal blowing is modelled as a boundary condition so the net-energy saving is estimated using experimental data from two different blowing devices. In a previous study for moderate Reynolds numbers, we found that it was possible to generate up to 5th order optimisation, but also that it was possible to reduce the skin-friction by up to 75% with substantial energy losses. In the present study, our Bayesian Optimisation framework is used for higher Reynolds numbers TBL using an Implicit Large Eddy Simulation approach. The simulations are performed with the high-order flow solver `Incompact3d` which is based sixth-order finite-difference schemes on a Cartesian mesh, a semi-implicit scheme for time advancement, a spectral solver for the Poisson equation and a 2D Domain Decomposition for supercomputer use. To better understand the flow, the different drag reduction mechanisms are investigated using the well-known Fukagata-Iwamoto-Kasagi (FIK) identity.

1.31 LES-based investigation of the angle of attack-dependence of flow past a cactus-shaped cylinder with four ribs

OLEKSANDR ZHDANOV[†] & ANGELA BUSSE

School of Engineering, University of Glasgow

In their natural environment, cacti can withstand high winds without being uprooted. Previous studies on cactus-shaped cylinders with many ribs showed a reduction of the mean drag and a decrease in the amplitude of aerodynamic force fluctuations over a range of Reynolds numbers compared to the standard circular cylinder. These investigations were inspired by the Saguaro cactus, a member of *Cactaceae* family originating from the Western Hemisphere, that has typically 10 to 30 ribs. In the Eastern Hemisphere, members of the *Euphorbiaceae* family have independently developed similar shapes but with a lower number of ribs in the process of convergent evolution. From a biomechanical point of view, the features of these two plant families that have evolved in similar environments are expected to have the same functions. Unlike to Saguaro-based cactus-shaped cylinders, the outer shape of succulents with low number of ribs does not resemble a circular cylinder and significant dependence of the aerodynamic forces on the angle of attack is expected.

In this study, the angle of attack dependence of the flow past a cactus-shaped cylinder with four ribs, inspired by the succulent *Euphorbia Abyssinica*, is investigated numerically at a biologically relevant Reynolds number ($Re = 20,000$). Large eddy simulations (LES) using the wall-adapting local eddy-viscosity (WALE) subgrid-scale model were performed for several angular orientations with respect to the freestream using OpenFOAM. As expected, the mean and fluctuating drag and lift coefficients show a strong variation with angle of attack.

Due to their similar overall shape, the results from the present LES are compared to experimental and numerical results for the square cylinder and square cylinders with rounded corners. In addition, the values of the aerodynamic coefficients and Strouhal number are compared to previous results of URANS simulations for the same shape and Reynolds number.

1.32 The late-time evolution of an isolated symmetrically unstable front [Poster]

AARON WIENKERS[†] & JOHN R. TAYLOR
DAMTP, University of Cambridge

Submesoscale fronts with large lateral buoyancy gradients and $O(1)$ Rossby numbers are common in the upper ocean. These fronts are associated with large vertical transport and are hotspots for biological activity. Submesoscale fronts are susceptible to symmetric instability (SI) – a form of stratified inertial instability which can occur when the potential vorticity is of the opposite sign to the Coriolis parameter. SI has linear eigenmodes which are capable of transporting buoyancy and geostrophic momentum. The unstable SI modes eventually break down through a secondary shear instability, leading to three-dimensional turbulence which further modifies the geostrophic momentum. An initially balanced front that is unstable to SI will evolve due to the momentum and buoyancy transport associated with SI and 3D turbulence.

Here, we consider an idealised problem with a front of finite width bounded by flat no-stress horizontal surfaces. The front is initially in thermal wind balance but there is no initial vertical stratification and the flow is unstable to SI. We study the evolution of the unstable front using a linear stability analysis and nonlinear numerical simulations. We find that the aspect ratio of the front and the ratio of the maximum horizontal buoyancy gradient to the Coriolis frequency are important parameters and influence the evolution of the front. Interesting behaviour emerges, particularly for fronts with large Rossby numbers. For example, fronts with relatively large horizontal density gradients develop bore-like gravity currents that propagate along the top and bottom boundaries. We then describe the energetics evolving towards the final adjusted state in terms of the dimensionless parameters of the system and understand these results in the context of the primary and secondary linear instability.

1.33 A Lattice Boltzmann Method in Generalized Curvilinear Coordinates

J. A. REYES BARRAZA & R. DEITERDING

University of Southampton

The Lattice Boltzmann method (LBM) is a rather new development in CFD. Instead of approximating the Navier-Stokes equations, the approach is based on solving a simplified version of the Boltzmann equation in a specific discrete space. It can be shown via the Chapman-Enskog expansion that the LBM recovers the Navier-Stokes equations (Chen and Doolen, 1998). The simplicity of the lattice Boltzmann algorithm can lead to dramatic reductions in computational time compared to traditional CFD solvers. On uniform grids and unsteady flow simulations, it can easily show performance gains up to two orders of magnitude (Deiterding and Wood, 2016), which has made the approach increasingly popular in recent years.

In the LBM, the discretisation of the physical space is coupled with the discretisation of momentum space (He and Luo, 1997). The advantage of this scheme is the exact treatment of the advection term, so it leads to zero numerical diffusion. On the other hand, this condition results in a method that uses only Cartesian grids. This aspect of the standard LBM limits its application, and solving problems with curved geometries becomes troublesome. Nonetheless, it is possible to implement standard numerical techniques on the LBM to use non-uniform meshes. Therefore, we propose an implementation of the LBM in generalized curvilinear coordinates, so the lattice Boltzmann equation (LBE) can be solved with non-uniform grids.

A second-order explicit method was implemented to solve the LBE in the computational domain, and several test cases were used for verification, including the 2D circular cylinder to show the capacity of the present method to perform simulations with curved-wall boundaries. The results of our method are consistent with the literature, and also show that our method has better treatment to curved walls than the standard Cartesian LBM confirming the capabilities of the proposed scheme.

References:

1. Shiyi Chen and Gary D. Doolen. Lattice Boltzmann method for fluid flows. *Annual Review of Fluid Mechanics*, 30:329–364, 1998.
2. Ralf Deiterding and Stephen L. Wood. Predictive wind turbine simulation with an adaptive lattice Boltzmann method for moving boundaries. *Journal of Physics: Conference Series*, 753, 2016.
3. Xiaoyi He and Li-Shi Luo. Theory of the lattice Boltzmann method: From the Boltzmann equation to the lattice Boltzmann equation. *Physical Review E*, 56:6811–6817, 1997.

1.34 Shear-thinning fluids can be slippery! Non-identifiability of parameters for the Bird-Cross-Carreau-Yasuda family of models when applied to blood rheology

DAVID J. SMITH¹, MEURIG T. GALLAGHER¹, RICHARD
A. J. WAIN^{1,2}, SONIA DARI¹ & JUSTIN P. WHITTY²

¹University of Birmingham

²University of Central Lancashire

Models of shear-thinning complex fluids, dating from the work of Bird, Carreau, Cross and Yasuda, have been applied in many important computational studies of blood flow for several decades. We will revisit these models, first to highlight a degree of uncertainty in the naming conventions in the literature, but more importantly to address the problem of inferring model parameters by fitting to rheology experiments. By refitting published data, and also by simulation, we find large, flat regions in the likelihood surfaces that yield families of parameter sets which fit the data equally well. Despite having almost indistinguishable fits to experimental data these varying parameter sets can predict very different flow profiles, and as such these parameters cannot be used to draw conclusions about physical properties of the fluids, such as zero-shear viscosity or relaxation time of the fluid, or indeed flow behaviours. We verify that these features are not a consequence of the experimental data sets through simulations; by sampling points from the rheological models and adding a small amount of noise we create a synthetic data set which reveals that the problem of parameter identifiability is intrinsic to these models. These issues can result in major predictive errors for even quite simple problems such as pressure-driven pipe flow, especially when the flow velocity is small.

1.35 Asymptotic dynamics of high dynamic range stratified turbulence

G. D. PORTWOOD^{1,2}, S. M. DE BRUYN KOPS² &
C. P. CAULFIELD^{3,4}

¹Los Alamos National Laboratory

²Department of Mechanical and Industrial Engineering, University of
Massachusetts

³BP Institute & DAMTP, University of Cambridge

Direct numerical simulations of homogeneous sheared and stably stratified turbulence are considered to probe the asymptotic high-dynamic range regime. We consider statistically stationary configurations of the flow that span three decades in dynamic range defined by the separation between the Ozmidov length scale, $L_O = \sqrt{\epsilon/N^3}$, and the Kolmogorov length scale, $L_K = (\nu^3/\epsilon)^{1/4}$, up to $\text{Gn} \equiv (L_O/L_K)^{4/3} = \epsilon/(\nu N^2) \sim O(1000)$, where ϵ is the mean turbulent kinetic energy dissipation rate, ν is the kinematic viscosity, and N is the buoyancy frequency. We isolate the effects of Gn , particularly on irreversible mixing, from the effects of other flow parameters of stratified and sheared turbulence, by allowing the forced flow to adjust towards stationarity. Specifically, we evaluate the influence of dynamic range independent of initial conditions, finding that for a wide variety of simulations with $36 \leq \text{Gn} \leq 900$, the flow always evolves such that $Ri \equiv N^2/S^2 \simeq 0.16$, and $F_r \equiv \epsilon/(NE_k) \simeq 0.5$, where S is the (imposed) shear, and E_k is the turbulent kinetic energy. We present evidence that the flow approaches an asymptotic state for $\text{Gn} \gtrsim 300$, characterized both by an asymptotic partitioning between the potential and kinetic energies and by the approach of components of the dissipation rate to their expected values under the assumption of isotropy. As Gn increases above 100, there is a slight decrease in the turbulent flux coefficient $\Gamma = \chi/\epsilon$, where χ is the dissipation rate of buoyancy variance. However, for this flow, there is no evidence of the commonly suggested $\Gamma \propto \text{Gn}^{-1/2}$ (dashed line) dependence when $100 \leq \text{Gn} \leq 1000$. Indeed, Γ remains very close to the upper bound $\Gamma \lesssim 0.2$ proposed in the classic Osborn (1980) parameterization, while the turbulent Prandtl number $Pr_T \equiv \kappa_M/\kappa_T = (P/S^2)/(B/N^2) \simeq 1$ for all values of Gn , where P is the turbulence production and B is the (vertical) buoyancy flux.

1.36 Numerical simulations of wall cooling performance and associated effects on transition in hypersonic flows with injection from porous surfaces

ADRIANO CERMINARA, RALF DEITERDING & NEIL SANDHAM

Aerodynamics & Flight Mechanics group, University of Southampton

Direct numerical simulations aimed to study the physics of wall cooling in a hypersonic boundary layer in the presence of injection through a porous wall have been performed. Two types of injection have been considered, namely slot injection [1] and injection through a layer of distributed porosity [2]. The simulations have been run using a high-order (up to 6th) method, consisting of a central differencing (CD) scheme, to achieve high resolution in the smooth flow regions, in conjunction with an identical order weighted-essentially-non-oscillatory scheme (WENO), that is locally activated in the sharp flow regions. Moreover an adaptive-mesh-refinement (AMR) technique is used on a Cartesian mesh in order to handle the smaller length scales in the porous region, preserving accuracy. Results show that slot injection is generally inefficient, because it requires very high blowing ratios, i.e. high mass flow rates of coolant injected into the boundary layer per unit time and surface, to achieve a significant cooling effect downstream of the injection point. A cross-validation study with experimental results [3], along with results from linear stability analysis and a parametric study of the sensitivity to different boundary-layer disturbance amplitudes, has demonstrated that the reason for the inefficiency of slot injection is that high perturbations associated to internal instability modes are induced in the boundary layer, even at the low blowing ratios, which results in an increase of the heat flux and ultimately leads to transition at the high disturbance amplitudes. In the case of injection through a porous layer, in contrast, this behaviour appears to be drastically reduced at the very low blowing ratios, which leads to much higher cooling performance, as a result of a more efficient film cooling effect. These results serve to assess the capabilities of transpiration cooling systems, in contrast to the widely used effusion cooling systems, for application on hypersonic vehicles, and to predict the cooling performance in different disturbance environment, with and without transition, which is important for a DNS-assisted design of new-generation thermal protection systems.

References:

1. Cerminara, A., Deiterding, R., and Sandham, N., *DNS of Hypersonic Flow over Porous Surfaces with a Hybrid Method*, AIAA 2018-0600 Paper, AIAA Aerospace Sciences Meeting, AIAA Scitech Forum, Kissimmee (FL), 2018
2. Cerminara, A., Deiterding, R., and Sandham, N., *Transpiration cooling using porous material for hypersonic applications*, Chap-

ter contribution to the book “Convective Heat Transfer in Porous Media”, T&F, in press, pp. 1-35, Nov 2018

3. Hermann, T., Ifti, H. S., McGilvray, M., Doherty, L., and Ger-aets, R. P., *Mixing characteristics in a hypersonic flow around a transpiration cooled flat plate model*, International Conference on High-Speed Vehicle Science and Technology, Moscow, Russia, 2018

1.37 Evaluating turbine wake steering techniques using scale-resolving simulations

GEORGIOS DESKOS, SYLVAIN LAIZET & RAFAEL PALACIOS

Department of Aeronautics, Imperial College London

Wind turbines operating within large-scale wind plants interact with each other through their wakes. A wind turbine operating within the full wake of an upstream turbine can experience mean power output reduction up to 40%. To this end, farm-level optimal control strategies through wake steering (re-direction) are being proposed as a remedy to avoid these adverse wake effects. However, most optimal control tools are based on empirical or semi-empirical models which provide only time-averaged predictions and ignore the unsteady flow features of the wake such as meandering and small scale-turbulence. Here, we present scale-resolving simulations of wake interactions obtained by the high-order finite-difference solver, Winc3D, for two utility-scale turbines operating in line and placed within realistic atmospheric turbulence conditions and at different set-ups (yaw & tilt angle and off-set distance) to study the physics of wake-wake and wake-turbine interactions. To parametrise the two wind turbines, we use a novel unsteady actuator line model enhanced with a closed-loop turbine-level controller. Analysis of a large number of farm-level control options shows that wake steering can be effectively used to maximise their power output while minimising the increase of power fluctuations and turbine loads.

1.38 Negating gust effects by actively pitching a wingIGNACIO ANDREU ANGULO[†]

University of Cambridge

Unsteady fluid mechanics is an essential component of the complex behavior of rotorcraft and flapping wing vehicles. In order to simplify this complex problem, low order models have been developed with the intention of capturing the main flow features. However, these models are often still too complex for implementation in real-time control. The present study analyses the ability of a low order model to simulate the flow around a pitching wing traveling through a gust. The flow and the plate have been modelled using a panel method that includes continuous shedding of point vortices from both edges of the wing, representing the shear layers. Moreover, the forces on the plate were estimated from the vorticity as described by the impulse method, carefully considering circulatory and non-circulatory components. Applying these results, an iterative process was used to adjust the wing inclination in order to maintain a zero lift value as the plate travels through the gust. The resulting pitch profile represents the control mechanism intended for the mitigation of gust effects and has been evaluated experimentally. Using a water tow tank, force and PIV data have been acquired on a plate that is pitched according to the computed profile as it travels through a gust. The comparison between the experimental and computational results demonstrates the ability of a low order model to predict loads for control purposes.

1.39 Nematic Liquid Crystal Flow During the Manufacture of Liquid Crystal Devices

JOSEPH R. L. COUSINS[†], S. K. WILSON & N. J. MOTTRAM

Department of Mathematics and Statistics, University of Strathclyde

Nematic liquid crystal (nematic) devices are ubiquitous in modern day life, and faster and more accurate manufacture of these devices is required to meet increasing global demand. The optimisation of the manufacturing process generally involves attempting to reduce manufacturing time by increasing flow velocities and filling speeds. However, these changes are often implemented without a full understanding of the possible consequences of flow-driven director misalignment and damage caused to the director anchoring within the device. An understanding of the flow of a nematic during manufacturing can therefore potentially improve both manufacturing efficiency and device quality.

In a common method of device manufacturing, nematic is dispensed in droplets onto a substrate and then compressed by a top plate moving downwards with a fixed constant speed, to ensure complete filling of the device. This process of compressing a film of nematic is similar to the classical squeeze film problem in fluid dynamics. We consider a nematic squeeze film in which the nematic is squeezed by the downward motion of the top plate, and the resulting flow velocity, pressure and director angle are investigated in the asymptotic limit of small reduced Reynolds number ($\delta Re \ll 1$), small Leslie angle ($\phi_L \ll 1$) and large Ericksen number ($Er \gg 1$), which represents a thin film of nematic where viscosity effects are strong compared to elasticity effects and there are no inertial effects. The director angle solution is obtained using the method of matched asymptotic expansions and the solution allows key insight into the behaviour of nematic during device manufacturing.

1.40 Jetting Behaviour in the Presence of Surfactants in Inkjet Printing

EVANGELIA ANTONOPOULOU[†], OLIVER G. HARLEN, MARK
A. WALKLEY & NIKIL KAPUR

University of Leeds

A key challenge in developing new applications of inkjet technology is to produce inks that can be jetted to form individual droplets and to transport functional components needed for the application. The development of mathematical models that allow fluid jetting behaviour to be determined as a function of fluid properties would allow optimisation to be carried out in-silico before creating the inks and verifying the performance.

Surfactants are often added to aqueous inks in order to modify the surface tension. However, the rapid expansion of the free surface during the fast jetting process means local areas of the surface will be depleted of surfactants leading to surface tension gradients, the effects of which on ink behaviour in jetting are unknown.

In this work, experimental studies of the jetting behaviour with and without the addition of surfactants are presented. In parallel we are developing a finite element based numerical simulation of inkjet break-up and drop formation in the presence of surfactants.

1.41 Experimental modelling of infectious aerosols from people with cystic fibrosisJESSICA PROCTOR[†]

University of Leeds

Airborne-person to person transmission of pathogens such as *Pseudomonas aeruginosa* and *Mycobacterium abscessus*, is a concern for those with cystic fibrosis (CF). This study aims to examine the aerosolisation of these bacteria generated under controlled conditions from different liquid suspensions, including artificial mucus with comparable properties to that from people with CF. The study is carried out using an ‘aerosol characterisation’ rig enabling sampling at different distances from the source under a constant flow rate. Bacterial strains are nebulised, using a Collison 3 jet nebuliser, down the rig where the aerosol passes through a laser diffractometer (Spraytec, Malvern), before sampling using an Andersen 6-stage impactor sampler. The survival of several strains of *P. aeruginosa* and *M. abscessus*, together with droplet size distributions were measured at distances of 0.5-4 m from the source. Results demonstrate that bacteria were able to survive over 4 m of travel, with the aerosol at this point having droplet sizes similar to that of the individual bacterium.

1.42 Evolution of hydroacoustic waves in deep oceanic waters with generalised sound-speed profiles

S. MICHELE & E. RENZI

Department of Mathematical Sciences, Loughborough University

We present a novel analytical model for the evolution of hydroacoustic waves in weakly compressible fluids characterised by depth variations of the sound-speed. Using a perturbation expansion up to the third order we decompose the initial set of governing equations in a sequence of linearised boundary value problems. Since forcing terms resonate the second order problem, two slow horizontal length scales and two slow time scales are necessary. Then we derive a novel expression for the second-order velocity potential for each normal mode and show that this forced solution does not exist in the case of constant homogeneous fluid layers. At the third order we derive the linear Schrödinger equation governing the evolution of the wave envelope for large length and temporal scales. This equation is similar to the case of dispersive gravity wave packets, hence similar interesting analyses are extended here. We show that the Schrödinger equation obtained in this work, now presents new terms depending on the sound-speed depth distribution. This result clearly contributes to enrich the corresponding dynamics, indeed, we show that for generalised sound-speed profiles the horizontal wavelength of each normal mode can be stretched or compressed with direct consequences on the propagation speed of the wavetrain envelope. Consequently, the analytical model presented here has also an important engineering application, since it allows improving the design of tsunami early warning systems.

1.43 A microfluidic assay to study the migration behaviour of marine bacteria in viscosity gradients

SASI KIRAN PASUPULETI, OSCAR GUADAYOL & STUART HUMPHRIES

Joseph Banks Laboratories, University of Lincoln

Microscale viscosity can strongly influence interaction between marine microbes such as bacteria and phytoplankton, and ultimately impact the ocean biogeochemistry. To investigate the effect of viscosity on the migration behaviour of marine bacteria, we have developed a microfluidic device producing stable viscosity gradients. The device comprises two layers, in the top layer viscosity gradients are generated by diffusive mixing of low and high viscous solutions in a gradient generator. The bottom layer consists an observation chamber in which GFP-expressing bacteria encounter a static viscous gradient, and the migration of bacteria in response to viscous gradient is monitored by microscopy. We applied this microfluidic assay to study the chemotactic behaviour of several types of marine bacteria in the viscosity gradients ranging from 1 – 50 cP.

1.44 Modelling flows in thermochemical nonequilibrium adaptive and mapped meshes

CHAY W. C. ATKINS & RALF DEITERDING

Aerodynamics and Flight Mechanics Group, University of
Southampton

In Computational Fluid Dynamics (CFD) simulations, Automated Mesh Refinement (AMR) can be used to balance the goals of adequate resolution and low simulation time by increasing the resolution only where it is needed. Additionally, close to surfaces, high aspect ratio cells can be used to capture the large gradients in a boundary layer with less cells than a Cartesian grid. In this work, Cartesian AMR methods and stretched, body fitted grids are used to efficiently model high enthalpy flow in thermochemical non-equilibrium. The use of non-equilibrium models is vital to accurately predict the aero-thermal environment experienced by a hypersonic vehicle.

The computational framework AMROC (Adaptive Mesh Refinement in Object-oriented C++), implements the Cartesian SAMR algorithm of Berger and Colella on parallel computers with distributed memory [1]. In previous work [2], a single-temperature TVD-MUSCL scheme for simulating reacting mixtures of thermally perfect gases on highly adaptive meshes had been developed. In the present work, an extended version of that solver has been coupled to the Mutation++ library [3] in order to model flows in thermochemical non-equilibrium. Park's two temperature model is used to model the differences in internal energy and a modified Arrhenius equation is used to account for chemical reactions. In addition to the non-equilibrium model, the ability to use stretched body fitted grids for viscous flow simulations has been incorporated to AMROC.

A number of studies have been carried out using the solver. The solver has been verified using a combination of the Method of Manufactured Solutions, comparisons to analytic results and code-to-code comparisons. The SAMR capabilities have been tested in simulations of inviscid flow over a double wedge. Comparisons between experimental and simulated results of hyper-velocity flow over a sphere demonstrate the importance of the non-equilibrium model for accurately predicting shock standoff distance. A cylinder exposed to high enthalpy, non-equilibrium flow in a shock tunnel is simulated, and good agreement is obtained with experimental results.

References:

1. R. Deiterding, "Block-Structured Adaptive Mesh Refinement-Theory, Implementation and Application," *ESAIM Proceedings*, vol. 34, pp. 97–150, 2011.
2. R. Deiterding, "A parallel adaptive method for simulating shock-induced combustion with detailed chemical kinetics in complex domains," *Computers & Structures*, vol. 87, pp. 769–783, 2009.

3. J. B. Scoggins and T. E. Magin, “Development of Mutation++ : MULTicomponent Thermodynamics And Transport properties for IONized gases library in C++,” in *11th AIAA/ASME Joint Thermophysics and Heat Transfer Conference*, 2014.

1.45 A Fluid Dynamics Model of Kidney Morphogenesis

VLADIMIR ZUBKOV

School of Computing, University of Brighton

Kidney development is initiated by the outgrowth of a ureteric bud of epithelial cells into a population of mesenchymal cells. Interactions between these two populations lead to the formation of the highly branched ureteric tree and the nephrons (basic structural and functional units of the kidney), presumably via the coordination of cell proliferation and morphogenetic responses.

While it is now possible to collect data showing how the structure of kidneys evolves, the biophysical mechanisms responsible for these changes remain to be determined. We present a mathematical model of kidney morphogenesis, in which the development of the kidney is described by a fluid dynamics model. We show that branching of the ureteric tree can be regulated by instability of the growing tip surface: ureteric tree tip cells, that moved further from the smooth tip surface, are subject to higher levels of growth factors and, as a result, have higher rates of proliferation and chemotactic attraction to growth factors which leads to further expansion of the cells from the tip and development of a new branch. The tip branching is stabilised by bending resistance of the tip surface. The balance between stabilising and destabilising mechanisms defines the number of the appearing branches.

1.46 Rivulet Flow Down an Inclined Permeable MembraneA. S. ALSHAIKHI[†], M. GRINFELD & S. K. WILSON

Department of Mathematics and Statistics, University of Strathclyde

We use the lubrication approximation to analyse the steady unidirectional flow of a slender rivulet flowing down an inclined permeable membrane. We assume that the rivulet is thin and that the ratio of the permeability of the membrane to the square of the capillary length is small.

We investigate the effect of the permeability and the inclination of the membrane on the length of the rivulet on the membrane. We assume that the flow in the rivulet is governed by the Navier–Stokes equations, and impose a no-slip condition on the tangential component of the velocity of the fluid at the fluid/membrane interface as well as a condition relating the normal component of the velocity of the fluid at the fluid/membrane interface and the pressure drop across the membrane.

We consider situations with prescribed flux and either fixed width or fixed contact angle. In the case of a rivulet with constant width, we find an exact solution for the shape of the rivulet, while in the case of a rivulet with constant contact angle, we derive and solve numerically a nonlinear ordinary differential equation for the shape of the rivulet. Perhaps our most interesting and unexpected results are the non-monotone dependence of the rivulet length on the inclination angle and the non-existence of rivulets for sufficiently large inclination angles.

1.47 Time-frequency analysis for wakes of accelerating ships

RAVINDRA PETHIYAGODA

Queensland University of Technology

Spectrograms have recently emerged as a useful method of visualising ship wakes from surface height measurements taken from a single location, with potential applications in ship detection and coastal management (coastal erosion). We present a linear dispersion curve that predicts the location of colour intensity in a spectrogram for a ship moving along an arbitrary path with arbitrary speed. We provide examples for two cases: a ship accelerating in a straight line, and a ship travelling in a circle with constant angular velocity. An example of nonuniqueness of the dispersion curve between the two cases is given where the difference in colour intensity due to the shape of the ship can be used as a distinguishing factor. This example sheds some light on potential difficulties for applications involving detection.

1.48 Hele-Shaw flows in doubly connected domains

SCOTT McCUE, LIAM MORROW, MICHAEL JACKSON, MICHAEL
DALLASTON & TIMOTHY MORONEY
Queensland University of Technology

In the commonly studied Hele-Shaw geometry, an essentially inviscid fluid (like air) is injected between two flat plates with viscous fluid (like oil) in between. The resulting Saffman-Taylor instability drives viscous fingering and complex interfacial pattern formation. The standard mathematical model for this scenario involves solving Laplace's equation in the unbounded viscous fluid domain, subject to boundary conditions on the interface that separates the two fluids. In reality, there is always a finite amount of viscous fluid bounded by (at least) two interfaces; however, experiments with inviscid fluid penetrating a viscous fluid are normally conducted so as to minimise the effects of the outer interface. Here we are interested in the case in which the two interfaces are close together, so that the effects of the outer interface can no longer be ignored in the model. We use a variety of mathematical tools (including linear stability analysis and a thin filament model) and the level set method to study this geometry, focussing on the viscous fingering patterns, the possibility of the inner interface bursting through the outer interface, and the effects of other non-standard influences such as rotating plates, lifting plates, or non-parallel plates.

1.49 Coalescence of Droplets with Dissimilar Surface Tension

THOMAS C. SYKES^{†1}, ALFONSO A. CASTREJÓN-PITA², J. RAFAEL
CASTREJÓN-PITA³, MARK C. T. WILSON¹, DAVID HARBOTTLE¹,
ZINEDINE KHATIR¹ & HARVEY M. THOMPSON¹

¹University of Leeds

²University of Oxford

³Queen Mary University of London

Droplet coalescence occurs in a variety of settings, from natural to emerging technologies, such as reactive inkjet printing and lab-on-a-chip microfluidic devices. The internal dynamics during coalescence determine the extent of fluid mixing within the coalesced droplet, with efficient mixing often critical to the application's viability. The fluid properties of the precursor droplets can significantly affect the internal dynamics, especially in the case that each droplet does not consist of the same fluid. Surface tension disparities are especially interesting, since they affect the internal dynamics both through the additional contribution to Laplace pressure and Marangoni flow.

This work investigates the coalescence of a sessile and an impacting droplet of different surface tension, in contact with a solid substrate. Two colour high speed cameras are used to capture the internal dynamics from both the side and below. This arrangement exposes both the detail of the flow through the depth of the droplet (side view), in addition to the intricate flow structures without distortion from the droplet's curved surface (bottom view), allowing surface and internal phenomena to be identified. Our results demonstrate significantly faster mixing compared to droplets with identical fluid properties, uncovering various intriguing internal flow mechanisms. Multiple fluid configurations and lateral separations are studied, with our results having practical implications for enhancing mixing within impacting and coalescing droplets of different surface tension.

1.50 Efficient Implementation of Elastohydrodynamic Integral Operators for Stokesian Filaments

ATTICUS L. HALL-McNAIR¹, MEURIG T. GALLAGHER¹, THOMAS D. MONTENEGRO-JOHNSON¹, HERMES GADÉLHA² & DAVID J. SMITH¹

¹University of Birmingham

²University of Bristol

Models for simulating the dynamics of flexible biological filaments have historically been mathematically complex and numerically expensive, with even simple simulation experiments taking in the order of hours or even days to solve on all but the most powerful computer hardware. This computational cost often stems from numerical stiffness associated with satisfying the inextensibility constraint common to many biological fibres. Recent work by Moreau, Giraldi & Gadéha (2018) demonstrated that a filament could be modelled efficiently by expressing the governing elastohydrodynamic problem via integral equations written in terms of the evolving tangent angle. Combined with a method of lines discretisation, this allows for a reduction in the required degrees of freedom for accurate simulation, alleviating the numerical stiffness of the system and enabling efficient computational modelling. In this presentation, I outline recent submitted work which builds upon the framework introduced by Moreau et al., augmenting and reformatting their formulation with the method of regularised stokeslets of Cortez et al. (2001, 2005). This enables the modelling of non-local hydrodynamics within and between filaments. Importantly, this is done in a numerically efficient manner, enabling fast and accurate simulation of arrays of filaments undergoing non-linear planar deformations. We present the continuous equations outlining the new elastohydrodynamic integral formulation (EIF) method, and the subsequent discretisations of them, before application to single and multiple filament problems in shear flow and sedimenting under gravity. We also consider the dynamics of active moment driven swimmers for two types of driving travelling-wave. From these simulations we reveal how filament interactions can lead to geometric buckling instabilities, and investigate optimal parameter pairings to produce fast swimming in active filaments.

1.51 Determining how the microstructure of the Endothelial Glycocalyx Layer affects its bulk fluid-dynamical properties

T. C. LEE , V. SURESH & R. J. CLARKE

University of Auckland

The Endothelial Glycocalyx Layer (EGL) is a hydrated, thin, brush-like layer that coats the inside of blood vessels. It is thought to serve as a protective barrier against damaging levels of fluid shear stemming from the flow of blood in the vessel lumen, as well as being implicated in a number of other biological functions, such as mechanotransduction and the immune response. The EGL is a fragile structure, and the difficulty in examining it in-vivo has motivated the development of theoretical models that can predict its elastohydrodynamics. In these previous studies the EGL has been modelled as an isotropic, homogeneous poroelastic layer. However, there is an increasing volume of experimental evidence to suggest that the EGL has a microstructural organisation that brings into question this assumption. This study uses Homogenisation Theory on an asymptotically-thin two-dimensional embedded surface, to analyse the extent to which organisational structure on the microscale can lead to observables on the macroscopic scale. It is hoped that this study might enable a means of inferring microstructural EGL organisation from bulk macroscopic measurements.

1.52 Effect of vapour pressure on the performance of a Leidenfrost engine

PRASHANT AGRAWAL¹, GARY G. WELLS¹, RODRIGO LEDESMA-AGUILAR¹, GLEN MCHALE¹, ANTHONY BUCHOUX², KHELLIL SEFIANE², ADAM STOKES², ANTHONY J. WALTON² & JONATHAN G. TERRY²

¹Northumbria University at Newcastle upon Tyne

²University of Edinburgh

In the Leidenfrost effect, as a result of thin film boiling, a vapour layer forms between a droplet and a surface heated to temperatures significantly higher than the liquid's boiling point. The vapour layer significantly reduces friction on the droplet, and acts as a thermal insulator increasing the droplet's lifetime. Due to this reduced friction droplets can self-propel (translate [1] or rotate [2]) on asymmetrically textured surfaces. The asymmetry rectifies the escaping vapour, producing a viscous drag on the levitating droplet. We have previously shown that on turbine-like substrates, these rotating droplets can transfer torque to additional surface tension coupled non-volatile solids [3], establishing the concept of a Leidenfrost heat engine. In this Leidenfrost engine, the power output depends on the vapour layer thickness, through the torque and angular speed of the levitating rotors. In this work, we demonstrate the ability to operate a Leidenfrost engine continuously and control its output power by mechanically altering the vapour layer thickness. This is done by replenishing the liquid and supporting the rotor weight using a bearing assembly. We observe a significant increase in the power output despite the added friction from the bearing. The design and operational principles described can be extrapolated to alternative liquid and solids to develop mm and sub-mm scale engines for applications in extreme environments with naturally occurring low pressures and high temperature differences.

We would like to acknowledge EPSRC for funding (EP/P005896/1 and EP/P005705/1).

References:

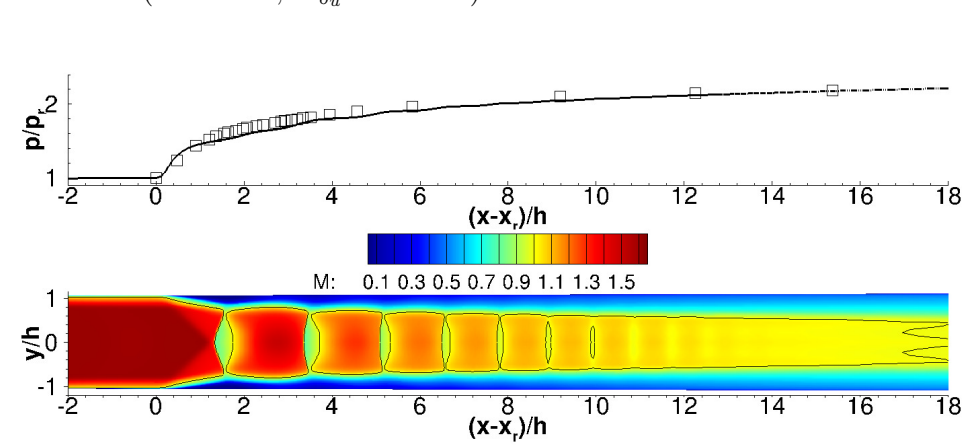
1. Lagubeau G., Le-Merrer M., Clanet C., Quéré D. 'Leidenfrost on a ratchet' *Nature Physics*, 2011, 7, 395–398.
2. Wells G., Ledesma-Aguilar R., McHale G., Sefiane K.A 'A Sublimation Heat Engine' *Nature Communications*, **2015**, 6, 6390.
3. Agrawal P., Wells G.G., Ledesma-Aguilar R., McHale G., Buchoux A., Stokes A., Sefiane K.A. 'Leidenfrost heat engine: Sustained rotation of levitating rotors on turbine-inspired substrates' *Applied Energy*, 2019,240,399-408.

1.53 Flow physics and sensitivity to RANS modelling assumptions of a multiple normal shock wave boundary layer interactionsKIRIL BOYCHEV[†], G. N. BARAKOS & R. STEIJL

CFD Laboratory, School of Engineering, University of Glasgow

The interaction of a shock wave with a boundary layer (SWBLI) occurs in many applications such as supersonic wind tunnel diffusers, and supersonic intakes. In the present work, Reynolds Averaged Navier Stokes (RANS), detached Eddy (DES), and scale-adaptive (SAS) simulations are used with the HMB3 CFD solver of Glasgow University to investigate the flow physics, and the sensitivity to modelling assumptions of multiple shock wave/boundary layer interactions (MSWBLI) inside a rectangular duct ($M = 1.61$, $Re_\delta = 162000$). Several eddy-viscosity models and an explicit algebraic Reynolds stress model are considered. A methodology for matching the experimental conditions before the start of the interaction and at the end of the interaction was first established. Based on the required grid resolution and the established methodology for matching the experimental conditions, a series of three-dimensional simulations were performed to investigate the effect of spanwise confinement. Using the same methodology, simulations of additional test cases were performed and compared to experiments. Across three test cases, spanning a range of conditions, the explicit algebraic Reynolds stress model was found to give the best agreement with the experiments and displayed consistency in predicting the MSWBLI. The ability of the model to better resolve the corner flows resulted in narrower corner separations than linear eddy-viscosity models. For the latter, the supersonic core-flow was closer to the duct wall and its larger re-acceleration resulted in strong local pressure peaks. A detailed account of the flow physics of MSWBLI will be presented at the conference.

Figure 4: Wall pressure (top) and Mach number contours (bottom) for a MSWBLI ($M = 1.61, Re_{\delta_u} = 162000$).



1.54 Effect of Ambient Pressure Oscillation on the Primary Break-up of Jet Spray

ZHEN ZHANG^{1,2} & DONG-HYUK SHIN¹

¹School of Engineering, University of Edinburgh

²Beijing Institute of Control Engineering, China

The present simulation study investigates the effects of ambient pressure fluctuation on cylindrical liquid jet sprays, using volume of fluid (VOF) method. This study is motivated by combustion instability on gas turbines where strong harmonic pressure fluctuation occurs. One previous study demonstrated that fluctuation of fuel mass flow rate, caused by fluctuating ambient pressure, is one of the key mechanisms of combustion instability (Lieuwen and Zinn, 1998). However, ambient pressure

fluctuation changes not only the fuel mass flow rate, but also ambient gas density, liquid surface tension, and viscosity. Especially, in liquid sprays, the ambient fluid density and surface tension can have strong effects on spray break-up. In order to investigate the multiple property changes, a new solver in OpenFOAM is developed. In the solver, liquid mass flow rate, ambient gas density, and liquid surface tension change simultaneously according to ambient pressure fluctuation. Simulations were conducted with the Reynolds number of jet flow below 2000 and Weber number around 2000, which are conducive to make the break-up available in the laminar case. The oscillating ambient pressure is shown to strengthen the surface instability of the liquid ligament to generate more and smaller droplets, which depends on the surface tension-pressure coefficient and the value of mean pressure and amplitude in the oscillation.

References:

1. Lieuwen & Zinn, "The role of equivalence ratio oscillations in driving combustion instabilities in low NOx gas turbines," Proceedings of the Combustion Institute, 1998.

1.55 Experimental simulation of the Vortex Ring State

D. PICKLES, R. GREEN & A. BUSSE

University of Glasgow

The fluid dynamics of a helicopter rotor present many challenging phenomena. The flow is dominated by a system of intertwined helical vortices that trail from the rotor blades that persist and remain in the vicinity of the rotor for a long time to dominate the wake, and subsequently cause significant interactional, vibration and aeroelastic effects. Of interest here is the vortex ring state (VRS), typically associated with the descent of a rotor into its own wake, where the trailed vortex system collapses from its usual helical structure to form a toroidal vortex ring of the same scale as the rotor diameter. The vortex ring is highly unsteady, and sheds off and reforms, leading to large thrust oscillations. It is often supposed that the phenomenon is the result of the behaviour of the trailed vortices, and subsequently computation and experimentation have revolved around modelling the rotor blade system. Instead, this presentation will describe results of an experiment where a specially designed ventilated open core annular jet is used to simulate the mean flow below a rotor, and the subsequent evolution of this flow field into a state analogous to the VRS is observed. Laser Doppler Anemometry (LDA) of the jet inlet and outlet planes highlights the formation of a conical region of reverse flow through the centre of the jet, which increases in size as the notional descent velocity increased. Planar Particle Image Velocimetry (PIV) and Smoke Flow Visualisation conducted in the University of Glasgow, de-Havilland wind tunnel was used to investigate the development and subsequent shedding of a large toroidal vortex notionally similar to that produced by a rotor operating in the VRS. The presentation will describe the experiment in detail and discuss preliminary results comparing the VRS of a rotor and the jet.

1.56 Robust Optimisation of Microfluidic Flow Systems [Poster]FOTEINI ZAGKLAVARA[†]

University of Leeds

The study of the flow and heat transfer in microfluidic systems is a subject of interest for many areas of engineering applications, such as microfluidic cooling systems, Polymerase Chain Reaction (PCR) diagnostic devices etc. The constant demand for better performance means that it is important to optimise the performance of such devices, so that they can meet key performance and cost targets.

This project aims to use both experimental and computational methods to study the flow and heat exchange in microfluidic channels where PCR takes place. Two main optimisation approaches will be compared; the first optimisation approach will be based on the robust shape optimisation of micro-channels, using 3-D conjugate heat transfer CFD and a small number of design variables, while the second one will use Topology optimisation to enable the size, shape and topology of the channels to be optimised simultaneously.

The ongoing work focuses on the robust optimisation of microchannels, using 3-D conjugate heat transfer CFD (COMSOL Multiphysics) and a small number of design variables. The DoE points are created, with the use of Morris Mitchell Latin Hypercubes. With the use of CFD and techniques such as RBF or MLSM, the response surface is generated and the optimum points are found (Pareto) for the selected objective functions, using different optimisation algorithms (Genetic Algorithm, Particle Swarm optimisation etc).

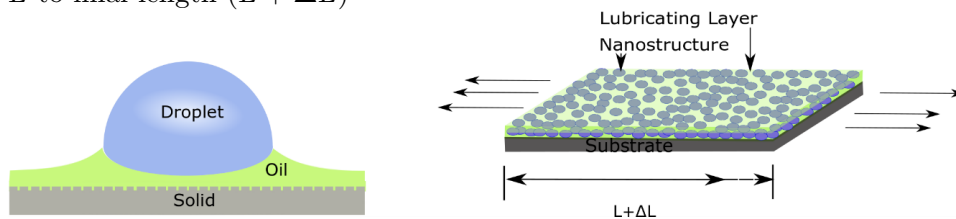
1.57 Droplet Mobility on the Flexible Slips (F-Slips) [Poster]

MUMTAHINA RAHMAN[†], GLEN MCHALE, RODRIGO
LEDESMA-AGUILAR & GARY G. WELLS

Northumbria University, Newcastle upon Tyne

Fluid-infused porous surfaces are crucial for many applications, such as wettability, microfluidics, self-cleaning, inject printing, fog collection etc [1,2]. Based on Nepenthes pitcher plants, Slippery Liquid Infused Porous Surfaces (SLIPS) [2] are introduced which shows promising result because they have lubricated surface on which it is easy to move droplets. This ease of movement of droplets on surfaces can come at the cost of droplet control. On a SLIPS, the interaction of the fluid-infused porous structure and the interfacial tensions of the contact line play an important role in the mobility of a droplet. Hence, it is possible to control the motion of a droplet by changing the parameters of the structured surface [1,3]. In this work we control the velocity of a droplet by applying a strain to the substrate containing the fluid. By increasing strain, at some point, the SLIPS property will break down and the underlying morphology of the surface will halt the moving droplet by pinning 1 . In this work we present a simple method to create a Flexible SLIP Surface (F-SLIPS) with the aim of controlling droplets. Glaco nanoparticles are spray coated on to a flexible material to make them superhydrophobic. Lubricating oil is applied to create slippery surface. The effects of stress and strain on flexible SLIPS is investigated and we investigate how the droplet's motion is effected by the mechanical strain placed on the underlying substrate.

Figure 5: a) Schematic of droplet on a SLIPS, b) Illustration of a SLIPS with nanostructure and lubricating layer, where upon stretch, the substrate along with nanoparticles and laminating layer goes from the initial length L to final length $(L + \Delta L)$

**References:**

1. Yao, X. *et al.* Adaptive fluid-infused porous films with tunable transparency and wettability. *Nat. Mater.* **12**, 1–6 (2013).
2. Wong, T. S. *et al.* Bioinspired self-repairing slippery surfaces with pressure-stable omniphobicity. *Nature* **477**, 443–447 (2011).

3. Coux, M., Clanet, C. & Quéré, D. Soft, elastic, water-repellent materials *r e.* **251605**, (2017).

1.58 On the aerodynamics of the gliding seeds of Javan cucumber

DANIELE CERTINI[†], C. CUMMINS, E. MASTROPAOLO,
N. NAKAYAMA & I. M. VIOLA

University of Edinburgh

Wind dispersed seeds inspired flight pioneers. Igo Etrich studied the Javan cucumber (*Alsomitra macrocarpa*) because it is an inherently stable glider [3] with one of the lowest terminal velocities (0.4 m s^{-1}). Unlike seeds from pioneer trees such as maples [4], Javan cucumber does not rely on wind, gusts and updrafts to cover distances up to hundreds of meters. It outperforms autorotating seeds like the maple seed [4] and equals pappose seeds like the dandelion [2]. This amazing flight is not only due to the flight mechanics but also to the aerodynamics provided by the shape. Our research aims to uncover the flow structures around the Javan cucumber. Here, we describe the morphology of real seeds and the airfoil with 3 D scans and image processing.

We argue that the flight mechanics of Javan cucumber cannot be understood using a two-dimensional wing. In fact, a rectangular flat plate with the same aspect ratio and wing span of Javan cucumber provides the correct forces (lift and drag) but, differently from the real seed, it is unstable in pitching ($dC_M/d\alpha > 0$). Conversely, a flat plate with a planar geometry resembling Javan cucumber is stable in pitching when it flies at an angle of attack of 12° , but it provides a lift coefficient $C_L = 0.85$ [5] that is more than double $C_L = 0.34$ of real seeds [1]. Finally, if the angle of attack was lowered to 5° , it would provide the correct lift force but it would be again unstable in pitching. More research is ongoing to demonstrate that the correct forces and stability can be achieved with a three-dimensional wing. This work aims to inspire the design of more efficient drones, as in the past the flight mechanics of Javan cucumber has inspired the design of aircrafts.

References:

1. Azuma, Akira & Okuno, Yoshinori 1987 Flight of a samara, *alsomitra macrocarpa*. *Journal of Theoretical Biology* **129** (3), 263–274.
2. Cummins, Cathal, Seale, Madeleine, Macente, Alice, Certini, Daniele, Mastropaolo, Enrico, Viola, Ignazio Maria & Nakayama, Naomi 2018 A separated vortex ring underlies the flight of the dandelion. *Nature* **562** (7727), 414.
3. Hertel, Heinrich 1966 Structure, form, movement .
4. Lentink, David, Dickson, William B, Van Leeuwen, Johan L & Dickinson, Michael H 2009 Leading-edge vortices elevate lift of autorotating plant seeds. *Science* **324** (5933), 1438–1440.
5. Minami, Shizuka & Azuma, Akira 2003 Various flying modes of wind-dispersal seeds. *Journal of Theoretical Biology* **225** (1), 1–14.

1.59 Self-propelled droplet transport on liquid surfaces

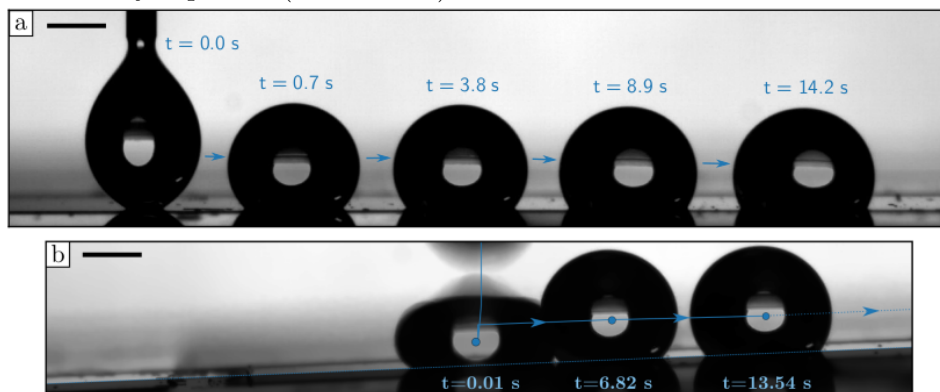
G. LAUNAY¹, M. S. SADULLAH², G. MCHALE¹,
R. LEDESMA-AGUILAR¹, H. KUSUMAATMAJA² & G. G. WELLS¹

¹Northumbria University, Newcastle-upon-Tyne

²Durham University

The ability to direct droplets on flat surfaces has many practical applications in microfluidics, bio-assay and analytical chemistry. To do this easily, and over long distances, it is necessary to combine a driving force and a highly mobile droplet. Here, we show that efficient droplet propulsion can be achieved using a dual length scale roughness to create slippery surfaces with a gradient of wettability. The micro-structured gradient in the roughness provides a directional force propelling the droplet via an imbalance in the contact angle [1]. The high droplet mobility is provided by a “liquid surface” created using a nanoscale roughness imbibed with oil [2] which prevents contact between the droplet and the solid. The resulting surfaces can propel droplets by several times their diameter, as well as against gravity (Figure 6). Furthermore, the strong vertical adhesion of these surfaces, allows impacting droplets to be captured prior to motion (Figure 1b), even when the substrate is completely inverted and the impacting droplets become hanging droplet.

Figure 6: Droplet self-propulsion on shaped liquid surfaces. (a) Droplet moving by several times its size on a flat surface. (b) Droplet self-propulsion on a tilted surface. Because of the strong vertical adhesion, the droplet is successfully captured (no rebound).



Acknowledgements: This work was supported by the Engineering and Physical Sciences Research Council [grant number EP/P026613/1].

References:

1. Shastry A., M. J. Case, and K. F. Böhringer. 'Directing Droplets Using Microstructured Surfaces' *Langmuir*, **2006**, volume 22, no. 14 : 6161– 67.
2. Wong T.S., S.H. Kang, S.K.Y. Tang, E.J. Smythe, B.D. Hatton, A. Grinthal and J. Aizenberg. 'Bioinspired Self-Repairing Slippery Surfaces with Pressure-Stable Omniphobicity' *Nature*, **2011**, volume 477, no. 7365 : 443– 47.

1.60 High-Order Relativistic Hydrodynamic Simulations using Rotated-Hybrid Riemann Solvers of the Kelvin–Helmholtz Instability and High Mach Number Flows

JAMIE TOWNSEND[†], LÁSZLÓ KÖNÖZSY & KARL W. JENKINS
Cranfield University

Two-dimensional relativistic hydrodynamic (RHD) simulations are performed using a newly developed Godunov-type finite volume solver, eCOS, to scrutinise current state-of-the-art intercell flux methodologies. A variety of popular Riemann solvers such as the: Rusanov, HLL, Roe and HLLC are used as well as innovative solutions that adopt rotated-hybrid Riemann solver technology. The rotated-hybrid class of Riemann solvers that arise from the amalgamation of the Roe and Rusanov/HLL solvers have shown great promise yet their application to RHD problems has not yet been tested. By applying a fewer-wave Riemann solver normal to shocks the Carbuncle problem can be avoided and by capitalising on a full-wave Roe solver orthogonal to shocks numerical dissipation is reduced. The robustness and ability to accurately resolve shear layers demonstrated by this solver make it an attractive candidate for RHD simulations. By performing numerical simulations at high Mach numbers and Lorentz factors a direct comparison between this technology and previously well-poised solutions can be understood. Furthermore, the two-dimensional Kelvin–Helmholtz instability is studied wherein the influence of Riemann solver choice can be quantified by means of growth-rate calculations and by reporting the energy power spectrum to gain insight into the manifest numerical dissipation. In all simulations a high-order spatial reconstruction technique is used that relies on the WENO concept in conjunction with a third-order TVD Runge–Kutta method for time integration.

1.61 The effect of heat transfer on boundary layer kinetic energy dissipation

LACHLAN JARDINE^{†1}, ANDREW WHEELER¹, ROB MILLER¹ &
BUDIMIR ROSIC²

¹University of Cambridge

²University of Oxford

For many engineering applications, their overall performance is influenced by the smallest scales of fluid motion. These dissipative flow structures are predominantly found in regions of high shear, such as boundary layers close to the surface. When heat is transferred through this surface, the boundary layer experiences large temperature gradients. How the near-wall temperature gradient and viscous dissipation are coupled remains unclear.

In this research, the effect of heat transfer on the dissipation of kinetic energy in a boundary layer is investigated. Both laminar and turbulent flows are examined using an isothermal, zero pressure gradient flat plate. For laminar flow, a compressible Blasius solution is formulated and compared with finite difference calculations. For turbulent flow, a semi-local scaling approach is taken and compared to DNS simulations. The simulations were conducted with freestream turbulence intensity of 5%. Transition is not studied in this investigation.

It is found that the leading-order effect of heat transfer, for both laminar and turbulent flow, is to rescale the boundary layer. By altering the thermofluid properties, heat transfer changes the history of the boundary layer and consequently the appropriate local non-dimensional reference scale. This study shows how the Reynolds number can be adapted to capture the effect of heat transfer.

This new understanding has been used to improve models for use in industrial design. An example of the magnitude of this effect is demonstrated on a cooled high-pressure turbine blade. This knowledge allows a designer to assess the effect of heat transfer on the overall performance.

1.62 Spontaneous Synchronization of Beating Cilia: An Experimental Proof Using Vision-Based Control

MOHAMED ELSHALAKANI[†] & CHRISTOPH H. BRÜCKER

Department of Mechanical Engineering and Aeronautics, City
University of London

Natural swimmers at low Reynolds number regimes make use of an emergence phenomenon known as hydrodynamic self-synchronization. The swimmer motors happen to oscillate in a specific non-symmetric manner and thus inducing a net swimming force to act on the swimmer body. This article investigates the formation of spontaneous coordination in a row of flexible 2D flaps (artificial cilia) in a chamber filled with a high viscous liquid ($Re = 0.12$). Each flap is driven individually to oscillate by a rotary motor with the root of the flap attached to its spindle axle. A computer-vision control loop tracks the flap tips online and toggles the axle rotation direction when the tips reach a pre-defined maximum excursion. This is a vision-controlled implementation of the so-called “geometric clutch” hypothesis. When running the control loop with the flaps in an inviscid reference situation (air), they remain in their individual phases for a long term. Then, the flaps are inserted in the chamber filled with a highly viscous liquid, and the same control loop is started. In this case, the flexible flaps undergo bending due to hydrodynamic coupling and come, after a maximum of 15 beats, into a synchronous metachronal coordination. The study proves in a macroscopic lab experiment that viscous coupling is sufficient to achieve spontaneous synchronization, even for a symmetric cilia shape and beat pattern.

1.63 A Lattice-Boltzmann Model of Electrocapillarity

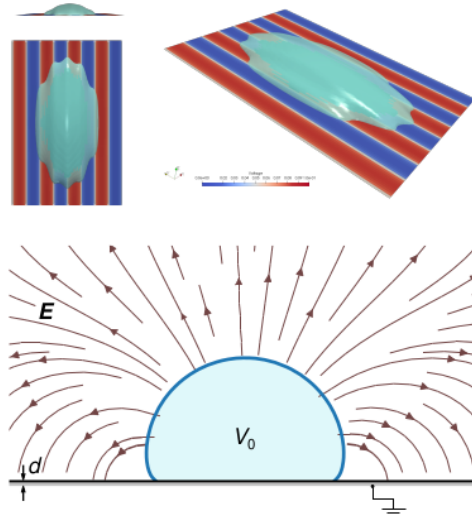
ÉLFEGO RUIZ-GUTIÉRREZ, GLEN MCHALE & RODRIGO
LEDESMA-AGUILAR

Northumbria University, Newcastle upon Tyne

Dielectrophoresis and electrowetting have become widely used techniques for controlling and manipulating small amounts of liquids. Applications of dielectrophoresis include the transport, and separation of liquids and other particles of different electric permittivity. Examples of electrowetting applications are electronic paper displays, adjustable lenses, and lab-on-a-chip devices. [1,2] In both cases, the underlying phenomena can be encompassed under electrocapillarity, the interaction of electric fields with multiphase systems where the effects of surface tension are comparable with electrostatic forces. Usually, one of the phases is a conducting liquid surrounded by an ambient dielectric or two liquids of different electric permittivities.

Fundamental aspects in electrocapillarity are still open for investigation; this mainly concerns the dynamical aspects, for example, the motion of contact lines and the shape that the liquid interface acquire in the presence of electric stresses. [2,3] This is important since most of the applications rely a precise control of the liquids and by placing electrodes in clever arrays. Simulations on electrocapillarity are timely as they may provide insights to address these aspects.

Figure 7: Example of simulations of droplet spreading by dielectrophoretic forces (top) and by electrowetting (bottom).



In this contribution, we propose a simple lattice-Boltzmann method that is capable of simulating electrocapillarity. We use a binary fluid

model that includes capillary phenomena and extend the algorithm to include the forces produced by electric fields. The electric field and the charges are derived from a potential function, which we obtain by a relaxation method. [4] We first validate our method by comparison against the experimental observations. Then, we examine the morphology of droplets under dielectrophoretic stresses.

Acknowledgements: The authors acknowledge support from EPSRC Grants Nos. EP/P024408/1 and EP/R036837/1,487 and from EPSRC's UK Consortium on Mesoscale Engineering Sciences (Grant No. EP/R029598/1).

References:

1. B.J. Kirby. *Micro-and nanoscale fluid mechanics: transport in microfluidic devices*. Cambridge university press, 2010.
2. Frieder Mugele. Fundamental challenges in electrowetting: from equilibrium shapes to contact angle saturation and drop dynamics. *Soft Matter*, 5(18):3377–3384, 2009.
3. A.M.J. Edwards, R. Ledesma-Aguilar, M.I. Newton, C.V. Brown, and G. McHale. Not spreading in reverse: The dewetting of a liquid film into a single drop. *Science Advances*, 2(9):e1600183, 2016.
4. É. Ruiz-Gutiérrez and R. Ledesma-Aguilar. Lattice-Boltzmann simulations of electrowetting phenomena. *Langmuir*, 2019. Just accepted. DOI: 10.1021/acs.langmuir.9b00098.

1.64 The role of protein concentration on the rheology of synovial fluid when modelling elastohydrodynamic lubrication of joint prosthesesL. NISSIM[†], H. BUTT, L. GAO, C. MYANT & R. HEWSON

Imperial College London

Joint replacements have been performed since the 1960s, the most common being hip and knee implants. Data collected from 2014 shows that, across the EU, on average 319 hip and knee replacements are carried out per 100 000 people. This equates to over 1.6 million surgeries annually. A number of factors including ageing populations, increasing life expectancy and improving joint designs mean that the number of replacement and revision procedures is only set to continue rising.

The difficulty in modelling synovial joints stems from complex geometry and the multi-component nature of the fluid. Proteins in the synovial fluid induce complex rheological behaviour [1][2], which is geometry specific due to the length scale of the protein which is of the same order as the fluid film thickness. It can be seen in the experimental work of Myant, Cann et al. [3][4] that protein matter collects at the inlet of the lubricated contact area and this aggregation leads to greatly increased film thickness as compared to those predicted by modelling the elasto-hydrodynamic lubrication (EHL) regime with the bulk synovial fluid properties.

In this work a ball on plate geometry is computationally modelled by coupling finite-difference derived EHL solutions with the transport of protein matter using a modified advection-diffusion equation to simulate aggregation and identify protein concentration changes. The local viscosity of the lubricating synovial fluid was updated to achieve transient simulations that capture the nature of Protein Aggregation Lubrication (PAL) and obtain film thickness predictions. Response surface based inverse methods were used to match the constants in the constitutive equations, giving agreement with observed phenomenon and providing general models for synovial fluid in constrained geometries.

References:

1. J. Hron, J. Málek, P. Pustějovská and K. R. Rajagopal, "On the modeling of the synovial fluid," *Advances in Tribology*, 2010.
2. T. Kitano, G. A. Ateshian, V. C. Mow, Y. Kadoya and Y. Yamano, "Constituents and pH changes in protein rich hyaluronan solution affect the biotribological properties of artificial articular joints," *Journal of Biomechanics*, vol. 34, no. 8, pp. 1031–1037, 2001.
3. C. Myant and P. Cann, "In contact observation of model synovial fluid lubricating mechanisms," *Tribology International*, vol. 63, pp. 97-104, 2013.

4. J. Fan, C. W. Myant, R. Underwood, P. M. Cann, and A. Hart, "Inlet protein aggregation: a new mechanism for lubricating film formation with model synovial fluids," *Proceedings of the Institution of Mechanical Engineers, Part H: Journal of Engineering in Medicine*, vol. 225, no. 7, pp. 696-709, 2011.

1.65 Experimental study of atmospheric stratification and urban flow and dispersion

DAVIDE MARUCCI & MATTEO CARPENTIERI

Department of Mechanical Engineering Sciences, University of Surrey

Poor urban air quality and the risk of spreading hazardous substances following industrial incidents or terrorist attacks in cities are an increasing problem. Predicting gas and particle dispersion can assist in preventing health hazards and planning emergency procedures. One of the main problems that affects models used for this purpose is the way they treat atmospheric stratification, very often present in environmental flows. The StratEnFlo project aimed to fill this gap.

Artificially thickened stable and unstable boundary layers were simulated in the EnFlo wind tunnel over a very rough surface. The effect of different parameters was investigated (among them, inlet temperature profile, capping inversion and surface roughness). These boundary layers were then employed as approaching flow for idealised urban models.

Experiments were then conducted on an array of rectangular blocks, where a pollutant tracer was also released from a point source at ground level. Mean and fluctuating velocities, temperatures and concentrations were sampled, together with heat and pollutant fluxes. The analysis of the data revealed that even in case of weak stratification there are important modifications inside and above the canopy on both the urban boundary layer and the plume characteristics.

Finally, the combined effects of a stable approaching flow and local surface heating were investigated in a bi-dimensional street canyon geometry. This represented an absolute novelty and the results highlighted how both local and incoming stratification can significantly affect the flow and dispersion at a microscale level in a complex way that depends on the particular case of study. This work helps in gaining new knowledge on the effects of stratification and encourages further work on the topic. The experimental database produced during the project is unique and of high quality. It can assist in developing, improving and validating numerical models, as well as developing parametrisations for simpler models.

1.66 FAST, NEAREST and flagellar regulation

M. T. GALLAGHER^{1,2}, G. CUPPLES^{1,2}, J. C. KIRKMAN-BROWN² &
D. J. SMITH^{1,2}

¹University of Birmingham

²Centre for Human Reproductive Science, Birmingham Women's and
Children's NHS Foundation Trust

Despite major technological advances in imaging and computing over the past decade, semen analysis in the human is limited to rudimentary methods such as sperm counting and analysis of fixed cells. There is no reliable and informative method to detect which sperm have both the motility and integrity to produce a healthy embryo. In an age where huge amounts of high-resolution data can be readily produced it is becoming increasingly important to be able to accurately and efficiently analyse large amounts of data, and to be able to use these analyses as a marker for clinical outcome. To address this, we have developed and released FAST (Flagellar Analysis and Sperm Tracking), a free-to-use package for the high-throughput detection and tracking of large numbers of beating flagella in experimental microscopy videos.

This new ability to track the detailed flagellar waveform allows for more than just measurements of motility. Alongside FAST we have been developing NEAREST (Nearest-neighbours for Easy Application of Regularised STokeslets), an open source software package enabling the rapid application of a meshless regularised Stokeslet method to solve mobility and resistance problems in Stokes flow. Combining FAST tracked flagellum with the numerical capabilities of NEAREST allows for detailed investigation into experimentally intractable quantities such as energy dissipation, disturbance of the surrounding medium and viscous stresses.

Finally, we will discuss how the analysis of modelling capabilities provided by these tools can be combined, together with models of the elastic behaviour of flagella and model-based learning algorithms to probe the secrets of flagellar regulation in swimming cells.

1.67 Bifurcation analysis of evaporating droplets on smooth surfacesMICHAEL EWETOLA[†] & MARC PRADAS

The Open University

Droplet evaporation is important in many processes including ink-jet printing, micro-patterning, coating, and cooling. Recent studies have shown that a droplet evaporating on smooth surfaces with periodic topographic and chemical variations experiences snap events characterized by a discontinuous change in the apparent and real contact angles respectively. The underlying properties of the surface induce a hierarchy of bifurcations, including pitchfork and saddle-node bifurcations. The bifurcation points, which can be predicted theoretically, correspond to critical volumes at which the droplet may change location by shifting laterally. In this study, we examine a droplet evaporating on a surface with combined topographic and chemical variations and observe that the combined heterogeneities enhance and annihilate these snap events. Further more, we observe that droplets break up at critical values of the topographic variation amplitude. In addition, we make use of a diffuse interface formulation coupled with the Navier Stokes equation to study the hydrodynamics of the droplet as it evaporates, observing a sequence of events in which the droplet base radius, contact angle, and mid-point rapidly change, in agreement with the theoretically predicted bifurcation point.

1.68 Finite Element Modelling of Microswimmers with Applications in Reproductive Biology

CARA V. NEAL[†], DAVID J. SMITH, MEURIG T. GALLAGHER &
THOMAS D. MONTENEGRO-JOHNSON

University of Birmingham

The journey of the human sperm to the egg is a complex and extremely important process. Sperm cells must navigate the intricate geometry of the fallopian tubes, generating active bending in order to swim through cervical mucus - a highly viscous, rheologically complex fluid. With rates of male infertility rising, it is becoming increasingly important to understand how sperm swim, and what might affect this process. While the field of microswimmers has gained significant attention in recent years, there are still several drawbacks to many of the ways in which we model swimmers. For example, methods are often computationally expensive, and many make the assumption that the fluid is Newtonian, despite the fact that this assumption has been shown to be invalid. In this talk, we will discuss a new method in which we can model both active and passive filaments in non-Newtonian fluids. This method uses a combination of a finite element technique, chosen due to its ability to handle the non-linear equations associated with non-Newtonian fluids, and the elastohydrodynamic integral formulation (EIF), developed by Hall-McNair et al. 2019. The EIF method is a particularly efficient way of modelling flexible filaments, accounting for the hydrodynamic interactions between them. The finite element method is formulated in such a way that the solution can be calculated on a coarse mesh, for decreased computational costs compared to more commonly used body-fitted meshes. After outlining the theory and implementation of these methods, we will conclude by presenting some results of the application to both passive filaments and sperm simulation within bounded domains.

1.69 Applying the Goldilocks Principle to predict coral habitat engineering

KONSTANTINOS GEORGOULAS[†]

University of Edinburgh

The ecosystem services provided by coral reefs are worth over \$100 billion annually and include coast line protection, tourism, food and medical derivatives. However, the health of the constituent corals can be significantly impacted by climate change. The occurrence and proliferation of reef-forming cold-water corals is reliant upon optimal current conditions, where provision of organic material is at a velocity suitable for prey capture by the coral. The occurrence of a significant proportion of dead skeletal framework on reefs highlights that when flow is sub-optimal, prey capture and ingestion rates are likely inadequate to facilitate survival.

The reef forming coral *Lophelia pertusa* has an optimal range of flow velocities in which they can capture food efficiently. This ‘Goldilocks Zone’, where the flow is neither too fast nor too slow, will promote coral growth compared to zones of sub-optimal flow velocity. Disruption of flow by the corals also creates sub-optimal velocity regions behind it, contributing to mortality of downstream corals.

A Computational Fluid Dynamics (CFD) model has been created in order to understand coral growth in ‘optimal conditions’, simulating current and possible future environments. Smoothed Particle Hydrodynamics (SPH) – a mesh-free Lagrangian method – is being used as its advantages over traditional grid methods are exploited in the coral growth model. The model is written in the C++ programming language and will be parallelized with the Open Multi-Processing (OpenMP) application programming interface to allow for time-effective high resolution simulations.

Our data and models of how corals modify their own flow environment, provides an explanation to the cold-water coral paradox of living in fast velocity environments, but requiring slow velocities for prey capture.

1.70 Low-order Prediction and Modelling of Intermittent Flow Separation and Reattachment in Unsteady 2D Flows

DESANGA FERNANDO & KIRAN RAMESH

Aerospace Sciences Division, University of Glasgow

Discrete-vortex numerical methods are a viable alternative to the traditional grid-based methods, particularly in the context of external aerodynamics flows. Recently, a discrete-vortex method has been successfully applied to high-amplitude, high-frequency unsteady manoeuvres where the aerodynamics is dominated by leading-edge vortex shedding. Here, the release of vortices from the leading edge is modulated using a Leading-Edge-Suction-Parameter (LESP) [“Discrete-vortex method with novel shedding criterion for unsteady aerofoil flows with intermittent leading-edge vortex shedding”. *J. Fluid Mech.* 751 pp. 500-538 (2014)]. This motivates the generalisation of this approach to the external aerodynamics problems with arbitrary flow separation/reattachment on the surface. However, most of the current approaches assume some “ad hoc” start and stop criteria for vortex shedding, such as continuous shedding from a given location. The concept of LESP is also limited to the cases where the shear layer detachment only occurs at the leading edge without any significant flow separation over the rest of the aerofoil.

The current study discusses a systematic method that can automatically determine the time and location of flow separation on arbitrary unsteady flows by using an integral boundary layer method. The formation of “Van Domellen singularities” in the boundary layer solution indicates the onset of unsteady flow separation. A novel viscous-inviscid coupling method is used to couple the boundary layer solution with the inviscid outer-flow field, which is calculated from the discrete-vortex method. Separated shear layers are represented by shedding discrete-vortex particles from the dynamically determined separation point. This novel method is physics-based, computationally efficient and mimics the arbitrarily separated/reattached flow fields over aerodynamic bodies.

The current paper will present the initial validations of this computational model for flows past a cylinder under a range of Reynolds numbers $Re = 10,000 - 1000,000$, and further results will be elaborated for NACA 0004 and NACA 0012 aerofoils under similar flow conditions.

1.71 Is climate change increasing atmospheric turbulence?

PAUL D. WILLIAMS

Department of Meteorology, University of Reading

Earth's atmosphere is a fluid that exhibits turbulence on length scales ranging from the planetary scale of thousands of kilometres to the Kolmogorov scale of a few millimetres. An important mechanism for generating atmospheric turbulence is the Kelvin–Helmholtz shear instability, which occurs mainly in the jet streams. The resulting clear-air turbulence is invisible and hazardous to flying aircraft. Anthropogenic climate change is modifying the jet streams by strengthening the vertical wind shear at aircraft cruising altitudes. Such a strengthening is expected to increase the prevalence of the shear instabilities that generate clear-air turbulence.

Here we use numerical simulations of the global atmospheric flow to analyse how shear-driven turbulence responds to climate change. We find that the probability distributions for an ensemble of 21 transatlantic wintertime clear-air turbulence diagnostics generally gain probability in their right-hand tails when the atmospheric carbon dioxide concentration is increased. By converting the diagnostics into eddy dissipation rates, we find that the ensemble-average airspace volume containing light turbulence increases by 59% (with an intra-ensemble range of 43%–68%), moderate by 94% (37%–118%), and severe by 149% (36%–188%). We find similar increases in all seasons worldwide, with some busy flight routes experiencing several hundred per cent more turbulence.

Our results suggest that clear-air turbulence will intensify in all aviation-relevant strength categories as the climate continues to change. We conclude that aircraft flights will become significantly bumpier in future. Flight paths may need to become more convoluted to avoid patches of turbulence that are stronger and more frequent, in which case journey times will lengthen and fuel consumption and emissions will increase.

1.72 Numerical simulations of grid-turbulence, and dissipation modelling in large-eddy simulations.RORY HETHERINGTON[†]

University of Leeds

Increased computing power and developments in turbulence modelling have led to a growing interest in large-eddy simulation (LES) for various engineering applications, e.g. aerodynamics, noise prediction, and turbo-machinery. In cases of spatially developing flows, such as flow past a cylinder, the flow field in the wake is known to be sensitive to inflow turbulence content. However, although LES solutions are sensitive to inlet condition, there exists no consensus on an optimal method for generating turbulent inflow.

No such confusion exists in experimental studies: inflow is passed through a grid to generate pseudo-homogeneous turbulence, a process thoroughly documented over the last few decades. However, with the advent of fractal grids, grid-generated turbulence studies have led to a reformulation of the classical form of equilibrium dissipation scaling.

In this study, LES subgrid-scale models are assessed for their suitability to describe non-equilibrium turbulence. In particular, drawbacks of algebraic and one-equation models are highlighted. A model for subgrid-scale dissipation of non-equilibrium turbulence is proposed, and tested on two classical flows: grid-turbulence, and flow past a cylinder. A new fractal grid design is recommended, and shown to reduce clumping in the vorticity field. Numerical simulations have been carried out in OpenFOAM, and supplemented with water flume particle-image velocimetry for validation where possible.

1.73 Contact line dynamics and hysteresis measurements on social surfaces

HERNAN BARRIO-ZHANG[†], ÉLFEGO RUIZ-GUTIÉRREZ, GARY
G. WELLS & RODRIGO LEDESMA-AGUILAR

Northumbria University, Newcastle Upon Tyne

Solids are not uniform and exhibit roughness at micrometric scales. The chemical and physical imperfections that cause roughness affect the interaction between a liquid-gas interface and the solid, namely on its apparent contact angle and pinning behaviour. This is the reason why surface topography has become a promising variable for controlling wettability, adhesion, mobility and liquid transport [1]. Contact Angle Hysteresis (CAH) is a measure of the static friction exerted by a solid surface on a liquid droplet [2]. Slippery Omniphobic Covalently Attached Liquid (SOCAL) surfaces are a novel way to produce surfaces with ultra-low CAH through acid-catalyzed graft polycondensation of dimethyldimethoxysilane [3]. This study focuses on the interaction of pure water droplets on ultra-smooth SOCAL surfaces. Our results show that when CAH approaches zero, its measurement becomes challenging. Hence, we develop a method to measure CAH by analysing the behaviour of the contact line during the slow relaxation of the liquid-gas interface on a SOCAL surface. By analysing the asymptotic behaviour of the contact line, we are able to quantitatively determine hysteresis.

References:

1. Yao X., Hu Y., Grinthal A., Mahadevan L. and Aizenberb J. ‘Adaptive fluid-infused porous films with tunable transparency and wettability’ *Nature Materials*, **2013**, 12, 529-534.
2. De Gennes P.G., Brochard-Wyart F., Quéré D., in ‘Capillarity and Wetting phenomena’; *Springer*, **2004**, 69
3. Wang L. and McCarthy T. ‘Covalently Attached Liquids: Instant Omniphobic Surfaces with Unprecedented Repellency’ *Angewandte Chemie - International Edition*, **2016**, 55, 244-248.

1.74 A computational model to predict the onset of secondary flows of blood in a cone and plate rheometer

NATHANIEL KELLY[†], DANIEL JELLIFFE, HARINDERJIT GILL,
KATHARINE FRASER & ANDREW COOKSON

University of Bath

Laminar-turbulent transition in shear thinning blood is an important consideration for design of safer cardiovascular devices, due to the fluid stresses associated with turbulence. Past studies have used a rheometry to study laminar shear stress on blood cells [1], however the onset of possible turbulent shear stresses has not been investigated. Hence, the aim of this study was to create a computational model to explore the onset of secondary flows as precursor to possible transition to turbulence within a cone and plate rheometer for Newtonian and shear-thinning blood rheology.

The Navier-Stokes equations were solved using finite volume solver OpenFOAM v5. An unstructured mesh containing approximately 300,000 cells was generated for a 45° sector of the cone and plate rheometer. A rotating wall velocity BC was applied to the cone surface with varying angular velocity, to control the rotational Reynolds number (Eq. 1). Newtonian and shear-thinning models of blood were used with turbulence modelled using Menter's $k - \omega$ SST RANS model. Secondary flow was assessed through relative torque calculation (theoretical torque/actual torque).

$$\tilde{R} = \frac{R\omega\alpha^2}{12\nu} \quad (1)$$

A comparison between the relative torque shows that secondary flow occurs at $\tilde{R} = 0.4$ for Newtonian blood analogues. This is in good agreement with experimental measurements and theoretical predictions [2], where transition to secondary flow occurs at $\tilde{R} = 0.5$. Compared to Newtonian, results for shear thinning showed a slight delay in transition to secondary flow which was also seen experimentally ($\tilde{R} = 1.4$). For low values of \tilde{R} vorticity plots show minimal secondary flow structures, however once \tilde{R} was increased beyond $\tilde{R} = 1.7$, secondary flow structures are clearly visible particularly at the periphery. This is in agreement with published experiments [2].

The results demonstrate that a cone and plate rheometer can be used to study secondary flow as a prelude to possible transition to turbulence. Further simulations will be performed on higher \tilde{R} values to observe behaviour at the laminar-turbulent transition.

References:

1. Chan, C et al. (2017). Shear Stress-Induced Total Blood Trauma in Multiple Species. *Artificial Organs*, 41(10), pp. 934-947.
2. Sdougos, H., Bussolari, S. and Dewey, C. (1984). *JFM*. 138(-1), p. 379.

1.75 Large eddy simulations of plumes in a stratified roomCAROLANNE VOURIOT[†]

Imperial College London

20% of all energy consumed in Europe is used to condition buildings, through heating or cooling. As people are spending an increasing amount of time indoors, it is predicted that the consumption of energy in buildings will rise still further in the upcoming years. This could be mitigated by switching to low energy options such as natural ventilation. Unlike mechanical ventilation or air conditioning, natural ventilation relies only on the flows created by density differences and/or wind around buildings. A feature of traditional architecture, it is being reintroduced into modern buildings as an attempt to reduce their environmental impact and to improve the living and working conditions of their occupants. With pollutant sources originating both indoors and outdoors, the ventilation system also needs to ensure that the air breathed by building occupants is of high enough quality.

Natural ventilation involves complex dynamics including buoyancy driven flows and stratified environments, which can be numerically simulated using large eddy simulations. We present a validation of Fluidity, an open source CFD code, for this application by looking at a typical case of displacement ventilation. We focus on the simulation of the flow within of a room containing a point source of heat and fitted with top and base openings. The results of the numerical simulations are compared to analytical predictions and experimental data from the literature. In particular, the plume and stratification created by the heat source are studied, both of which should be accounted for during the design of a ventilation system. We believe that the use of Fluidity in this setting will enable rapid prototyping of new buildings and promoting clean air quality in building by assessing exposure to pollutants.

1.76 Sedimentation of tephra from stratified plumesDANIEL WARD[†]

University of Leeds

Volcanic ash can be hazardous to public health and the aviation industry, the 2010 eruption of the Icelandic volcano Eyjafjallajökull, for example, led to widespread disruption of flights across Europe. It is therefore important to be able to accurately predict the spread and deposition of tephra from a volcanic eruption. Volcanic eruptions that occurred in the past often have no data on parameters such as source buoyancy flux and plume height, with data on tephra accumulation often being the only record of eruptions. It is possible, therefore to use an inversion method to approximate source parameters based solely on available data.

When a volcano erupts, a buoyant plume is produced, providing the mechanism for tephra transport and dispersal. In a stratified environment, a buoyant plume first rises to its neutral buoyancy level, where it then spreads laterally, forming an umbrella region. Tephra may settle out of the plume (or be re-entrained) at any point in the flow, after which it accumulates on the ground. Different sizes of particles are likely to be distributed accordingly, providing data such as grain-size distribution and particle mass for use in inverting for source parameters.

Using the spectral element code Nek5000, direct numerical simulations of a buoyant plume in a stratified environment are conducted with advection of tephra simulated using Lagrangian particle tracking. This will develop understanding of the dispersal dynamics of tephra from a volcanic plume and comparing results to existing models of particle dispersal facilitates the improvement of these models and aids in predictions of ash fall from volcanic eruptions, as well as improving existing inversion methods.

1.77 Elasticity suppresses fluidisation of yield-stress material under vibrationsASHISH GARG[†], MATTHIAS HEIL & ANNE JUEL

University of Manchester

The rheology of yield-stress fluids has been the subject of extensive research in recent years. However, the mechanics of fluidisation of such materials due to external forcing remains poorly understood. Using a combination of experiments and theory, we investigate the fluidisation of a sessile drop of yield-stress material on a pre-existing layer of the same fluid due to vertical sinusoidal oscillations. We find that molten tempered chocolate and a microgel solution of carbopol exhibit different fluidisation behaviours despite having the same yield stress. The experiments show that the carbopol drop deforms harmonically with the driving frequency for low values of the driving acceleration unlike chocolate, which remains rigid. Above a critical value of the acceleration, transient axisymmetric spreading occurs. Chocolate spreads viscoplastically whereas the carbopol drop exhibits large-amplitude harmonic deformation and spreads significantly less. The time scale of spreading is significantly reduced in carbopol where the drop rapidly reaches a new stable state of harmonic deformation. To achieve a similar extent of spreading, carbopol requires 3-4 times more forcing. Informed by the rheological measurements, we model chocolate and carbopol as a viscoplastic and an elastoviscoplastic fluid, respectively. We derive a depth-averaged model for the dynamics of the drop in the limit of a slender axisymmetric drop and compute solutions using finite-difference methods. We find that the harmonic deformations of the carbopol drop are associated with elastic deformations and that the yield-stress controls the critical acceleration at which spreading is initiated. The extent of the spread for a given acceleration results from the interaction between elastic and viscous forces and the yield-stress alone does not determine fluidisation.

1.78 Parallel-in-time integration of Dynamo Simulations

ANDREW CLARKE[†]

University of Leeds

The precise mechanisms responsible for the natural dynamos in the Earth and Sun are still not fully understood. Numerical simulations which couple the flow of a conducting fluid with magnetic effects, using the equations of magnetohydrodynamics (MHD), are used to investigate the dynamo effect. These simulations are extremely computationally intensive, and are carried out in parameter regimes many orders of magnitude away from real conditions.

Parallelization in space is a common strategy to speed up simulations on high performance computers, but eventually a scaling limit is reached due to increasing overheads from communication. Additional directions of parallelization are desirable to utilise the high number of processor cores available in current and future massively parallel high-performance computing systems.

Parallel-in-time methods can deliver speed up in addition to that offered by spatial partitioning but have not yet been applied to dynamo simulations. We investigate the ability of parallel in time methods to speed up dynamo simulations in two different areas. First, we have investigated the feasibility of using the parallel-in-time algorithm Parareal to speed up initial value problem simulations of the kinematic dynamo – a simplification of the dynamo problem which concentrates on the magnetic field effects. Secondly, we investigate the ability of this technique to speed up simulations of Rayleigh Bénard convection, as convective flows are thought to drive many natural dynamos, such as the Earth's core.

The pseudo-spectral python based code Dedalus is used in numerical simulations. Results for kinematic dynamo studies show that both the Roberts flow and Galloway-Proctor flow dynamos can benefit from extra speed up using parallel in space and time methods over parallel in space alone. Results for the Galloway-Proctor flow are promising, with speed ups of 300 found with 1600 cores. Early results for Rayleigh-Bénard convection will be presented.

1.79 Multiphase plumes in a stratified ambient

NICOLA MINGOTTI & ANDREW W. WOODS

BP Institute, University of Cambridge

We report on experiments of turbulent particle-laden plumes descending through a stratified environment. We show that provided the characteristic plume speed exceeds the particle fall speed, then the plume is arrested by the stratification and initially intrudes at the neutral height associated with a single-phase plume of the same buoyancy flux. If the original fluid phase in the plume has density equal to that of the ambient fluid at the source, then as the particles sediment from the intruding fluid, the fluid finds itself buoyant and rises, ultimately intruding at a height of about 0.58 ± 0.03 of the original plume height, consistent with new predictions we present based on classical plume theory. This is key for predictions of the environmental impact of any material dissolved in the plume water which may originate from the particle load. We also show that the particles sediment at their fall speed through the fluid below the maximum depth of the plume as a cylindrical column whose area scales as the ratio of the particle flux at the source to the fall speed and concentration of particles in the plume at the maximum depth of the plume before it is arrested by the stratification. We demonstrate that there is negligible vertical transport of fluid in this cylindrical column, but a series of layers of high and low particle concentration develop in the column with a vertical spacing which is given by the ratio of the buoyancy of the particle load and the background buoyancy gradient. Small fluid intrusions develop at the side of the column associated with these layers, as dense parcels of particle-laden fluid convect downwards and then outward once the particles have sedimented from the fluid, with a lateral return flow drawing in ambient fluid. As a result, the pattern of particle-rich and particle-poor layers in the column gradually migrates upwards owing to the convective transport of particles between the particle-rich layers superposed on the background sedimentation. We consider the implications of the results for mixing by bubble plumes, for submarine blowouts of oil and gas and for the fate of plumes of waste particles discharged at the ocean surface during deep-sea mining.

1.80 Predicting orientation of suspensions of elongated particles in three-dimensional thin channel flowG. CUPPLES¹, D. J. SMITH¹, M. HICKS² & R. J. DYSON¹¹University of Birmingham²Linear Diagnostics Ltd, Birmingham

Flow linear dichroism is a biophysical spectroscopic technique that exploits the shear-induced alignment of elongated particles in suspension. This talk is focussed around the broad aim of optimising the sensitivity of this technique by improving the alignment of these particles, with a specific application of a handheld synthetic biotechnology prototype for waterborne-pathogen detection. I will describe a model of steady and oscillating pressure-driven channel flow and orientation dynamics of a suspension of slender microscopic fibres. The model couples the Fokker-Planck equation for Brownian suspensions with the narrow channel flow equations, the latter modified to incorporate mechanical anisotropy induced by the particles. The linear dichroism signal is estimated through integrating the perpendicular components of the distribution function via an appropriate formula that takes the bi-axial nature of the orientation into account. For the specific application of pathogen detection via binding of M13 bacteriophage, I will explore the impact of the channel depth, width, pressure gradient and frequency of oscillations on the alignment in the system. I will also discuss the practical ability for oscillatory flow, compared to steady flow, for the analysis of smaller sample volumes.

1.81 DNS of a turbulent rotating jet

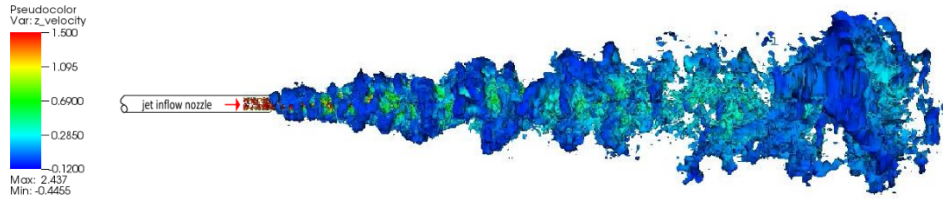
SAMUEL D. DUNSTAN[†] & YONGMANN M. CHUNG

University of Warwick

In this study direct numerical simulation (DNS) of the canonical jet subject to axial rotation is investigated. The recycling method is imposed so that there is fully developed turbulent pipe flow at the jet inlet [1]. The Reynolds number used was $Re_D = 4900$.

The spectral element solver, Nek5000 [2], is used. The inflow pipe domain is $15D$ in length and consists of 10.6×10^6 grid points. The jet domain proper is $0 < x/D < 112.5$, $r/D < 57.5$ and $0 \leq \phi < 2\pi$ and with the number of grid points being 135×10^6 . 80% of grid points are within $x/D \leq 50$ and $r/D \leq 7.5$, in the main region of interest. A grid independence test was performed, monitoring fundamental time averaged flow descriptors such as centreline velocity.

Figure 8: Iso-surfaces of pressure $p/\rho U_j^2 = -0.005$ for the non-rotating turbulent jet.



The turbulent jet simulation was performed first without rotation (Figure 8). The results are consistent with the findings of previous numerical studies [3, 4], with vortex rings forming initially in the near field and later, self similarity in the far field. Rotation in the straight turbulent pipe is applied via two methods, the Coriolis body force and slip wall rotation. Comparisons are made with previous investigations into the rotating pipe [5–7]. The log law region is observed to move upward, while streamwise fluctuations have a lower peak value for a higher pipe wall rotation rate (Figure 9).

In the initial simulations of the turbulent jet with rotation applied, faster breakdown occurs and the jet cone is quickly subjected to a lengthwise contraction and radial and azimuthal redistribution (Figure 10). These observations are consistent with [8, 9]. The rotating turbulent jet simulations are on-going and results will be presented in the next meeting.

Figure 9: Streamwise velocity, (a) semi-log plot for the straight pipe with wall axial rotation and (b) fluctuations.

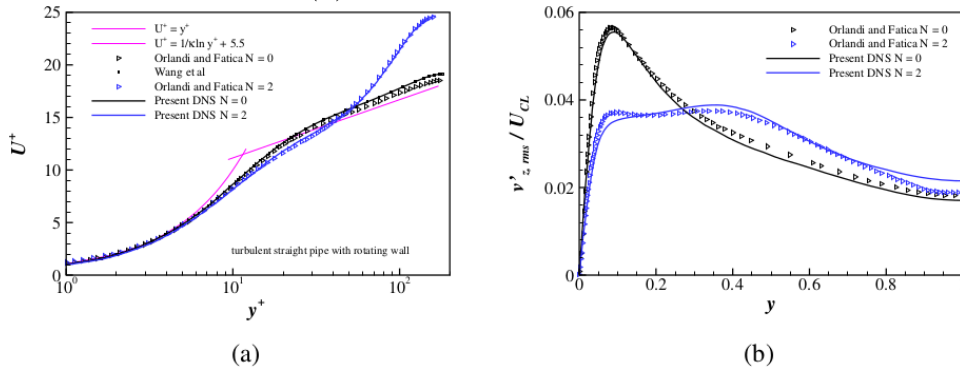
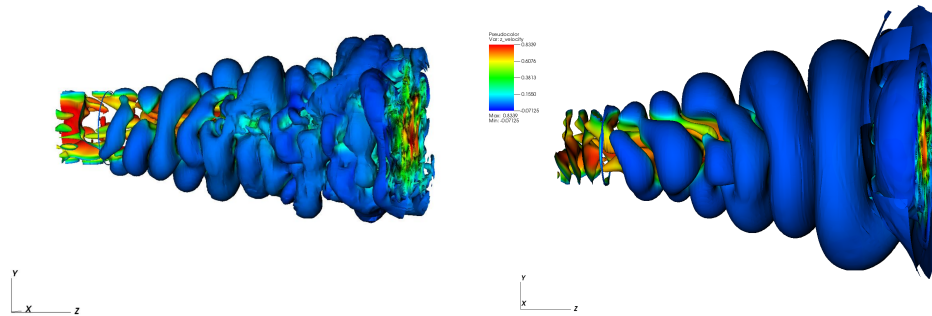


Figure 10: Jet near field at the onset of rotation. Iso-surfaces of pressure $p/\rho U_j^2$ at 60 contour levels of range and coloured by streamwise velocity. Rotational reference $\Omega = 0.21$. (a) at $t = 0$ and (b) at $t = 25$.



References:

1. Z. X. Wang, R. Orlu, P. Schlatter, and Y. M. Chung. Direct numerical simulation of a turbulent 90 degrees bend pipe flow. *International Journal of Heat and Fluid Flow*, 73:199–208, 2018.
2. P. F. Fischer, J. W. Lottes, and S. G. Kerkemeir. Nek5000 user documentation, 2008.
3. J. Kim and H. Choi. Large eddy simulation of a circular jet: effect of inflow conditions on the near field. *Journal of Fluid Mechanics*, 620:383–411, 2009.
4. T. B. Gohil, A. K. Saha, and K. Maralidhar. Direct numerical simulation of naturally evolving free circular jet. *ASME: Journal of Fluids Engineering*, 133(11):111203, 2011.
5. P. Orlandi and M. Fatica. Direct simulations of turbulent flow in a pipe rotating about its axis. *Journal of Fluid Mechanics*, 343:43–72, 1997.

6. L. Facciolo, N. Tillmark, A. Talamelli, and P. H. Alfredsson. A study of swirling turbulent pipe and jet flows. *Physics of Fluids*, 19(3):035105, 2007.
7. R. Mullyadzhanov, S. Abdurakipov, and K. Hanjalic. On coherent structures and mixing characteristics in the near field of a rotating pipe jet. *International Journal of Heat and Fluid Flow*, 63:139–148, 2017.
8. I. R. Atthanayake, P. Denissenko, Y. M. Chung, and P. J. Thomas. Formation-breakdown cycle of turbulent jets in a rotating fluid. *Journal of Fluid Mechanics*, In press, 2019.
9. D. Frank, J. R. Landel, S. B. Dalziel, and P. F. Linden. Anticyclonic precession of a plume in a rotating environment. *Geophysical research letters*, 44(18):9400–9407, 2017.

1.82 The impact of shark skin denticles on the turbulent flat plate boundary layer

CHARLIE LLOYD^{†1}, JEFFREY PEAKALL¹, ALAN BURNS¹, GARETH KEEVIL¹ & ROBERT DORRELL²

¹University of Leeds

²University of Hull

The skin of sharks, unlike that of most other fishes, is comprised of small tooth-like structures called dermal denticles. The hydrodynamic function of shark skin has been of interest for several decades, with most attention being focussed on the riblet features which are often present on the denticle crown. In the present study we investigate the impact of three-dimensional shark skin denticles on a flat plate boundary layer flow. We adopt 2D Laser Doppler Anemometry (LDA) to measure boundary layer profiles over 3D printed arrays of two types of shark skin denticle; one based on a smooth *Poracanthodes sp.* sample, and the other a ribletted denticle of the same dimensions as the first, but with parallel riblets protruding from the denticle crown. Boundary layer measurements are taken in a recirculating flume at four flow rates, corresponding to Reynolds numbers of $Re_\theta \approx 400 - 1200$, based on the momentum thickness. This relates to dimensionless denticle heights of $h^+ \approx 8 - 30$.

The results show that drag reduction is not achieved for either of the denticle plates at any of the tested Reynolds numbers. However, the skin friction coefficient is significantly larger for the smooth denticle compared to the ribletted; the hydraulically smooth regime is maintained up to a denticle height of $h^+ \approx 15$ for the ribletted denticle, contrary to the smooth denticle which increases the skin friction coefficient by over 10% at this h^+ . The results also show that as the roughness height increases, the difference in skin friction between the ribletted and the smooth denticles also increases.

If there are hydrodynamic advantages to complex three-dimensional shark skin denticles outside the scope of this work, such as the reduction of boundary layer separation, then our results indicate that riblets significantly minimise any increase to skin friction that may occur as a result.

1.83 Structural and physical determinants of solute transport in complex microvascular networks

ALEXANDER ERLICH¹, PHILIP PEARCE², GARETH NYE³, PAUL BROWNBILL³, ROMINA PLITMAN MAYO⁴, OLIVER JENSEN¹ & IGOR CHERNYAVSKY^{1,3}

¹School of Mathematics, University of Manchester

²Department of Mathematics, MIT

³Maternal and Fetal Health Research Centre, St Mary's Hospital, Manchester

⁴School of Mechanical Engineering, Tel Aviv University

Across mammalian species, solute transport takes place in complex microvascular networks. However, despite recent advances in three-dimensional (3D) imaging, there has been poor understanding of geometric and physical factors that determine solute exchange and link the structure and function. Here, we use an example of the human placenta, a vital fetal life-support system, where the primary functional exchange units, terminal villi, contain disordered networks of fetal capillaries and are surrounded externally by maternal blood. We show how the irregular internal structure of a terminal villus determines its exchange capacity for a wide range of solutes. Integrating 3D image-based geometric and diffusive-advective-reactive transport features into new non-dimensional parameters, we characterise the structure-function relationship of terminal villi via a simple and robust algebraic approximation, revealing transitions between flow- and diffusion-limited transport at vessel and network levels. The developed theory accommodates for nonlinear blood rheology and tissue metabolism and offers an efficient method for multi-scale modelling. Our results show how physical estimates of transport, based on scaling arguments and carefully defined geometric statistics, provide a useful tool for understanding solute exchange in placental and other complex microvascular systems.

1.84 The Dynamics of Anisotropic Ice in Simple ConfigurationsDANIEL RICHARDS[†], SAM PEGLER, SANDRA PIAZOLO & OLIVER HARLEN

University of Leeds

Understanding the anisotropic flow of ice is likely a key factor for the reliable prediction of mass loss from the Earth's ice sheets, potentially to be the largest contributor to future sea-level rise over the course of the next few centuries. Our ability to project sea-level rise is limited by our ability to model the flow of ice. A potentially key ingredient is the anisotropy caused by the strain-dependent crystal lattice alignment of ice grains, which can be shown to cause the viscosity to vary by a factor of at least 9 in different directions, indicating a dominant control. Even though anisotropy is thus likely to have a large influence on flow configurations seen in ice sheets, its effects are currently poorly understood. For example, it is an open question as to how anisotropy influences the flow of glaciers and ice streams, the flow of ice around obstacles, at ice stream junctions and across grounding lines, regions which are key to controlling the large-scale mass balance.

This work compares the current state of the art methods for modelling anisotropy, which combines the modelling of the rheology with a director field for the crystal orientation. Analogies, both mathematical and physical, are drawn with fibre-suspension flows. Initial results show that the director-field model can represent the evolution of the crystal orientation to leading order when comparing behaviour with experiments of ice under compression and shear (Qi *et al.* 2019, Craw *et al.* 2018). This model is then coupled with various rheological models of anisotropic ice that have been proposed in the glaciological literature, yielding an evaluation of the validity of these models.

1.85 Supersonic wind tunnels: Effects of nozzle geometry

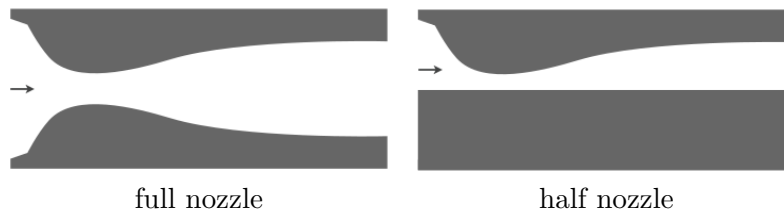
KSHITIJ SABNIS[†] & HOLGER BABINSKY

University of Cambridge

Experiments on supersonic flows are typically conducted in wind tunnels with either a “full” or “half” two-dimensional nozzle geometry, and these are generally considered to be equivalent. However, we have recently shown that the pressure distribution within the nozzle sets up secondary flows within the tunnel’s sidewall boundary-layers. These transverse velocities are different for the two nozzle configurations. The secondary flows significantly affect the sidewall boundary-layer thickness as well as the topology of streamwise vortices which exist within the corner boundary-layers. The nature of the flow in these corner regions, and thus the momentum contained within them, is therefore quite distinct for the two nozzle geometries.

The differences in corner boundary-layer are expected to be particularly salient in experiments focused on the response of the floor boundary-layer to an incident oblique shock. Established models in the literature (Xiang, 2019) show that that the location of corner separation strongly influences the flowfield elsewhere.

We therefore have an understanding of two key elements in this problem: first, we have found that the nozzle geometry determines the corner boundary-layer; secondly, the strong influence of corner separation on the overall flowfield is recorded in the literature. In order to link both findings, it is important to evaluate the influence of the corner boundary-layer on shock-induced corner separation. An oblique shock incident on the floor-boundary layer is introduced to both nozzle geometries. The difference in separation behaviour between the two nozzles is explained in the context of the distinct corner flows exhibited. Furthermore, the effects of these differences on floor boundary-layer separation elsewhere in the flowfield are analysed and compared with established models.



1.86 On the Lift Augmentation Mechanism of an Asymmetrically Pitching FoilSHŪJI ŌTOMO^{†1}, KAREN MULLENERS², KIRAN RAMESH³ & IGNAZIO MARIA VIOLA¹¹University of Edinburgh²École Polytechnique Fédérale de Lausanne³University of Glasgow

Research on unsteady aerodynamics has significantly grown in recent years due to its relevance to micro-air vehicles, mechanical swimmers, and flapping-foil energy harvesters. In these applications, a leading-edge vortex (LEV) might occur, resulting in a strongly non-linear relationship between forces and kinematics. We present experimental (force measurement and particle image velocimetry) and theoretical (Theodorsen's theory) studies on unsteady lift generated by a pitching wing and the corresponding dynamics of the LEV. We experimentally investigate the lift generation mechanism of a pitching NACA 0018 aerofoil section in a water flume at a Reynolds number of 3.2×10^4 . Time-resolved direct force measurement and two-dimensional particle image velocimetry (PIV) are performed. We employ smoothed triangular pitching kinematics to have a constant pitch rate for most of the period of oscillation, minimising the effect of pitching acceleration (i.e. non-circulatory forces). The reduced frequency is varied from 0.22 to 0.88 and pitching amplitude from 4° to 64° . We examine the effect of changing the amount of asymmetry in pitching kinematics. We find that the asymmetric kinematics allows to augment net lift. For the reduced frequencies $k_\xi \geq 0.4$ (k_ξ is the reduced frequency based on the faster part of asymmetric pitching kinematics), the wing experiences its maximum lift at the beginning of the deceleration phase before reaching the maximum angle of attack. This occurs for every pitching amplitude and any asymmetric configuration. These experimental results and those of Theodorsen's theory are in qualitative agreement. The connection between the LEV formation and the lift force is currently under investigation by computing the LEV circulation.

1.87 Evaporation-driven transport through soft hydrogels

MERLIN A. ETZOLD, M. GRAE WORSTER, & PAUL F. LINDEN
DAMTP, University of Cambridge

We will present an experimental and theoretical study of water transport in hydrogel, motivated by transpiration through leaves. A small region at the base of a saturated hydrogel bead is brought in contact with liquid water. The remainder of the surface is exposed to the atmosphere in a continuously purged relative humidity chamber. The bead shrinks until a steady state is reached in which the evaporated water is replenished through the bead from the reservoir that supplies its base. The steady-state bead size is highly sensitive to changes in bottom pressure or atmospheric conditions surrounding the bead.

We explain these results with a one-dimensional model. The hydrogel swells until equilibrium is reached between the internal swelling pressure and the elastic forces of the polymer chains that contribute to the distributed osmotic pressure in the bead. Water transport in steady state is maintained by a gradient in osmotic pressure, which is caused by a gradient in polymer fraction. Changes in the evaporation rate lead to an adjustment of the pressure gradient, which causes the polymer concentration gradient to change. If the bottom pressure is changed, the partial shrinkage of the hydrogel leads to a decreased permeability and therefore to an adjustment of the pressure gradient as well.

Apart from the biological importance, similar transport processes are relevant for a plethora of technical applications employing hydrogels, such as soft contact lenses, tissue engineering, drug delivery and hazardous material handling.

1.88 Aerodynamic Optimisation of Supersonic Aerofoils Based on Deep Neural Networks

AARON FERIA-ALANIS[†] & ANTONIOS F. ANTONIADIS

Cranfield University

The scope of this research is the development, implementation and analysis of transonic and supersonic aerofoil optimisation by Deep Neural Networks (DNN) based on inverse design [1].

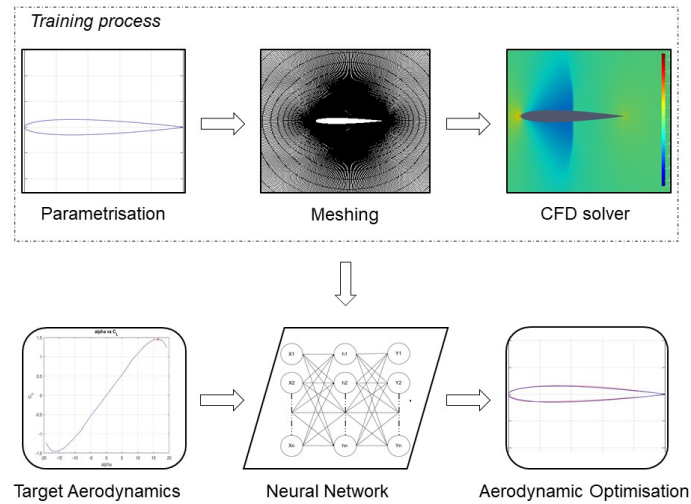
Deep learning techniques combined with comprehensive and complete database of aerodynamic data can form the pillars of aerodynamic shape optimisation [2]. The work-flow of the computational framework is shown in Figure 11; the training process initialises the parameterisation of the aerofoils. The parameterisation scheme performs the necessary dimensional reduction of the features in the database. Several airfoil parameterisation algorithms are assessed and evaluated e.g., Parsec, CST, iCST. The analysis demonstrated that the Class/Shape Transformation (CST) parameterisation scheme is the most suitable for this research. A automated mesh technique is designed and implemented to capture essential fluid dynamics phenomena of the flow (e.g., shock wave, rarefaction, shock-wave boundary layer interaction) around the aerofoil. The aerodynamic computations are performed for 320 aerofoils with angles of attack ranging from -10 to 10 and Mach numbers ranging from 0.8 to 3.0. Spatial discretisation is accomplished with the Jameson-Schmidt-Turkel (JST) scheme and with convergence is reached by the backward Euler implicit numerical scheme [3]. The database is constructed with the CST parameters for all aerofoil and their respective aerodynamic characteristics from the CFD solver. The deep neural network is then trained, validated (cross-validation) and evaluated against the database. An extensive investigation of the effect from different DNN configurations takes place in this research. The DNN used in this work is a ten layered feed forward back propagation with Bayesian Regularization neural network for the regression problem.

Acknowledgements: The authors acknowledge the computing time on the High-Performance Computing facility, Delta at Cranfield University. This research is funded by the National Council for Science and Technology (CONACYT - Mexico).

References:

1. Artificial Neural Network based inverse design: Airfoils and wings, Gang Sun, Yanjie Sun, Shuyue Wang, Aerospace Science and Technology, Vol. 42, pages: 415-428, 2015
2. Neural Networks based airfoil generation for a given C_p using BezierPARSEc parameterization, Athar Kharal and Ayman Saleem, Aerospace Science and Technology, Vol. 23, pages: 330-344, 2012
3. Numerical Solution of the Euler Equations by Finite Volume Methods: Central versus Upwind Schemes, Murat UYGUN and

Figure 11: The ANN is trained using the data from the CFD simulations and the parameters from the parameterisation scheme. After the training process the ANN is used to predict the shape parameters for desired transonic/supersonic aerodynamic characteristics.



Kadir KIRKKPR, Journal of Aeronautics and Space Technologies, Vol. 2, pages: 47-55, 2005.

4. Universal Parametric Geometry Representation Method, Brenda M. Kulfan, Boeing Commercial Airplane Group, Seattle, Washington 98124, Journal of Aircraft Vol. 45, No. 1, January-February 2008
5. Direct Numerical Simulation of 2D Transonic Flows Around Airfoils, Tapan K. Sengupta, Ashish Bhole, N.A. Sreejith, Computers and Fluids, Vol. 83, pages: 19-37, 2013

1.89 Adjoint-based optimal control of an inkjet waveformPETR KUNGURTSEV[†] & MATTHEW P. JUNIPER

Department of Engineering, University of Cambridge

A drop-on-demand inkjet printhead contains narrow microchannels, each with a piezoelectric actuator and a small orifice. The actuator is an active control element: when an electric current is applied to it, the actuator deforms and creates acoustic waves which in turn push a droplet out of the orifice. After each pulse, acoustic reverberations remain in the channel until they decay or propagate out of the channel. Also, the orifice meniscus remains deformed and oscillates until the surface energy is transferred to the fluid. If the next pulse is applied before the reverberations have sufficiently died away, or the meniscus is still deformed, the next droplet can differ from previous droplets, reducing print quality.

The total energy of the system consists of the acoustic oscillations energy and the surface energy. We model the flow using thermoviscous acoustic equations, and derive a reduced order model for the meniscus dynamics. We apply the adjoint method to derive the sensitivity of the total energy with respect to the actuation pulse shape, or the waveform, and use gradient-based algorithms to damp the residual acoustic waves and minimize the meniscus deformation by the time the next droplet is demanded. We propose a method for optimal control of the acoustic flow coupled with a free surface, and demonstrate how to decrease the residual energy by several times.

1.90 On the formation of hydraulic jump for low- and high-viscosity liquids

ROGER E. KHAYAT & YUNPENG WANG

Department of Mechanical and Materials Engineering,
University of Western Ontario

The free-surface flow formed by a circular jet impinging on a stationary disk is analysed theoretically to predict the location and height of the jump. For a high-viscosity liquid, the formulation reduces to a problem, involving only one parameter: $\alpha = \text{Re}^{1/3}\text{Fr}^2$, where Re and Fr are the Reynolds and Froude numbers based on the flow rate and the jet radius. We show that the jump location coincides with the singularity in the thin-film equation when gravity is included, suggesting that the jump location can be determined without the knowledge of downstream flow conditions such as the jump height, the radius of the disk, which corroborates earlier observations in the case of type I circular hydraulic jumps. Consequently, there is no need for a boundary condition downstream to determine the jump radius. Our predictions confirm the constancy of the Froude number Fr_J based on the jump radius and height as suggested by the measurements of Duchesne et al. (2014). For low- and high-viscosity liquids, the height of the jump is sought subject to the thickness value at the disk edge, based on the capillary length and minimum flow energy. The edge thickness is found to be negligible for high-viscosity liquids (Wang & Khayat 2018, 2019).

References:

1. Duchesne, A., Lebon, L. & Limat, L. 2014 Constant Froude number in a circular hydraulic jump and its implication on the jump radius selection. *Europhys. Lett.* **107**, 54002.
2. Wang, Y. & Khayat, R.E. 2018 Impinging jet flow and hydraulic jump on a rotating disk. *J. Fluid Mech.* **839**, 525-560.
3. Wang, Y. & Khayat, R.E. 2019 The role of gravity in the prediction of the circular hydraulic jump radius for high-viscosity liquids. *J. Fluid Mech.* **862**, 128-161

1.91 Vesicle transport and cytoplasmic streaming in the pollen tube

R. J. DYSON¹, J. TYRRELL¹, Y. CHEBLI², D. J. SMITH¹ &
A. GEITMANN²

¹School of Mathematics, University of Birmingham

²Department of Plant Science, McGill University

The rapid elongation of the pollen tube in seed plants cannot occur without the transport of sufficient cell wall and membrane material to the growing apex. The movement of this material, delivered via exocytic secretory vesicles, can be categorised under two regimes: ‘long distance’ movement in the shank (via active transport along actin filaments), and ‘short distance’ movement in the apex (where vesicles diffuse and advect freely). Many current models of vesicle transport focus on diffusion in the apical region alone, neglecting advective effects as well as the resulting distribution profile in the pollen tube shank. Using the method of regularised Stokeslets with an adjustment made for axisymmetry, we produce a complete advective velocity profile for cytosolic flow in the tube based on the drag induced by the active transport of vesicles along actin. We use this to calculate exocytic and endocytic vesicle motion in the tube, incorporating vesicle uptake and deposition at the wall, and generating insight into pollen tube growth dynamics.

1.92 Computational Aerodynamic Solutions of Hovering Rotors by High-Order Schemes on Unstructured Grids

PAULO A. S. F. SILVA[†], FRANCESCO RICCI, PANAGIOTIS
TSOUTSANIS, KARL W. JENKINS & ANTONIOS F. ANTONIADIS

Cranfield University

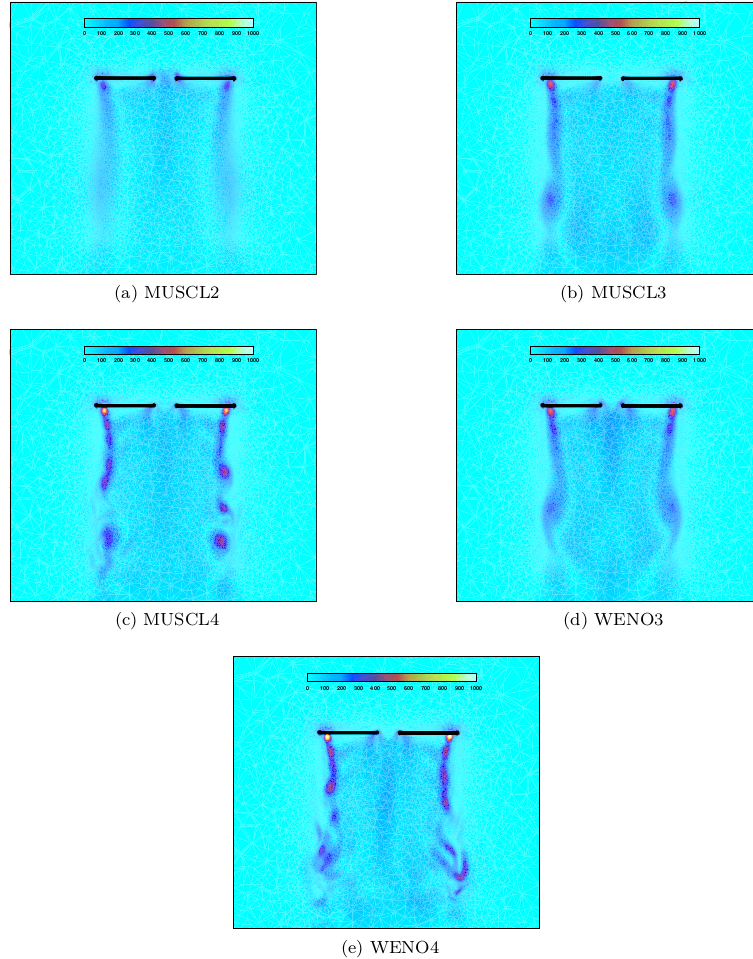
This paper concerns the development, implementation and assessment of high-order finite volume schemes for hovering rotors. The high-order numerical schemes are implemented on rotating reference frame and for the mixed-element unstructured grid framework. The Reynolds averaged Navier-Stokes equations are approximated with up to fourth-order accurate spatial schemes, the Spalart Allmaras model [1] in the implementation described by Antoniadis et al. [2]. Two classes of spatial discretisation schemes are implemented and evaluated, the Monotonic Upwind Scheme for Conservation laws (MUSCL) and Weighted Non-Oscillatory (WENO). Convergence is accelerated with the Lower-Upper Symmetric Gauss-Seidel (LU-SGS) [3] implicit backward Euler time integration. A single reference frame approach is adopted where the governing equations are formulated based on absolute velocities, the HLLC Riemann solver [4] is modified as well as the implicit solver to account for the rotational nature of the simulated problems. We evaluate our implementation on well established rotor configurations: Caradonna and Tung [5], UH-60a [6] and PSP [7]; and compare with experimental measurements. Our findings indicates that the fourth-order MUSCL and WENO are promising in capturing and preserving the vortex trajectory, as show Fig. 12. We carry out a grid sensitivity analysis were evaluated the Figure of Merit for the PSP and UH-60a case, as see in Fig. 13 Both schemes predict the blade tip vortex interaction, contraction, convection and strength of the vortices up three full revolutions. In the presence of shocks, both high-order schemes accurately predict the shock position and strength.

Acknowledgements: The authors acknowledge the computing time on the High-Performance Computing facility, Delta at Cranfield University. During this study, Paulo A. S. F. Silva was supported by the Coordenação de Aperfeiçoamento de Pessoal de Nível Superior - Brasil (Capes) - Finance Code 001 (No 88881.128864/2016-01).

References:

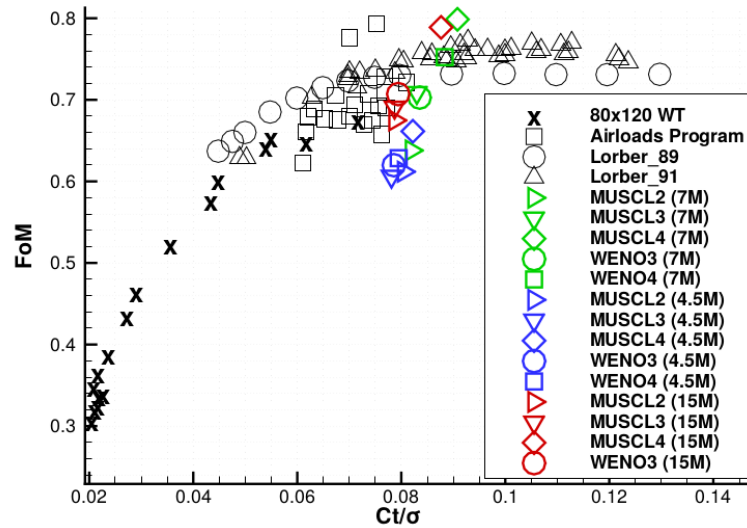
1. M. L. Shur, M. K. Strelets, A. K. Travin, P. R. Spalart, Turbulence modeling in rotating and curved channels: assessing the spalart-shur correction, AIAA journal 38 (5) (2000) 784–792.
2. A. F. Antoniadis, P. Tsoutsanis, D. Drikakis, Assessment of high-order finite volume methods on unstructured meshes for rans solutions of aeronautical configurations, Computers & Fluids 146 (2017) 86–104.
3. M. Parsani, K. Van den Abeele, C. Lacor, E. Turkel, Implicit lu-sgs algorithm for high-order methods on unstructured grid with

Figure 12: Vorticity magnitude contours for a longitudinal section of Caradonna and Tung rotor [5].



- p-multigrid strategy for solving the steady navier–stokes equations, *Journal of Computational Physics* 229 (3) (2010) 828–850.
4. E. F. Toro, *Riemann solvers and numerical methods for fluid dynamics: a practical introduction*, Springer Science & Business Media, 2013.
 5. F. X. Caradonna, C. Tung, Experimental and analytical studies of a model helicopter rotor in hover.
 6. P. LORBER, R. STAUTER, A. LANDGREBE, A comprehensive hover test of the airloads and airflow of an extensively instrumented model helicopter rotor, in: *AHS, Annual Forum*, 45 th, Boston, MA, 1989.
 7. A. N. Watkins, B. D. Leighty, W. E. Lipford, K. Z. Goodman, J. Crafton, J. W. Gregory, *Measuring surface pressures on rotor*

Figure 13: Computed Figure of merit at $M_{tip} = 0.63$ and pitch angle equal to 12° for UH-60a in all schemes and meshes and experimental data [8, 9, 6, 10].



blades using pressure-sensitive paint, AIAA Journal 54 (1) (2015) 206–215.

8. P. M. Shinoda, H. Yeo, T. R. Norman, Rotor Performance of a UH-60 Rotor System in the NASA Ames 80-by 120-Foot Wind Tunnel, Tech. rep.
9. W. G. Bousman, Power measurement errors on a utility aircraft, Tech. rep., NATIONAL AERONAUTICS AND SPACE ADMINISTRATION MOFFETT FIELD CA AMES RESEARCH ... (2002).
10. P. F. Lorber, Aerodynamic Results of a Pressure-Instrumented Model Rotor Test at the DNW, Journal of the American Helicopter Society 36 (4) (1991) 66–76.

1.93 Simulation of turbulent flows with Nek5000DANIEL FENTON[†]

School of Engineering, Cardiff University

Nek5000 is a high-order spectral element code developed for the numerical simulation of a vast array of fluid dynamic systems, with applications in fields such as turbulence and combustion for highly accurate direct numerical simulation (DNS). Whilst more computationally expensive, DNS of a turbulent flow possesses the benefit over the alternative large eddy simulation (LES) of not requiring modelling on the smallest length scales, in so far as DNS produces explicit solutions to the Navier-Stokes and continuity equations. In fact, the small-scale effects can play a significant role in the evolution of certain systems, for example the near-wall flow of a turbulent channel, and consequently DNS leads to a more accurate statistical study of the flow properties. The objective of this work is to assess the use of Nek5000 in terms of its applicability to the study of turbulence in relatively high Reynolds number incompressible Newtonian flows, by means of comparison to well established benchmark results obtained by other studies. The performance of the code in more complex turbulent flows will also be assessed.

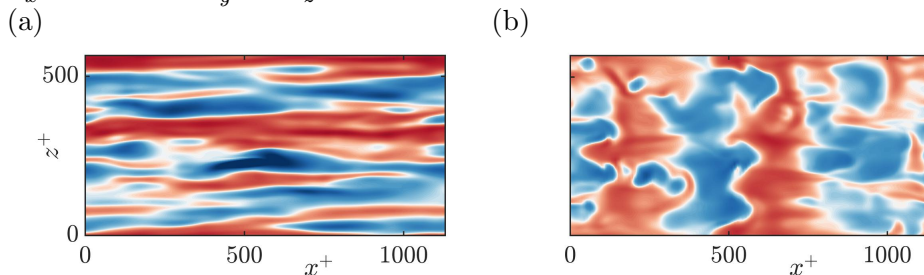
1.94 Drag reduction by anisotropic permeable substrates – analysis and DNS

GARAZI GÓMEZ-DE-SEGURA[†] & RICARDO GARCÍA-MAYORAL

Department of Engineering, University of Cambridge

We explore the ability of anisotropic permeable substrates to reduce turbulent skin-friction drag, studying the influence that these substrates have on the overlying turbulence. For this, we perform DNSs of channel flows bounded by streamwise-preferential permeable substrates, where the flow within the permeable substrate is modelled using Brinkman’s equation. The results confirm theoretical predictions, and the resulting drag curves are similar to those of riblets. For small permeabilities, the curves exhibit a linear regime [1,2], where drag reduction is proportional to the difference between the streamwise and spanwise permeabilities. This linear regime breaks down for a critical value of the wall-normal permeability [3], beyond which the performance begins to degrade. We observe that the degradation is associated with the appearance of spanwise-coherent structures, as shown in Fig. 14, and which is attributed to a Kelvin-Helmholtz-like instability of the mean flow. This feature is common to a variety of obstructed flows, and linear stability analysis can be used to predict it. For large permeabilities, these structures become prevalent in the flow, outweighing the drag-reducing effect of slip and eventually leading to an increase of drag. These results and the models subsequently developed provide design guidelines to produce a drag-reducing permeable substrate. For the substrate configurations considered, the largest drag reduction observed is $\approx 20 - 25\%$ at a friction Reynolds number $Re_\tau = 180$, which is at least twice that obtained for the riblets studied by Bechert *et al* [4].

Figure 14: Instantaneous realisations of the streamwise velocity at $y^+ \approx 2.5$ for (a) a substrate in the linear drag-reducing regime, with permeabilities $K_x^+ = 3$ and $K_y^+ = K_z^+ = 0.023$; and (b) in the drag-increasing regime, with $K_x^+ = 117$ and $K_y^+ = K_z^+ = 0.9$.



References:

1. Luchini *et al.*, *J. Fluid Mech.* **228**, 87–109 (1991)
2. Jiménez, *Phys. Fluids* **6**, 944 (1994)
3. Gómez-de-Segura *et al.* *Submitted to Journal of Fluid Mechanics*
4. Bechert *et al.*, *J. Fluid Mech.* **338**, 59–87 (1997)

1.95 Particle-laden gravity currentsMARTIN C. LIPPERT[†] & ANDREW W. WOODS

BP Institute, University of Cambridge

We explore the dynamics of sedimenting gravity currents produced when issuing a mixture of particles and fresh water into a flume tank filled with fresh water. The negative buoyancy of the gravity currents is provided by monodispersed Silicon-Carbide particles. We present novel experiments in which we use light-attenuation techniques to visualise the shape of these currents.

The particles have diameters between 10 and 100 micrometres and the Reynolds number of the gravity currents are in the range from 500 to 1500. The experiments show that the height of the gravity current reduces with distance from the source. Using dye, we visualise a continuous emergence of source liquid from the top of the gravity current along the entire length of the current, indicating that the current does not remain well-mixed.

Our experiments are complemented by a simple theoretical model based on the conservation of volume and momentum fluxes, taking into account the separation of the liquid and the particles. The model quantifies the sedimentation of particles as well as the velocity, height and run-out length of the gravity currents. The model assumes a constant settling velocity of the particles, corresponding to their Stokes' velocity.

We find that our experimental measurements on the gravity currents are in good accord with the model predictions in the investigated range.

1.96 Sound generation by entropy perturbations passing through cross-sectional area changes

DONG YANG, JUAN GUZMÁN & AIMEE S. MORGANS

Department of Mechanical Engineering, Imperial College London

Entropy perturbations are also known as temperature variations or “hot spots”. Physically, they can be generated by any unsteady heat release, unsteady heat transfer and viscous effect. These entropy fluctuations remain silent when advected by a non-accelerated mean flow but generate additional sound when accelerated. In many laboratory-scale experiments which study this phenomenon, mean-flow acceleration is achieved by using sudden cross-sectional area changes, such as a hole. Several analytical models that predict entropy noise in nozzles exist for a wide range of parameters. These models are often based on inviscid flow and no separation in the mean flow. However, for the cases with sudden cross-sectional area changes, the mean flow may separate, especially at a sudden expansion. This makes previous models inadequate in predicting the associated sound generation.

In the present work, we develop an analytical model based on the Green’s function method which can identify the detailed sound source in the cases with mean flow separation. Sound generations by entropy perturbations passing through both a sudden flow contraction and expansion are studied. Numerical simulations which introduce low-amplitude entropy fluctuations upstream of the cross-sectional area changes are also performed to validate the model.

1.97 Shape sensitivity analysis of thermoacoustic instability in an annular combustor using an adjoint Helmholtz solverSTEFANO FALCO[†]

Department of Engineering, University of Cambridge

Thermoacoustic oscillations, due to the interaction between unsteady heat release and sound waves, are a serious threat to gas turbines and rocket engines. These instabilities often appear in the late stages of the design process, the main reason being that they are extremely sensitive to small changes in the parameters of the system. Tools for finding cheaply and accurately the most stabilizing design changes are therefore needed.

In this study, a finite element solver for computing the thermoacoustic modes and their sensitivities is presented. The relevant equation is an inhomogeneous Helmholtz equation with distributed heat release and acoustic impedance boundary conditions. It is a nonlinear eigenvalue problem for the angular frequency that is solved using a fixed-point iteration. The solver is written using the open-source computing platform FEniCS and consists of both a direct and an adjoint solver.

The first-order shape derivative in Hadamard form for the eigenvalues is derived considering the eigenvalues as objective in a constrained shape optimization problem.

A two-dimensional model of the annular chamber present at Cambridge University Engineering Department is then studied. The combustor has an unstable longitudinal mode. The thermoacoustic modes of the annular combustor are computed and the influence of small geometry modification is assessed using the direct-adjoint solver.

1.98 High density ratio lattice Boltzmann simulations [Retracted]

1.99 On dispersion in heterogeneous porous rocks

NEERAJA BHAMIDIPATI[†] & ANDREW W. WOODS

BP Institute, University of Cambridge

We study the dispersion of tracer by a pressure-driven flow through a porous rock of finite thickness which is bounded above and below by impermeable seal rock. We assume that the heterogeneity of the rock is due to an assemblage of high permeability lenses within the formation. We further assume that the lenses are at randomly assigned vertical locations and that they are sufficiently far apart horizontally so that the flow field associated with individual lenses is independent of other lenses in the formation. We define a dilution coefficient $\alpha_{cr} = l/L_{cr}$ where l is the length of each lens and L_{cr} is the distance between successive lenses. When the distance between the lenses is $L \geq L_{cr}$ ($\alpha = l/L \leq \alpha_{cr}$) the lenses are in the dilute limit where their flow fields are sufficiently decorrelated. For each lens, if a passive tracer is released into the flow through this formation, the permeability contrast between the lens and the formation causes a finite longitudinal shearing of the tracer. If the tracer passes through a series of such lenses, the net distortion of the tracer is given by the net effect of the distortions associated with each lens. Since these are positioned randomly across the channel, the streamlines in the centre of the channel tend to be influenced more than the streamlines at the edge of the channel, and this leads to an effective shear of the flow when averaged over many lenses. However, owing to the random position of the lenses, there is a variability of the actual displacement of the tracer relative to this mean, and when averaged over many lenses this appears as an effective dispersivity. We compare the results of the numerical calculations for the flow through a series of lenses, in which each lens is located at different vertical positions within the aquifer, with a continuous model given by the advection-dispersion equation for the transport of the tracer at each height in the formation, using the mean speed and mean dispersivity at that height. Our calculations show that once the flow has passed through 4-5 lenses, there is good agreement of the numerical calculations and the continuous model. This illustrates that initially the spreading of the tracer is controlled by the dispersivity, leading to the tracer spreading at a rate proportional to $t^{1/2}$, but that later the spreading is controlled by the shear at a rate proportional to t . We find that the transition between these two regimes occurs at a time $\tau = 2\bar{D}/\Delta U^2$ where \bar{D} is the mean longitudinal dispersivity and ΔU is the shear strength.

1.100 Internal gravity waves, shear, and mixing in forced stratified turbulence

CHRISTOPHER J. HOWLAND[†], JOHN R. TAYLOR &
COLM-CILLE P. CAULFIELD

DAMTP, University of Cambridge

Wind and tides are two primary drivers of the ocean circulation. Some of the energy input is dissipated through small-scale turbulence in boundary layers near the top and bottom of the ocean, but a large fraction of the energy input is converted to internal gravity waves. Energy is thought to cascade from large scales to small scales through wave-wave interactions, down to a scale of approximately 10m. At yet smaller scales, stronger wave-wave interactions, shear instabilities and wave breaking lead to turbulent mixing, albeit through turbulence that is strongly affected by stratification.

This irreversible mixing is vital for maintaining the density profile of the deep ocean, and it also controls the level of biological activity in the upper ocean. In the pycnocline, where energy is typically supplied through internal waves, it is not clear whether shear-driven mixing or more efficient convective mixing is more prevalent.

To determine the importance of internal waves for modifying the nature of mixing in stratified turbulence, we perform direct numerical simulations of a Boussinesq fluid subjected to background shear and different types of large-scale forcing. We compare the results of simulations forced by purely horizontal motions against those forced by internal gravity waves. We therefore identify how key quantities such as mixing efficiency and vertical diffusivity vary with the type of forcing, and isolate the mechanisms responsible for the differences. We also investigate how well existing parametrisations of mixing capture the behaviours of the flows and how much information observational-style sampling can capture in each type of flow.

1.101 A unified approach to the study of turbulence over smooth and drag-reducing surfacesJOSEPH I. IBRAHIM[†] & RICARDO GARCÍA-MAYORAL

Department of Engineering, University of Cambridge

Some complex surfaces, such as riblets, anisotropic permeable coatings and superhydrophobic surfaces, can reduce turbulent skin-friction drag through the use of small-scale texture. Essentially, they achieve this by impeding the streamwise flow less than the spanwise and wall-normal fluctuations. As a result, the quasi-streamwise vortices associated with the near-wall cycle of turbulence are ‘pushed’ away from the surface with respect to the mean flow. Provided that surface manipulations are small, the flow will perceive the texture in a homogenised fashion, whereby the different velocity components, on average, experience different ‘virtual origins’ with respect to some reference plane. The change in drag is then observed as a positive outward shift of the mean velocity profile.

Virtual origins for the streamwise and spanwise velocities have typically been imposed using Robin boundary conditions that introduce a slip-length coefficient. These take the form $u = \ell_x \partial u / \partial y$ and $w = \ell_z \partial w / \partial y$, respectively. We extend this framework to applying a virtual origin for the wall-normal velocity as well, where $v = \ell_y \partial v / \partial y$, and conduct direct numerical simulations with different ‘slip lengths’ for the different velocities. We show that these boundary conditions affect the flow by setting the virtual origins for the mean flow and the turbulent fluctuations, embodied principally in the quasi-streamwise vortices of the near-wall cycle. The virtual origin for the mean flow is set by the streamwise slip length, ℓ_x , while that for the turbulence is set by ℓ_y and ℓ_z . We characterise these origins in terms of ℓ_x , ℓ_y and ℓ_z , and we show that, other than by the shift in origin, the turbulence in the flow remains essentially smooth-wall-like.

1.102 On analytical solutions for the mean wind profile in an urban canopy

OMDUTH COCEAL

NCAS, University of Reading

There is continuing interest in simple models for the mean wind profile within urban canopies. Analytical models such as the exponential velocity profile have proved popular as a first approximation. However, the existence of analytical solutions usually depends on assumptions whose physical validity is not always justified in the parameter regimes in which they are applied. We here instead propose a method for obtaining approximate analytical solutions that conform to more physically realistic urban canopy models, and illustrate it with one-parameter and two-parameter models. The inherent flexibility of the approach allows its application in other contexts.

1.103 The effect of rotor wakes on compressor flow field within the multistage machinesPAWEL J. PRZYTARSKI[†] & ANDREW P. S. WHEELER

Department of Engineering, University of Cambridge

Flows within the multi-stage compressors feature complex interactions between stationary and rotating blades coupled with high free-stream turbulence effects. These flowfields are difficult to study experimentally while standard modelling techniques are unfit to reliably capture the physics of the flow. In the present work we focus on the role of periodic forcing from rotor wakes on compressor flowfield.

We employ high fidelity simulations of two compressor blade geometries and use new numerical method that allows us to mimic the multi-stage environment. To do that we sample the velocity field behind the blade and feed it through the inlet. By continuously recycling the flowfield we reach a type of ‘repeating stage’ simulation that is free of any assumptions regarding inflow turbulence, such as intensity, lengthscales or spectrum.

We use those results to address the question of the true nature of turbulence in a multi-stage environment as well as show how periodic and turbulent unsteadiness affects boundary layer transition mechanisms. We then show how rotor wake interactions are crucial for entropy generation within the passage and that this is a consequence of a feedback mechanism that leads to elevated turbulence production.

1.104 Detour induced by the piston effect in double-diffusive convection of near-critical fluidsZHAN-CHAO HU[†] & XIN-RONG ZHANGDepartment of Energy and Resources Engineering,
Peking University, Beijing

The nonlinear oscillatory double-diffusive convection in a thermodynamically near critical binary fluid layer is investigated. The setup of the problem can be interpreted as the Rayleigh-Bénard convection subjected to a stabilizing concentration gradient. The bifurcation of the system is first studied. Two subcritical bifurcation branches are depicted, which, together with the trivial branch of pure diffusion, are connected by two hysteresis loops. To understand the role of the piston effect, the Boussinesq counterpart of the near-critical system is considered and compared. Results show the onset of convection is significantly altered by the piston effect. For the Boussinesq system, the lower boundary layer becomes unstable, brings on finite amplitude perturbations and leads to the final state. However, the near-critical system features a two-stage evolution. In the first stage, the lower boundary layer becomes unstable and then returns to stability. As soon as the temperature field relaxes into the second stage, a change of criterion occurs, and the fluid becomes unstable again. The remaining convection motions serve as small perturbations, which amplify and finally result in finite-amplitude convection. By this means, the near-critical system becomes insensitive to the existence of the other equilibrium state in hysteresis loops, and detours relative to the Boussinesq system are observed.

1.105 Turbulence in the Body of Gravity CurrentsCAROLINE MARSHALL[†]

University of Leeds

While the ubiquitous nature of gravity currents means they have been extensively studied, this research has focused almost exclusively on the head of the flow. The body is typically neglected, despite forming the largest component of most natural flows. This work aims to quantify the three-dimensional turbulent structure of the body of constant-influx solute-based gravity currents using a combination of three-dimensional direct numerical simulation (DNS), and planar and tomographic particle image velocimetry (PIV).

DNS was used to investigate the influence of both Reynolds and Schmidt numbers on the formation of large-scale coherent structures within the flow body. These structures are of interest due to their ability to transport mass, momentum and temperature, and therefore influence properties such as erosion and deposition in particle-laden flows. In this case, Reynolds number was varied by altering the degree of slope. Planar PIV was used to investigate the effect of varying Reynolds number on the body by changing either the degree of slope or the rate of fluid influx.

This work describes the structure of the body of constant-influx gravity currents for the first time, and highlights the three-dimensional turbulent nature of the flow. The cross-stream and vertical velocity components of the flow were found to be of similar magnitude in this simple ducted domain. The influence of both the Reynolds and Schmidt numbers on the formation of coherent structures within the body were investigated, and the impact of these structures on flow dynamics was established.

1.106 A new approach to modelling polydisperse sprays with phase exchange based on the Fully Lagrangian Approach

OYUNA RYBDYLOVA, YUAN LI & TIMUR ZARIPOV

University of Brighton

The focus of this study is development and implementation of a new mathematical model for simulations of sprays. The model is based on the Fully Lagrangian Approach (FLA). According to this approach, particles/droplets are treated as a continuum (or a set of continua). The dispersed phase parameters are calculated from the solution of ODE systems along chosen particle/droplet trajectories. Unlike conventional Lagrangian particle tracking methods, however, particle/droplet number density is calculated using the continuity equation in the Lagrangian form. This approach was shown to be promising as in comparison to conventional methods, it requires less computational resources to obtain admixture number density distribution with the same order of accuracy. The FLA is being further developed to take into account polydispersity of droplets in sprays, droplet evaporation and condensation. To achieve this, the continuity equation in the FLA has been generalised by introducing a particle distribution function (PDF). This function represents the distribution of droplets over space, sizes, and time. The set of Lagrangian variables has been increased to include initial droplet size. This approach has been applied to 1D and 2D flows of evaporating droplets for validation against analytical solution. The new model has been implemented as a stand-alone in-house code and as an additional library to OpenFOAM.

**1.107 Aerosol generation from liquid droplet impact on solid surfaces
[Poster]**ISLAM SALEM[†]

University of Leeds

The number of nuclear facilities that are becoming obsolete and require decommissioning is already large and accelerating. Traditional methods of nuclear decommissioning are very expensive, it was estimated that the decommissioning of all UK nuclear sites would cost in the excess of £100 billion (NDA, 2013). The common methods of decontamination results in a large amount of waste and are labour intensive, due to the repetitive nature of these processes. A fairly new technique is spray decontamination, where a decontamination gel is jet sprayed into a wall (containing radioactive waste); penetrating voids, then the washed waste is collected and treated. Liquid jets made up of the decontamination gel break up into droplets, sized in the millimetre domain due to the Plateau-Rayleigh instability. These droplets then impact a solid substrate, resulting in either spreading, splashing or rebounding. An undesirable outcome is splashing in this case, due to the formation of micron sized aerosol droplets which are light enough to become airborne, contaminating the environment in the process. The interest in the topic is not only solely due to its practical and natural significance but also due to the rich theoretical (fluid mechanics) insight that can be gained from it (Raman, et al., 2016). This project is motivated by the desire and the benefit to understand the nature of a liquid droplet impact on a solid substrate with a particular interest in droplet splashing.

1.108 Quantifying the effect of morphological features of river channels on discharge relationsDUNCAN LIVESEY[†]

University of Leeds

Satellite-based passive microwave sensors can be used to estimate the discharge of large rivers. Microwave sensors track changes in emitted microwave intensity from river reaches which can be correlated with changes in water surface area in the reach. Changes in surface area, and so microwave intensity, can be used to estimate discharge by using a rating equation. These rating equations are reach specific and require calibration either from hydraulic models or in situ measured data.

In situ gauging stations monitor stage (water height) and estimate discharge through a cross-section of a river using a stage-discharge rating equation. These rating equations are based on at-a-station hydraulic geometry (AHG) and have been well investigated but much less work has been done on relating surface area over a reach to discharge. Further work on the relation between water surface area and discharge in a river reach is required to better constrain these relations and so improve the estimation of discharge. This work focusses on how morphological features of river channels, such as river meanders, can affect these surface area – discharge rating equations.

1.109 Fluid dynamics of single/multiple droplets onto a substrate with a topographical feature

K. H. A. AL-GHAITHI[†], M. C. T. WILSON, O. G. HARLEN &
N. KAPUR

University of Leeds

The use of inkjet printing to manufacture printed electronics has been receiving increasing attention due to the technique's potential for roll-to-roll manufacturing, lower cost and flexibility. As the droplets used for printing become smaller $O(10\mu\text{m})$, substrate topographical features (designed or due to minor variations) can affect the dynamics and equilibrium morphologies of the printed liquid. Here, the interaction of droplets with a surface featuring an open microchannel are explored. Such a feature could represent a designed structure and allow us to investigate the effect of its dimensions on the printed morphology. A 3D GPU-enabled multiphase Lattice Boltzmann Method is used. The GPU speed-up enables running parametric studies in affordable simulation time. This implementation also captures partial wetting and contact angle hysteresis. The latter is significant as stable continuous printed lines form only if the receding contact angle is very low or zero [1]. The model is validated using experimental data from the literature.

The effect on dynamics and equilibrium morphologies of a single droplet as the depth and width of the feature change is investigated using the developed simulation methodology. Varying the width and depth of the microchannel relative to the droplet size reveals six different morphologies varying from complete imbibition into the microchannel to almost just a spherical cap. An example morphology is seen in Fig. 15. In addition, a series of droplets that form a continuous printed line are simulated to ascertain what depths and widths of the feature cause breaks in continuity of the line.

Acknowledgements: The authors thank EPSRC and Dupont Teijin Films (DTF) for supporting this work. We would particularly like to thank Andrew Bates and Kieran Looney from DTF.

References:

1. Schiaffino S., and Sonin A. A. 'Molten droplet deposition and solidification at low Weber numbers' *Physics of Fluids*, **1997**, 9, 3172-3187.

Figure 15: Top View of the equilibrium morphology for a droplet impacting a feature with depth and width of 0.2 and 0.4 times the in-flight droplet diameter respectively.



1.110 Pulse propagation in quasi-laminar gravity currents [Retracted]

1.111 Energy cascade in a homogeneous swarm of bubbles rising in a vertical channel

BRUNO FRAGA¹, CHRIS C. K. LAI², WAI HONG RONALD CHAN³ & MICHAEL DODD³

¹School of Engineering, University of Birmingham, UK

²Physics Division, Los Alamos National Laboratory, USA

³Center for Turbulence Research, Stanford University, USA

The cascade of kinetic energy is a defining characteristic of fluid turbulence. For single-phase flows, the Richardson-Kolmogorov phenomenology provides a satisfactory first approximation of the energy cascade with which many existing turbulence models/theories are based. However, the phenomenology has not been demonstrated in two-phase flows where the production by the dispersed phase is an additional source of liquid turbulent kinetic energy.

We use bubble-resolved, direct numerical simulations to investigate the energy cascade in homogeneous swarms of air bubbles rising a vertical channel. We consider millimeter-sized bubbles with a bubble Reynolds number of 500. The von Karman-Howarth-Monin (K-H-M) equation is adapted for the two-phase flow and used to quantify the interscale energy transfer and to compute the scale-by-scale energy budget.

A parametric study on bubble size influence on the inter-scale energy transfer under constant void fraction is performed to better understand the mechanisms of wake-to-wake interaction. The use of an Eulerian-Lagrangian algorithm allows us to generate rigid bubbles of constant size. The difference between rigid and deformable bubbles in terms of turbulent kinetic energy production is analysed by comparing the former results with an equivalent case solved using a Volume-of-Fluid algorithm.

1.112 Numerical Simulation of a Bubble Swarm: Void Fraction and Bubble Size Analysis

ERNESTO RAMA NOVO & BRUÑO FRAGA

School of Engineering, University of Birmingham

There are many unknown mechanisms dictating how energy is transferred among the different scales of a flow with the presence of bubbles. In order to analyse this phenomenon within a CFD framework, an in-house direct numerical simulation (DNS) code is employed. The aforementioned code consists on a finite difference scheme with the added functionality of an immersed boundary method (IBM) used to model any interaction with the second phase present in the flow.

Experimental results show that in such flows the behaviour of the normal homogeneous isotropic turbulence spectra ($-5/3$ being the rate at which energy is transferred in the inertial subrange) changes for a certain range of scales, being a direct result of the presence of the bubbles. The introduction of a bubble swarm plays a significant role in the behaviour of the flow resulting in pseudo turbulence generation - the void fraction has a direct impact on the flow characteristics, causing a greater turbulence enhancement and velocity fluctuations of the bubbles as it increases becoming a fundamental parameter to study. A change in behaviour of the energy cascade for varying diameters is also expected since the size of the bubble has a direct effect on the range of wavelengths at which energy is transferred. Simulations with different diameters are carried out in order to investigate how altering this length scale affects the overall picture of the energy cascade while keeping the void fraction constant (0.5 %) after the code has been validated.

1.113 Development and verification a green approach towards isolating essential oils from *Rosmarinus officinalis* using ultrasound-assisted supercritical CO₂

MING-CHI WEI¹, SHOW-JEN HONG², DA-HSIANG WEI², PEI-HUI LIN³ & YU-CHIAO YANG^{2,4}

¹Department of Applied Geoinformatic, Chia Nan University of Pharmacy and Science, Tainan 71710, Taiwan

²Department and Graduate Institute of Pharmacology, Kaohsiung Medical University, Kaohsiung 80708, Taiwan

³Department of Surgery, Davis Heart and Lung Research Institute, The Ohio State University Wexner Medical Center, Columbus, Ohio 43210, USA

⁴Department of Medical Research, Kaohsiung Medical University Hospital, Kaohsiung, Taiwan

Rosmarinus officinalis Lamiaceae is valuable as a medicinal plant as well as a functional food. *R. officinalis* leaves are an important source of essential oils (0.6-2%) and reveal several bioactivities. However, the content of aromatic component varies with climate, plant genotype, drying, extraction, and analytical methods. It is doubtlessly that the biological activities of essential oils of this herb depend on its chemical compositions. Four different isolation techniques, including ultrasound-assisted supercritical carbon dioxide (USC-CO₂) extraction, heat-reflux extraction (HRE), conventional supercritical carbon dioxide (SC-CO₂) extraction and hydrodistillation (HD) were utilized to produce essential oils from dried leaves of *R. officinalis*. The extracts were further analyzed using gas chromatography (GC) with flame ionization detection and gas chromatography with mass spectrometry (GC-MS). The highest yield of oil was obtained via USC-CO₂ extraction (2.34%, weight of the extracted oil/weight of dry plant) while utilizing lower extraction temperature (50°C) and pressure (27.5 MPa), and less organic solvent consumed (0 mL) and time duration (90 min). In addition, the results showed that at a lower pressure of 11.0 MPa, the yield of oils decreased when the temperature was increased from 28 to 55°C, while at higher pressures (17.5, 22.5, 27.5, and 32.5 MPa), the opposite trend was observed. Furthermore, a second-order rate model and a mass transfer model based on Fick's second law were validated under USC-CO₂ extraction. The energy barrier in the current study procedure was obviously lower than that of the others extraction methods, based on the lower of activation energy. Furthermore, the results obtained from Fick's second law indicated that the intraparticle diffusion is the controlling factor in the current study procedure. Consequently, the results obtained from the current research can clearly informed of the sensory system for the utilization of *R. officinalis* to the consumer.

1.114 Production of essential oil from *Lavandula angustifolia* through a green procedure and its theoretical solubility consideration

YU-CHIAO YANG^{1,2}, SHOW-JEN HONG¹, DA-HSIANG WEI¹,
PEI-HUI LIN³ & MING-CHI WEI⁴

¹Department and Graduate Institute of Pharmacology, Kaohsiung Medical University, Kaohsiung 80708, Taiwan

²Department of Medical Research, Kaohsiung Medical University Hospital, Kaohsiung, Taiwan

³Department of Surgery, Davis Heart and Lung Research Institute, The Ohio State University Wexner Medical Center, Columbus, Ohio 43210, USA

⁴Department of Applied Geoinformatic, Chia Nan University of Pharmacy and Science, Tainan 71710, Taiwan

Lavandula angustifolia (Lavender) is one of the most popular plants essential oils (5–6%) used in the world for various industrial purposes, including pharmaceutical, food, perfumes and cosmetic industries. Biological activity of the Lavender essential oil has been attributed to the presence of major constituents, linalool, linalyl acetate, lavandulyl acetate, 1,8-cineole and camphor, which have antibacterial, antioxidant, anticancer and the others activities. Lavender oils were extracted using ultrasound-assisted supercritical carbon dioxide (USC-CO₂) extraction with different dynamic times, temperatures, pressures and CO₂ flow rate to obtain the best extraction yield of oils using single-factor experiments. In addition, the heat-reflux extraction, hydrodistillation and conventional SC-CO₂ extraction methodologies are also used for comparison. The content of aromatic ingredients in the oils was determined by the gas chromatography (GC) and gas chromatography with mass spectrometry (GC-MS). The results indicated that the highest yields of volatile oils and volatile components were obtained with USC-CO₂ using a dried flower with a mean particle size of 0.36 mm at a CO₂ flow rate of 0.35 g/min, temperature of 51°C and pressure of 27.0 MPa for over 95 min, which is superior to the other extraction techniques based on its higher extraction yield and extraction efficiency. It was also showed that the dominant components in the oils were linalool and linalyl acetat, based on the total average content. To evaluate the feasibility of USC-CO₂ procedure and for establishing optimum operation conditions, the solubility of essential oil in SC-CO₂ using the dynamic extraction method were further determined. Furthermore, the thermodynamic properties of essential oil in the SC-CO₂ system were estimated following the theory developed by the three density-based models. The results obtained from the current research provide consumers the information of healthy eating and health consumption.

1.115 A Droplet Mop

JOSH SACZEK¹, GUANQI WANG¹, VLADIMIR ZIVKOVIC¹, BEN XU²
& STEVEN WANG¹

¹School of Engineering, Newcastle University

²Faculty of Engineering and Environment, Northumbria University

The need for sterile conditions is paramount within the chemical industry especially the pharmaceutical sector where cleaning of manufacturing facilities and production equipment is one of its most focused concerns. Any cleaning system must adequately clean surfaces, minimize the risk of contamination, but also reduce cleaning liquid consumption and enable it to be recycled (Murakami et al., 2000). This is currently achieved via a multitude of techniques but broadly either chemical, physical or a combination of the two. These more traditional cleaning methods either introduce a chemical which could contaminate the product or a mixing device which itself would require potential cleaning. Herein, we introduce a third category of cleaning approach, potentially overcoming both of these two issues; this new approach massively minimizes liquid consumption and, we anticipate that it can be applied for a great variety of cleaning processes. Based on the preliminary results, we predict that a 7 cm² droplet can effectively clean a 200 – 300 cm² contaminated surface.

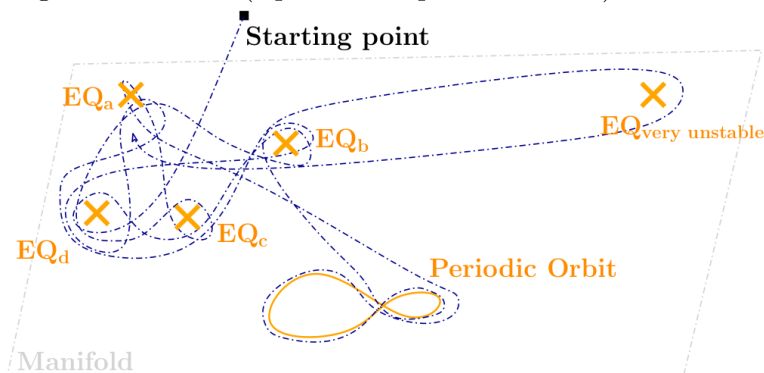
1.116 Feedback stabilization of a Plane Couette Flow Exact Coherent Structure

GEOFFROY C. P. CLAISSE[†] & ATI S. SHARMA

Aerodynamics and Flight Mechanics
University of Southampton

Turbulence can be interpreted as a finite dimensional dynamical system [1]. Each solution of the Navier-Stokes equations (NSE) is associated to the motion of a point in a state-space. This theory was strengthened by the discovery in shear flows of invariant solutions of the NSE, referred to as Exact Coherent Structures (ECS). In this theory, the turbulent inertial manifold is depicted as a network of ECS acting as unstable attractors of the turbulent dynamical state (Fig. 16). The turbulent dynamical state is thought to escape the neighbourhood of an ECS along its unstable eigenspace [2]. Nonetheless, this mechanism remains unproven, and recent work suggests the state may leave via the stable manifold [3]

Figure 16: Dynamical representation of the chaotic evolution of a turbulent state along different ECS (equilibria or periodic orbits).



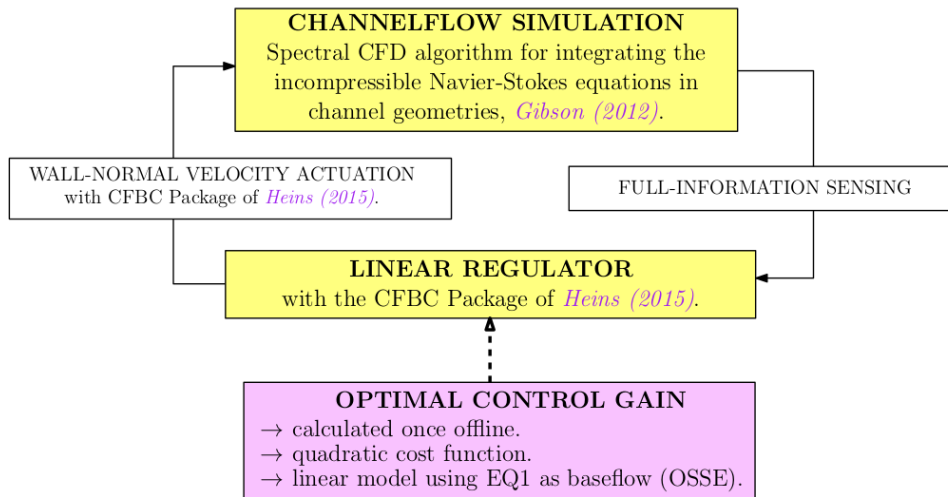
Here, we focus on the stabilization via state-space control theory of the unstable eigenspace of the Nagata [4] lower-branch (EQ1), known as the least unstable Plane Couette Flow ECS.

The application of state-space control theory to stabilize ECS requires a linearised state-space model. This linearization is very high-dimensional. To reduce the state-dimension, we derived a divergence-free model similarly to the Orr-Sommerfeld Squire model, and validated it against the literature [5, 2]. It results in a boundary-actuated full-matrix state-space model: the Orr-Sommerfeld Squire model Extended for an ECS as baseflow (OSSE). The OSSE model depicts faithfully the dynamical evolution of the flow in the neighbourhood of an ECS for small perturbations and it enables access to linear control theory. We then built a full-information state-feedback optimal

controller actuating via wall-transpiration and targeting the unstable eigenspace of EQ1. The optimal control derives from the solution of a high-dimensional Riccati equation, computationally expensive but now accessible thanks to the OSSE model. Finally, we were able to stabilize EQ1 within linear simulations.

We are now in the process of determining the radius of stability of the stabilized EQ1 in non-linear simulations run in *Channelflow* [6] (Fig. 17), which will give insights on the mechanisms responsible for the chaotic evolution of the turbulent state.

Figure 17: Configuration of the non-linear DNS simulation run in *Channelflow* [6]. Full-information of the flow is fed to the regulator, which in turn actuated via wall transpiration thanks to the *CFBC Package* [7]. The optimal control gain is determined thanks to the solution of the Riccati equation associated to the OSSE model.



References:

1. Eberhard Hopf. A mathematical example displaying features of turbulence. *Communications on Pure and Applied Mathematics*, 1(4):303–322, 1948.
2. J F Gibson, J Halcrow, and P Cvitanovic. Visualizing the geometry of state space in plane Couette flow. *Journal Of Fluid Mechanics*, 611:107–130, 2008.
3. M. Farano, S. Cherubini, J. C. Robinet, P. De Palma, and T. M. Schneider. How hairpin structures emerge from exact solutions of shear flows. *Journal of Fluid Mechanics*, 858:1–12, 2019.
4. M. Nagata. Three-dimensional finite-amplitude solutions in plane Couette flow: bifurcation from infinity. *Journal of Fluid Mechanics*, 217:519–527, 1990.

5. T. R. Bewley and S Liu. Optimal and robust control and estimation of linear paths to transition. *Journal of Fluid Mechanics*, 365:305–349, 1998.
6. JF Gibson. Channelflow: a spectral Navier-Stokes simulator in C++. *University of New Hampshire*, (July):1–41, 2012.
7. Peter H Heins. *Modelling, Simulation and Control of Turbulent Flows Peter Hywel Heins*. PhD thesis, University of Sheffield, 2015.

1.117 Coherent patterns and bypass laminar turbulent transition in boundary layersJOSEPH OLOO[†] & VICTOR SHRIRA

Keele University

In the classical scenario of laminar-turbulent transition the key role is played by linear instabilities of the basic flow. Here we focus on a specific bypass scenario where the existence/absence of linear instabilities is immaterial and the transition is caused by a nonlinear mechanism resulting in the “collapse” (blow-up) of finite amplitude initial perturbations. Novel essentially 2-d evolution equations are derived asymptotically for long-wave finite amplitude perturbations and large but finite Reynolds numbers. Two types of boundary-layer flows are considered: weakly stratified boundary layers and 3-d boundary layers. The resulting pseudo-differential nonlinear evolution equations are obtained in the distinguished limits and describe interplay between nonlinearity, weak dispersion, stratification and dissipative effects. Their key feature is that the transverse scale of perturbations is assumed to be the same as the longitudinal one, while across the boundary layer structure of the solution is provided by the solution of the corresponding linear boundary value problem. We show that the initial perturbations exceeding certain threshold collapse, i.e., develop a singularity in finite time. For the initial conditions representing a Gaussian hump in the velocity field the dependence of the domain of collapsing regimes on the boundary-layer parameters has been found.

1.118 A dam-break driven by a moving source: a simple model for a powder snow avalanche

JOHN BILLINGHAM

School of Mathematical Sciences
The University of Nottingham

We study the two-dimensional, irrotational flow of an inviscid, incompressible fluid injected from a line source moving at constant speed along a horizontal boundary, into a second, immiscible, inviscid fluid of lower density. A semi-infinite, horizontal layer sustained by the moving source has previously been studied as a simple model for a powder snow avalanche, an example of an eruption current, Carroll et al. (*Phys. Fluids*, vol. 24, 2012, 066603). We show that with fluids of unequal densities, in a frame of reference moving with the source, no steady solution exists, and formulate an initial/boundary value problem that allows us to study the evolution of the flow. After considering the limit of small density difference, we study the fully nonlinear initial/boundary value problem and find that the flow at the head of the layer is effectively a dam-break for the initial conditions that we have used. We study the dynamics of this in detail for small times using the method of matched asymptotic expansions. Finally, we solve the fully nonlinear free boundary problem numerically using an adaptive vortex blob method, after regularising the flow by modifying the initial interface to include a thin layer of the denser fluid that extends to infinity ahead of the source. We find that the disturbance of the interface in the linear theory develops into a dispersive shock in the fully nonlinear initial/boundary value problem, which then overturns. For sufficiently large Richardson number, overturning can also occur at the head of the layer.

1.119 Large-eddy simulation of enhanced mixing for water treatment applicationsBOYANG CHEN[†] & BRUÑO FRAGASchool of Engineering
University of Birmingham

In environmental engineering, wastewater must be collected and conveyed to a treatment facility to remove pollutants. With regards to energy consumption, the largest expense in wastewater treatment occurs in secondary treatment, particularly for activated sludge processes. We develop a numerical tool to enhance and assess the cost-effectiveness of real aeration systems in wastewater treatment. Aeration in an activated sludge process is based on pumping air into a tank, promoting the mixing and redistribution of the dissolved oxygen to facilitate the microbial growth. The microbial feeds on organic material, forming flocks which can easily settle out in the wastewater. A well-designed aeration system is key to an effective and sustainable wastewater treatment. However, the design of these facilities often obeys to rules-of-thumb that usually lead to an excessive energy expense.

The in-house finite-difference-based Large-Eddy Simulation code BubLPT was applied to investigate the principle of aeration system in wastewater treatment. The solver uses an Eulerian-Lagrangian point-particle model to couple liquid and gas phases. The parallelization of the code is supported by a hybrid MPI-OpenMP implementation. This model is used to investigate the best strategy for homogeneous aeration under constant void fraction. In order to implement it, three setups are modelled and assessed: one-plume, two-plume and bubble screen. The dissolved oxygen in the water tank is modelled as a passive tracer. The mixing produced by these three strategies is quantified by both instantaneous evolution of the flow field and statistical analysis of the dissolved oxygen concentration. The results obtained with the three strategies are compared and discussed. The results are also being validated by experimental data from a real wastewater treatment facility. Ongoing work on the integration of solid sludge particles in the mixing process is being currently implemented.

1.120 Droplet Retention and Shedding on Slippery Substrates

B. V. ORME[†], G. MCHALE, R. LEDESMA-AGUILAR &
G. G. WELLS

Northumbria University, Newcastle Upon Tyne

Droplets in contact with most solid surfaces experience contact line pinning, making the movement or removal of these droplets a challenge. Taking a hydrophobic structure or porous material and imbibing this with a lubricating liquid the issue of droplet pinning is resolved. However, the ability to control droplet positioning and movement becomes difficult [1]. Therefore a pinning point, in the form of a structure, to which the droplets will be attracted, can be added to the surface [1]. In this work we use is a step to create a lubricant menisci at the corner attracting the droplet by capillary forces, similar to the Cheerios Effect [1–3]. The adhesion force to this object is quantified by measuring the detachment angle and it is found that this angle can either be increased or decreased by changing either the step height, tilting direction, lubricant thickness, initial droplet position or a combination of these [4]. If the parameters are chosen in a specific configuration the surface can be inverted and the droplet will hang upside down. Furthermore, the final stationary position has little impact on detachment angle if the initial droplet position differs, meaning that the surface retains a memory of the droplet’s initial conditions. Applications for such surfaces range from microfluidics to inkjet printing or fog harvesting.

Acknowledgements: B. V. O. would like to thank Northumbria University for funding via postgraduate research studentship and Dr. Andrew Edwards for assistance during sample production.

References:

1. Hui Guan, J. *et al.* Drop transport and positioning on lubricant-impregnated surfaces. *Soft Matter* **13**, 3404–3410 (2017).
2. Vella, D. & Mahadevan, L. The ‘Cheerios effect’. *Am. J. Phys.* **73**, 817–825 (2004).
3. Karpitschka, S. *et al.* Liquid drops attract or repel by the inverted Cheerios effect. *Proc. Natl. Acad. Sci.* **113**, 7403–7407 (2016).
4. Orme, B. V. *et al.* Droplet Retention and Shedding on Slippery Substrates (Submitted to Langmuir)

1.121 A multicompartment SIS stochastic model with zonal ventilation for the spread of nosocomial infections: detection, outbreak management and infection control

MARTÍN LÓPEZ-GARCÍA, MARCO-FELIPE KING &
CATHERINE J. NOAKES

University of Leeds

In this work, we study the environmental and operational factors that influence airborne transmission of nosocomial infections. We link a deterministic zonal ventilation model for the airborne distribution of infectious material in a hospital ward, with a Markovian multicompartment SIS model for the infection of individuals within this ward, in order to conduct a parametric study on ventilation rates and their effect on the epidemic dynamics. Our stochastic model includes arrival and discharge of patients, as well as the detection of the outbreak by screening events or due to symptoms being shown by infective patients. For each ventilation setting, we measure the infectious potential of a nosocomial outbreak in the hospital ward by means of a summary statistic: the number of infections occurred within the hospital ward until end or declaration of the outbreak. We analytically compute the distribution of this summary statistic, and carry out local and global sensitivity analysis in order to identify the particular characteristics of each ventilation regime with the largest impact on the epidemic spread. Our results show that ward ventilation can have a significant impact on the infection spread, especially under slow detection scenarios or in overoccupied wards, and that decreasing the infection risk for the whole hospital ward might increase the risk in specific areas of the health-care facility. Moreover, the location of the initial infective individual and the protocol in place for outbreak declaration both form an interplay with ventilation of the ward.

This talk is based on the manuscript:

López-García M, King M-F, Noakes CJ (2019) *A multicompartment SIS stochastic model with zonal ventilation for the spread of nosocomial infections: detection, outbreak management and infection control*. Risk Analysis, DOI: 10.1111/risa.13300.

1.122 Evaluating CFD against a zonal ventilation model for predicting airborne pathogen transfer under different hospital ward ventilation configurations

ROSIE JONES[†], MARCO-FELIPE KING, MARTÍN LÓPEZ-GARCÍA & CATHERINE J. NOAKES

University of Leeds

With 37,000 attributable deaths across Europe and an annual financial burden of \$6.5 billion in the US; healthcare acquired infections (HCAI) are a global issue. HCAI are those that develop during admission to a health-care facility. Hospital guidance for ventilation regimes currently focus on patient comfort and are not comprehensively exploited as a tool to reduce airborne infection transmission.

We investigate the applicability of zonal ventilation models of 6 hospital multi-bed wards in López-García et al. (2019). A zonal ventilation model was used to analyse scalar contaminant spread through wards with a single infective source. Steady state, computational fluid dynamic (CFD) modelling with temperature boundary conditions and species transport was used to recreate the ward ventilation combinations. Different ventilation regimes were investigated to determine optimal reduction of airborne contaminants.

Both models demonstrate the ability to recognise the typical path the overall contaminant spread. However, without including thermal properties and a consideration of location of inlets/outlets the zonal model under-predicts the contaminant concentration by up to 80% in the zones located closest to the infective source. In zones further from the infectious source where contaminants are homogeneously mixed, both the analytical and CFD ward concentrations differ by up to 12%.

This investigation concludes that the analytical models are unable to accurately predict airborne pathogens dispersion in complex air flows, whereby restricting their implementation to areas that are homogeneously mixed: far from of the infectious source. CFD modelling is able to capture the complex, varying flow of a hospital ward and should continue to be utilised to investigate ventilation as a resource to reduce the burden of HCAI.

References:

1. López-García M, King M-F, Noakes CJ (2019): *A multicompartment SIS stochastic model with zonal ventilation for the spread of nosocomial infections: detection, outbreak management and infection control*. Risk Analysis, DOI: 10.1111/risa.13300.

1.123 Dune-Dune Repulsion

K. A. BACIK^{†1}, C. P. CAULFIELD^{2,1}, S. LOVETT³ &
N. M. VRIEND^{1,2}

¹DAMTP, University of Cambridge

²BPI, University of Cambridge

³Schlumberger Cambridge Research

Dunes are coherent sedimentary structures which arise spontaneously due to the dynamical interplay between granular matter and the flow of the overlaying fluid. Natural dunes rarely occur in isolation. Aeolian dunes form vast dune fields and subaqueous bedforms occur in groups. As of now, the mechanisms which regulate the large scale organisation of dune fields are poorly understood. In particular it is unclear if the dune configurations we observe are stable or transient. Here we investigate the long-time behaviour of a quasi-2D dune corridor using a subaqueous experiment in an annular geometry. In our experiment, a corridor of individual isolated dunes emerges spontaneously from a thin layer of sediment destabilised by the overlaying turbulent flow. We show that the corridor structure appears to be robust and that stabilisation is achieved by long-range dune-dune interactions. Our experiments reveal that by altering the flow, dunes strongly affect the shape and the migration rate of their downstream neighbours which leads to an effective dune-dune repulsion. Here, we discuss the repulsion mechanism in detail and explore its consequences for the system-level dynamics of the dune corridor.

1.124 Nonlinear feedback control of the bi-modal flow behind a three-dimensional blunt bluff bodyD. AHMED[†] & A. S. MORGANS

Department of Mechanical Engineering, Imperial College London

The wake behind many three-dimensional blunt bluff bodies in close proximity to ground exhibits reflectional symmetry breaking. In the turbulent flow regime, this manifests as wake flow switches between one of two asymmetric wake positions, either side-to-side or top-to-bottom. These switches occur over long, random timescales, with the wake recovering symmetry in the long time-average. This work employs Large Eddy Simulations to investigate feedback control to suppress this wake bi-modality, with a view to minimizing the form drag generated by the associated oscillatory dynamics.

A canonical simplified road vehicle geometry – the squareback Ahmed body – is considered. A model for the supercritical pitchfork bifurcation model is used to imitate its side-to-side wake bi-modality. The model is based on an expansion of the Navier-Stokes equations non-linearly around the critical bifurcated point. This model is used to derive a non-linear, single-input single-output, feedback controller, whose objective is to re-symmetrise the wake. The control law for the system is designed using a Hamiltonian-Jacoobi-Issacs cost functional, with the centre-of-pressure on the Ahmed body base considered as the input signal and synthetic jets (zero net mass flux) placed just upstream of the separation point used as actuators. The controller is applied with success to the representative model of the supercritical pitchfork bifurcation, in the presence of additional noise, and is currently being applied in Large Eddy Simulations of the turbulent Ahmed body wake.

1.125 Influence of moving ground use on the unsteady wake of a small-scale commercial road vehicleALEKSANDRA ANNA REJNIAK[†] & ALVIN GATTO

Brunel University London

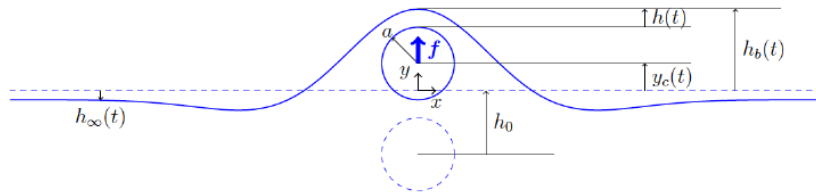
Wind tunnel testing is a key tool used in ongoing efforts to reduce road vehicle fuel consumption. Accurate reproduction of a realistic flow environment is important, with moving ground use now commonplace. Several previous investigations have considered the impact a moving ground has on the flow-field. For road vehicles with low ground clearance (racing cars), its use is generally accepted as being essential. For less specialised examples, such as commercial vehicles, the need, given a higher ride height, is considered less critical. However, much of this previous work considers only a time-averaged perspective; time-resolved details remain incomplete. This work scrutinizes that aspect. Wind tunnel test results are presented for a 1/24th-scale road vehicle, representative of a Heavy Goods Vehicle, for both moving and stationary ground flow conditions. Particular focus resides within the separated wake, with drag, base surface pressure, and wake velocities quantified, compared, and evaluated. The influence of wheel rotation is also included. All tests were conducted at a Reynolds number, based on model width, of 2.3×10^5 . Mean results show that moving ground use decreases drag with a 12% increase in base surface pressure. Subtle differences in wake topology are also observed, with a stationary ground promoting areas of significantly reduced flow-speed directly behind the vehicle. This feature is absent with moving ground use. The presence of a moving ground is also found to decrease the characteristic frequencies of wake pumping and vortex shedding mechanisms.

1.126 Exit dynamics of a 2D cylinder from the water

INTESAAF ASHRAF, ANOUCHKA LILOT AND STÉPHANE DORBOLO
UR-CESAM, GRASP, University of Liege, Belgium

Penguins, dolphins and submarine have to leave water surface to air for various reasons. However, the pop up dynamics of an object from liquid to air is not fully understood. This study is an attempt to bridge this gap. In this work, we study and quantify the exit dynamics of a 2D cylinder, that is fully submerged in a water tank. The cylinder moves upwards at a constant velocity in a vertical direction till cylinder pops out of the water into the air. The experiments were performed at varying speed and height. The simultaneous force measurement was also taken. The image of cylinder moving was taken at high speed came. The image acquisition was taken 3000Hz.

Figure 18: Characteristics lengths of cylinder moving upward



The characteristics distance, as shown in Fig. 18, of upward moving cylinder was characterized as a function of time. We observed three different regimes during this process. In first regime, as the cylinder move upwards, a bump is observed. The size of the bump increases, as the cylinder moves closer to the water and air interface (Fig. 19). In second regime, as the cylinder keeps moving upwards and moves inside the bump, as shown in the Fig. 20. The cylinder body is closest to the interface. It is called crossing regime. In third regime, as the cylinder keep moving upwards and leaves the water surface interface. The drainage of the liquid from the cylinder surface takes place, as shown in the Fig. 21.

Acknowledgements: This work is financially supported by PDR WORKFLOW (FNRS). SD is a FNRS Senior Research Associate.

Figure 19: Bump formation due to upward movement of the cylinder

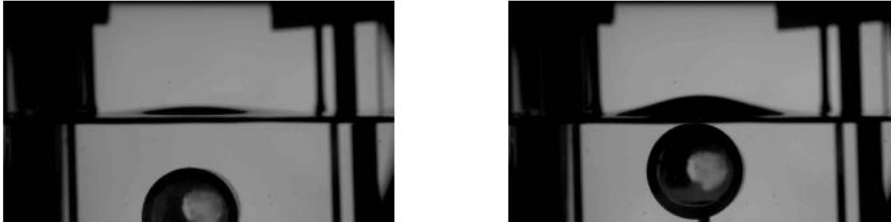
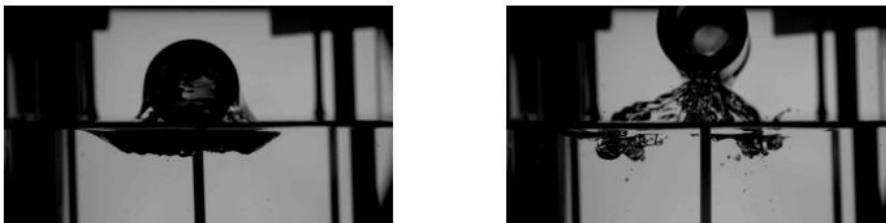


Figure 20: Crossing Regime of the cylinder



Figure 21: Drainage Regime of the cylinder



**1.127 Coarse grained models for reactive flows in porous media:
homogenisation and numerical simulations**

FEDERICO MUNICCHI & MATTEO ICARDI

University of Nottingham

One of the greatest difficulties in the study of transport phenomena in porous media is the inherent multiscale nature of the vast majority of processes of interest. A precise model or simulation describing the local, pore-scale, phenomena would be needed but it is of little practical applicability due to the rapid oscillations of the concentration and flow fields, hence the need for a coarse grained model, equivalent to the first one but involving smoother fields that can be accurately evaluated with much lower computational effort.

A variety of methods can be employed to perform this procedure: asymptotic homogenisation is a powerful and versatile tool for the up-scaling of transport and reaction equations in porous and heterogeneous media. For example, Taylor dispersion in porous media has been approached in this way [2], and examples in the literature deals with the problem of heterogeneous (surface) reaction [1].

In this contribution, we illustrate the limits of standard homogenisation theory in the presence of fast surface reactions and how the use of spectral decomposition and two-scale asymptotics techniques leads to a closed formulation for the coarse grained model. This methodology consists in splitting the original complex problem into a set of simpler sub-problems that can be solved on a relatively small representative periodic cell rather than the whole domain. Furthermore, we provide details on the numerical implementation of such model in the open source finite volume library OpenFOAM[®], and we compare its performance and accuracy against fully resolved simulations. Finally, we discuss the limitations of the presented methodology in the case of absorption/desorption surface reactions.

References

1. Grgoire Allaire, Robert Brizzi, Andro Mikelić, and Andrey Piatnitski. Two-scale expansion with drift approach to the Taylor dispersion for reactive transport through porous media. *Chemical Engineering Science*, 65(7):2292–2300, 4 2010.
2. J.L. Auriault and P.M. Adler. Taylor dispersion in porous media: Analysis by multiple scale expansions. *Advances in Water Resources*, 18(4):217–226, 1 1995.

1.128 Three-dimensional numerical simulations of a thin film falling vertically down the inner surface of a rotating cylinderUSMAAN FAROOQ^{†1}, JASON STAFFORD², CAMILLE PETIT¹ &
OMAR K. MATAR¹¹Department of Chemical Engineering, Imperial College London²Department of Mechanical Engineering, University of Birmingham

Whilst gravity driven flow down the inside and outside of a stationary vertical cylinder has been investigated in some detail (Mayo et al., 2013), the flow of thin films associated with a rotating cylinders is rare, and typically the cylinder's orientation will be horizontal (Pougatch and Frigaard, 2011). In this study the cylinder is orientated vertically, where a thin liquid film flows down a concave surface which itself has an imposed velocity in the azimuthal direction. A key feature of this setup is the presence of waves inclined in the expected direction of flow. The imposed azimuthal velocity influences the shape and speed of the waves, with an angle being developed which is intrinsically dependent on the magnitude of the imposed velocity.

An investigation of the wave dynamics is performed using high resolution three-dimensional direct numerical simulations and a volume-of-fluid approach to treat the interface. The impact of cylinder Reynolds number on the stability of these falling, rotating films is examined. As Reynolds number increases, the centrifugal force increases, producing a stabilising effect (Iwasaki and Hasegawa, 1981). Key features, such as the transition from a 2D to a more complex 3D wave regime and the thickness of the film are heavily influenced by this stabilising effect and are investigated. An analysis of the predicted films provide a detailed insight into the relationship between the wave dynamics and internal flow fields.

1.129 Numerical Study of the Wave Kinetic Equation for Drift Wave/Zonal Flow InteractionsKRISTOFFER SMEDT[†]

University of Leeds

The Wave Kinetic equation can be a useful tool for bridging the scale separation between small scale perturbations and the larger scale structures their interactions can help create or sustain. These are of great interest in magnetic confinement fusion, where the magnetic field and density gradient lead to small scale drift waves. In an analogous manner to Rossby waves and zonal flows in geo- and astrophysics, drift waves can deposit energy into the zonal bands. As the zonal flows has a large impact on the transport properties of the plasma, this interaction is of great interest in fusion research.

In this short study, a numerical model based on the wave-kinetic equation was developed from a reduced version of the equation. The reduction was based on simple geometric considerations from tokamak plasmas, and the numerical model was applied to provide insight into the dynamics of the equation. Two cases were studied for the same geometry and initial parameters; one with a strong mean initial zonal flow and one with a weak zonal flow. Initial results indicated that a weak initial shear zonal flow was enhanced significantly by the presence of small-scale perturbations, in contrast to the case for strong zonal flow. Additionally, position/wavenumber phase-space structures seemingly formed, suggesting that a phenomena similar to particle-trapping may occur for wave packets according to the wave kinetic formulation.

1.130 Influence of stack chimneys on the displacement ventilation of an enclosed geometryDANIEL FIUZA DOSIL[†]

Imperial College London

Approximately 3 billion people, predominately from low- and middle-income countries, cook and heat their homes by burning solid fuels in open fires or simple stoves. This results in extremely poor indoor quality, which has been linked to diseases that produces 3 millions of premature deaths per year.

Motivated by the search of solutions for enhancing the natural ventilation and indoor air quality of rural dwellings, we investigate the effects of a chimney stack on the ventilation of an enclosed geometry. In this study, we model the effects of a chimney stack on the dynamics of a naturally-ventilated enclosed geometry with a localised source of buoyancy. We present a theoretical model to describe the dynamics of the displacement ventilation regime with a chimney. Additionally, the effects of the pressure losses along the length of the chimney and their influence on the ventilation are discussed. Small scale experiments, using the salt-bath modelling technique, has been conducted with different chimney lengths to validate the theoretical models and to illustrate different flow regimes.

1.131 Shaping supersonic contoured nozzles for cold spraying metallic particlesALDO RONA & LUIZA F. ZAVALAN[†]

Department of Engineering, University of Leicester

Cold sprayed metallic coats can provide an appropriate surface finish for a range of applications, including marine propellers, boat keels, and ablating surfaces in aerospace. Cold spraying can coat surfaces at a comparatively lower environmental impact with respect to plasma spray or chemically bonded sprays. In a metal cold spray, the kinetic energy imparted to the metal particles by a high speed gas provides the means for particles to plastically deform and deposit on the target substrate. Therefore, a uniform particle distribution of uniform velocity is typically desirable to achieve a good quality deposition rate and to reduce wastage from particles failing to splatter on the target substrate. This work revisits the method of characteristics technique for designing axisymmetric nozzles for generating lightly laden jets. By Computational Fluid Dynamics, the performance of current commercial cold spray nozzles is compared with new nozzle profiles, designed with a smooth throat and for a parallel (axial) outflow. The two-phase flow is modelled by the compressible Reynolds-Averaged Navier-Stokes equations with k-omega turbulence closure, for the primary (gas) phase, and a Lagrangian discrete phase model is solved for the particle transport. Two-way coupling renders the kinetic interaction between the two phases. Particle dispersion is modelled by a discrete random walk model. Preliminary results indicate that the best performing shapes differ from the classic minimum-length bell-shaped nozzle for space propulsion and are closer to the contoured walls of supersonic wind tunnels. Plans for testing prototype nozzles are under development in collaboration with The Welding Institute (TWI), Cambridge, under the auspices of the EPSRC Doctoral Training Programme IMPaCT.

1.132 Impact of surfactants on inertia-induced undulations on the surface of capillary bubbles

A. BATCHVAROV¹, M. MAGNINI², L. KAHOUADJI¹,
R. V. CRASTER³ & O. K. MATAR¹

¹Department of Chemical Engineering, Imperial College London

²Department of Mechanical, Materials and Manufacturing
Engineering, University of Nottingham

³Department of Mathematics, Imperial College London

This work focuses on numerical investigation of the effect of soluble and insoluble surfactants on elongated bubbles in circular microchannels. Analytical and numerical work on the subject in the context of creeping flows ($Re \ll 1$) shows that surfactants tend to accumulate at the bubble tail and modify its shape (Ratulowski and Chang, 1990; Park, 1992; Stebe and Barthes-Biesel, 1995; Olgac and Muradoglu, 2013). More recent work on surfactant-free elongated bubbles shows that in the presence of high inertia ($Re \gg 1$), tail undulations become more apparent at the back of these bubbles (Magnini, 2017). With this work we study the effect of soluble and insoluble surfactants on bubble tail undulations. The CFD simulations of the flow are performed using a hybrid front-tracking code (Shin et al., 2018).

Acknowledgements: We acknowledge the contribution of Drs Damir Juric and Jalel Chergui (both from LIMSI, CNRS, France), Dr Seungwon Shin (Hongkik University, South Korea).

1.133 DNS for the dynamics of 3D surfactant-laden bursting bubbles

R. CONSTANTE-AMORES[†], L. KAHOUADJ, A. BATCHVAROV &
O. K. MATAR

Department of Chemical Engineering, Imperial College London

Bursting bubbles play an important role in both industrial applications and nature. It has been estimated that around 10^{18} – 10^{20} bubbles burst per second over the world ocean, exchanging chemical components or heat from the ocean to the atmosphere. This exchange is due to the formation of a central jet, which results in droplets according to the Plateau–Rayleigh instability. The free-surfactant dynamics is well known in literature, however, the effect of the addition of surfactant on the free surface has not been reported yet. We have performed 3D Numerical Simulation of surfactant-laden bursting bubbles to ensure that the entire physics are captured as Marangoni stresses, which rise due to superficial gradients of the surface tension, act in the tangential components of the interface. Neglecting gravitational effects, the Laplace number is the only dimensionless parameter which controls the system which measures the importance of the surface tension forces respect to the viscous forces, i.e., $La = \rho\sigma R/\mu^2$, where ρ , μ , σ and R are the liquid density, viscosity and surface tension, and the initial radius of the droplet. Non-dimensional simulations varying the Peclet number ($Pe = UR/D$, where U is the velocity and D is the diffusion coefficient), which compares the ratio of the time scales for molecular diffusion to convective transport, were launched to analyse the fate of the jet. Results regarding the surfactant concentration distribution on the free surface, the surface tension gradients and the importance of Marangoni stresses will be presented.

1.134 From walking to shooting modes in droplet vibrations

L. KAHOUADJI, O. K. MATAR & R. V. CRASTER

Imperial College London

A vibrated drop constitutes a very rich physical system, blending both interfacial and volume phenomena. A remarkable experimental study was performed by M. Costalonga (PhD. Université Paris Diderot, 2015) highlighting sessile drop motion subject to horizontal, vertical and oblique vibration. Several intriguing phenomena are observed such as drop walking and rapid droplet ejection (shooting mode). We perform three-dimensional direct numerical simulations taking into account the dynamic of the contact line motion determined by the generalized Navier-slip model associated with a front-tracking-based multiphase method.

Acknowledgements: Drs Damir Juric and Jalel Chergui (LIMSI, CNRS, France), Dr Seungwon Shin (Hongik University, South Korea); Engineering and Physical Sciences Research Council, UK.

1.135 Implementation and verification of CFD model for crude-oil fouling

GABRIEL F. N. GONÇALVES^{†1}, MIRCO MAGNINI² &
OMAR K. MATAR¹

¹Imperial College London

²University of Nottingham

Deposition of solids at the walls of process equipment may generate severe efficiency and cost related issues (Wagterveld, 2013). With the objective of the simulating crude oil fouling in industrial conditions, a two-phase multi-component solver with heat transfer and phase change was implemented in the OpenFOAM open-source framework. The model utilizes the volume-of-fluid method for tracking the interface between fouling layer and working fluid, and momentum and energy conservation equations are solved for the mixture. The solidification model of Svendsen (1993) is used for the calculation of the mass transfer rate, which is assumed to take place at the interface and at the walls. The implementation was verified with previous calculations performed in a commercial CFD platform.

1.136 Turbulent flows over sparse canopiesAKSHATH SHARMA[†] & RICARDO GARCÍA-MAYORAL

Department of Engineering, University of Cambridge

The study of canopy flows has wide ranging applications, which include reducing crop loss, energy harvesting and improving heat transfer. Based on the geometry and spacing of the canopy elements, they can be grouped into three regimes – dense, intermediate and sparse. In the dense regime, the canopy elements are closely packed and the overlying turbulent eddies cannot penetrate within them. In the sparse limit, the spacing between the canopy elements is large and the turbulent eddies can penetrate the full height of the canopy. The intermediate regime lies between these two limits. In the present work, we investigate turbulent flows within and over sparse canopies using direct numerical simulation. We find that such canopies affect the surrounding flow through two distinct mechanisms. The first is through the flow induced directly by the presence of the canopy elements as obstacles. When this element-induced flow is filtered out, the remaining background turbulence exhibits a balance of the viscous and the Reynolds shear stresses within the canopy layer similar to that over smooth walls. From this, a scaling based on the sum, at each height, of these two stresses is proposed. Using this height-dependent scaling, the background turbulence fluctuations within the canopies show similarities to those over smooth walls. This suggests that the background turbulence within the canopy scales with the local stress at each height, rather than the total drag as in smooth walls. This effect is essentially captured when the canopy is substituted by a drag force that acts on the mean flow alone, aiming to produce the correct local stress without modifying the fluctuations directly. This forcing is shown to produce better estimates for the turbulent fluctuations within sparse canopies compared to a conventional, homogeneous-drag model.

1.137 CFD Based Optimisation of Swirl Inducing Multi-Nozzle Annular Jet Pump

ANDREW MORRALL

Engineering Department, Lancaster University

A jet pump is a fluidic device that has no internal moving parts, instead driving media by means of energy exchange between two fluids; the motive fluid and the pumped, secondary fluid. Though the efficiency of jet pumps compared to traditional turbomachinery devices is comparably low, they are often used in applications that require high reliability, or the ability to pump solid materials, owing to the jet pump containing no moving parts. The multi-nozzle annular jet pump uses nozzles arranged circumferentially around a pipe bore to inject the motive fluid. The orientation of these nozzles is designed to induce swirl downstream of injection, however, the effect this has on the flow is little understood and has received little attention in academia.

This optimisation studies a single-phase, air based, multi-nozzle annular jet pump using the CFD code ANSYS[®] FLUENT. Various geometric parameters of the pump are altered to find the optimal level of performance and efficiency. Results and the numerical setup, including turbulence model selection and spatial refinement, are verified against experimental analyses, comparing static wall pressure and axial velocity. Preliminary results show good agreement with experimental data, and highlights the significant impact the nozzle orientation, size and quantity has on the induced flow and efficiency levels of the pump.

1.138 Flow-induced symmetry breaking in growing bacterial biofilms

PHILIP PEARCE

Department of Systems Biology, Harvard Medical School

Bacterial biofilms are matrix-bound multicellular communities. Biofilms represent a major form of microbial life on Earth and serve as a model active nematic system, in which activity results from growth of the rod-shaped bacterial cells. In their natural environments, from human organs to industrial pipelines, biofilms have evolved to grow robustly under significant fluid shear. Despite intense practical and theoretical interest, it is unclear how strong fluid flow alters the local and global architectures of biofilms. Here, we combine highly time-resolved single-cell live imaging with 3D multi-scale modeling to investigate the effects of flow on the dynamics of all individual cells in growing biofilms. Our experiments and cell-based simulations reveal that, in the initial stages of development, the flow induces a downstream gradient in cell orientation, causing asymmetrical droplet-like biofilm shapes. In the later stages, when the majority of cells are sheltered from the flow by the surrounding extracellular matrix, buckling-induced cell verticalization in the biofilm core restores radially symmetric biofilm growth, in agreement with predictions from a 3D continuum model.

1.139 SPT: Slender Phoretic Theory of Chemically Active FilamentsPANAYIOTA KATSAMBA¹, SÉBASTIEN MICHELIN² &
THOMAS D. MONTENEGRO-JOHNSON¹¹School of Mathematics, University of Birmingham²LadHyX, Département de Mécanique, Ecole Polytechnique

Artificial microswimmers have the potential to revolutionise non-invasive medicine and microfluidics. A large class of these swimmers self-propel by generating concentration gradients in a surrounding solute, and recent work has suggested that fabricating such swimmers from flexible, thermoresponsive filaments allows their precision navigation. In order to efficiently model such swimmers, we develop a Slender Phoretic Theory (SPT) for the chemohydrodynamics of microscale autophoretic filaments of arbitrary centreline, as a one-dimensional substitute for inefficient numerical solution of 3D partial differential equations. We show that, unlike other slender body theories, azimuthal effects that appear at first order for curved shapes have a leading order contribution to the swimming kinematics, and consider the effects of curvature for U-, S- and helical filament shapes.

1.140 Recasting Navier-Stokes Equations

S. KOKOU DADZIE & M. H. LAKSHMINARAYANA REDDY

School of Engineering and Physical Sciences, Heriot-Watt University

Experiments show that liquid flows through nanoscale structures can be four to five order of magnitude faster than predicted by conventional fluid flow theory. A convincing physical explanation of these high fluid velocities through the nano-tubes is still lacking. Adding solid nanoparticles into liquids dramatically increase the fluid thermal conductivities so that the Fourier's law of heat transfer alone is insufficient to understand their transport properties. The meaning of a fluid velocity in the derivation of the conventional flow equations has been severely questioned over the past decade. Meanwhile, several models have been proposed to substitute the Navier-Stokes. Some of these are, for example, Volume Diffusion (or Bi-velocity hydrodynamic models, Ghost effect system Navier-Stokes equations and many others. Here, starting with the conventional Navier-Stokes equations, we introduce a transformation technique similar in nature to Lorentz transformation. It involves transforming the velocity field variable within the standard fluid flow equations. In doing so, we show the existence of a class of systematically thermo-mechanically consistent mass diffusion type of fluid flow set of equations. Our new models are more complete form of those previously proposed to substitute the original Navier-Stokes. The new class of equations appear better suited for: compressible flows, flow involving thermal stresses and other transport processes. As an illustration, our new model for compressible flows is applied to the description of shock wave profiles in monatomic gases where the Navier-Stokes is well-known to fail. Two other of the new models termed "pressure-diffusion" and "thermal-diffusion" Navier-Stokes are also used to re-interpret experimental data of Rayleigh-Brillouin light scattering in gases.

1.141 Variability of stochastically forced zonal jetsLAURA COPE[†]

DAMTP, University of Cambridge

Zonal jets are strong and persistent east-west flows that arise spontaneously in planetary atmospheres and oceans. They are ubiquitous, with key examples including mid-latitude jets in the troposphere, multiple jets in the Antarctic Circumpolar Current and flows on gaseous giant planets such as Jupiter and Saturn. Turbulent flows on a beta-plane lead to the spontaneous formation and equilibration of persistent zonal jets. However, the equilibrated jets are not steady and the nature of the time variability in the equilibrated phase is of interest both because of its relevance to the behaviour of naturally occurring jet systems and for the insights it provides into the dynamical mechanisms operating in these systems.

Variability is studied within a barotropic beta-plane model, damped by linear friction, in which stochastic forcing generates a kind of turbulence that in more complicated systems would be generated by internal dynamical instabilities such as baroclinic instability. This nonlinear (NL) system is used to investigate the variability of zonal jets across a broad range of parameters. Comparisons are made with two reduced systems, both of which have received attention in recent years. A quasilinear (QL) model, in which eddy-eddy interactions are neglected, permitting only nonlocal interactions between eddies and the zonal mean flow, is studied in addition to a model employing direct statistical simulation (DSS) in which the flow statistics, truncated at second order in equal-time cumulants, are solved for directly. Each system reveals a rich variety of jet variability. In particular, the NL model is found to admit the formation of systematically migrating jets, a phenomenon that is observed to be robust in subsets of parameter space. Jets migrate north or south with equal probability, occasionally changing their direction of migration.

1.142 Potential flows through periodic domains with multiple objects per periodPETER J. BADDOO[†] & LORNA J. AYTON

University of Cambridge

Abstract: In this work it is shown that recent advances in conformal geometry can be leveraged to obtain analytic solutions for potential flows in periodic domains. The solutions are constructed in a parametric circular domain and then conformally mapped to the periodic physical domain. By expressing the problem in terms of the transcendental Schottky-Klein prime function, the ensuing solutions are valid for domains of arbitrary connectivity, i.e. any number of objects per period window. Moreover, the conformal mapping to the desired physical domain may be constructed using a new periodic Schwarz-Christoffel formula. The solutions are appropriate for a range of scenarios in periodic domains including uniform flows, vortex flows and flows induced by moving boundaries.

2 Posters

2.1 Methods for investigating dissolution in surfactant solutions

RACHEL HENDRIKSE[†]

University of Leeds

Surfactants are present in many everyday products such as detergents and shampoos. Under certain conditions, surfactants will aggregate into different structures in solution. These different structures alter the rheology of the solution, and the exact structure formed is concentration dependant. This poses an interesting situation in which the rheology changes as the material dissolves. This research uses different simulation techniques to investigate both equilibrium phase behaviour, as well as the dissolution process. Most research focuses on understanding equilibrium behaviour, and non-equilibrium processes have been much less studied and are not as well understood.

Small scale modelling of the ‘clustering’ behaviour of surfactant molecules in solution helps us to understand the effects of the small scale on the rheology of the material. This poster will focus on the use of Lattice Monte Carlo (LMC) and Dissipative Particle Dynamics (DPD) methods. Both methods model molecules as a chain of ‘beads’. LMC confines these beads to a lattice structure, whereas DPD is an off-lattice mesoscopic simulation technique which involves a set of particles moving in continuous space. While LMC can only be used to study the equilibrium behaviour of solutions, DPD can be used to study the dissolution process as well. This poster will compare the two methods, and show how DPD can be used to study the movement of surfactant molecules into an aqueous solution.

Incorporating small scale dissolution phenomena into large scale models, for example via multi-scale CFD approaches is challenging and has received little attention in the literature. This is largely due to challenges capturing small scale phenomenon in a large scale simulation. One of the aims of this research is to investigate the feasibility of a coupled DPD-CFD model. This poster will discuss how such a model is implemented, and outline how a DPD-CFD model could work.

2.2 Accurate Lattice Boltzmann Simulations of Gas Permeability through Nanoporous Media

DIAN FAN, ANH PHAN & ALBERTO STRIOLO

Department of Chemical Engineering, University College London

The mesoscale lattice Boltzmann (LB) simulation protocol is often used to predict fluid permeability, although the reliability of such predictions strongly depends on the boundary conditions implemented. While, in the ideal scenario, no slip is expected at solid-liquid interfaces, in some cases gas does slip, yielding pronounced differences in gas and liquid permeability. This phenomenon is experimentally known as the Klinkenberg effect. Comparing LB results obtained implementing classical slip boundary conditions against non-equilibrium molecular dynamics (MD) simulation results for methane gas flowing through nanopores reveals important non-physical errors. This discrepancy might account for the overestimation of the Klinkenberg effect, often reported in the literature when LB simulations are applied to nanoporous media. An improved slip boundary condition is proposed and implemented to minimize non-physical slip. It is shown that estimated apparent permeability and permeability corrections are consistent with MD results and experimental measurements. We achieved a numerical consistency of the Klinkenberg effect across molecular, mesoscopic, and macroscopic scales, which indicates the extended applicability of the LB method to predicting slip and transitional gas flow behaviors by the improved boundary condition.

2.3 Predicting Spray Impact on and Carry-Over from Complex Shaped Surfaces

LIAM GRAY[†]

University of Leeds

Sprays are typically formed when a product is atomized to obtain a desired droplet size distribution and in turn increase its efficiency. The applications of sprays are varied, from fuel injectors to personal care products. One constant however is the inherently complex nature of the spray generation process. Due to the small time and length scales involved an experimental approach becomes difficult when trying to capture the entire process. Therefore, a heavily validated numerical model is to be developed within ANSYS Fluent to model the spray generation and fate of the droplets after impacting the target surface (carry-over).

The focus of this research is on sprays generated from aerosol cans and the carry-over of droplets which leads to respiratory discomfort. We aim to better understand how spray generation and topological variations in target surface affect carry-over and possible routes in minimising this negative effect.

The numerical model aims to incorporate the four main stages in spray generation: the primary atomization phase, the secondary atomization phase, the droplet transport and the droplet-wall interaction. The starting point of our model is to incorporate the carrier jet which transports the product. A species transport approach is employed to model the mass fraction of each species. This is then validated against experimental data within the literature. Further additions to the model are also discussed, including an impingement wall and introduction of droplets. The numerical model is currently still in development.

2.4 Fluid Transport Correlations in Partially Filled Pipes for Nuclear Decommissioning

CHRISTOPHER CUNLIFFE[†] & DAVID DENNIS

University of Liverpool

The efficient transfer of fluids in a partially filled pipe flow regime is ubiquitous to nuclear decommissioning operations. Factors such as the hazardous nature of the fluid and the need to minimise blockages and leakages, mean there is an emphasis on low volumetric flow rates with a reliance on passive flow conditioning techniques such as gravity driven flows. As a result, the partially filled configuration naturally becomes more prevalent. To expand the operational limits of this transportation method, a knowledge of the fundamental parameters which characterise the behaviour and dynamics of the flow and how these parameters change relative to each other is required. Understanding the underpinning transport correlations will maximise the operational envelope of this flow regime potentially lowering waste production, reducing long-term storage requirements and minimising associated costs and environmental consequences. A large scale non-active experimental test rig has been developed at the National Nuclear Laboratory Workington facility taking the form of a gravity fed low gradient linear pipe line fitted with a bespoke control and data acquisition software for the analysis of the behaviour and dynamics of the fluid. Initial trials have been run using water to identify the accessible flow regimes in this configuration providing an elementary characterisation of the flow. The Manning equation has been employed as a validation method and to test the approximate behaviour of the flow in this open hydraulic flow regime. Electrical Resistance Tomography will be employed to examine the internal flow structure across the pipe cross-section to gain an understanding of the interaction between the different flow phases. Future work will be developed from the initial Newtonian characterisation with the focus being on non-Newtonian and multiphase flows, feeding into a strategy to facilitate nuclear decommissioning operations.

2.5 Massively Parallelized Models of Fluid-Solid Multiphase Flow

DAMILOLA ADEKANYE[†]

University of Leeds

In environmental systems the hydrodynamics of flows, such as turbidity currents, interacting with solid boundaries are dependent on the morphodynamics of the substrate. Turbidity currents are underflows driven by the action of gravity on the density difference between ambient fluid and a turbid mixture of fluid and sediment. The flows are non-conservative, as the interstitial fluid is miscible with the ambient fluid, and particulate material is eroded and deposited at the boundaries. An important problem in the numerical modelling of turbidity currents is achieving efficient coupling between the hydrodynamics of the flow and morphodynamics of the bed. This challenge has remained largely unresolved as particle transport is controlled by processes at small spatial and temporal scales, whilst the system scales of interest may be many orders of magnitude larger.

The core aim of the research project is to numerically investigate the three-dimensional flow structure of turbidity currents, the processes of sediment erosion and aggradation, and the formation of sinuous submarine channels. In order to achieve this a numerical model is under development, with the objective of efficiently coupling the hydro and morphodynamics. The computational expense of conventional modelling approaches has precluded the study of highly turbulent environmental flows with deformable boundaries. In this research project, an in-house lattice Boltzmann method (LBM) code, which was written to run on massively parallel graphics processing units, is developed further and applied to the study of fluid-solid multiphase flows with environmental context.

Work in the early stages of the project has focused on the validation of a saline gravity current LBM model, as a precursor to a turbidity current model, which would include deformable boundaries. The results from this stage of the study show good agreement with published high resolution simulations, and experimental studies.

2.6 The Zhang–Viñals Equations for Pattern Forming Problems

REECE COYLE[†]

University of Leeds

A layer of fluid that is vibrated in a periodic and vertical motion can display a fascinating range of patterns that emerge on the fluid surface, termed Faraday waves. The form and stability of these patterns have been investigated theoretically since the first experimental reports of Faraday in 1831, and work has led to models that not only display rich dynamics in terms of global pattern formation, but may have unexplored potential in describing localised states. One such model is the so called Zhang–Viñals equations, which describe the Faraday setup for a fluid of low viscosity in a high aspect ratio domain. Although the model struggles to achieve qualitative agreement with experiments in the limit of small viscosity, it displays some of the fundamental dynamics necessary to explore pattern formation theoretically. The use of an uncontrolled approximation within the derivation of the Zhang–Viñals equations is examined with careful consideration of the region where localised states are expected to form, guided by previous experimental work and results from a linear stability analysis based on the full Navier–Stokes equations. Establishing the Zhang–Viñals equations as a reliable model for localised pattern formation problems is the first step in an overall goal to theoretically explore the formation of oscillons, a time-dependent local structure that has been found to exist in the Faraday setup for a variety of fluids.

2.7 Folding and necking of layered viscous structuresOLIVIA GOULDEN[†]

University of Leeds

Viscous structures comprising layers of different viscosities arise widely throughout nature, with important examples including the Earth's ice sheets and lower crust. It is well documented that such structures can deform to produce folds and buckles when subject to compressive stresses. Observations of exposed rock and radar data of ice sheets have both indicated the widespread existence of large-scale folds and small-scale wrinkles of immersed layers. Recent observations of centimetre-scale folding in the Greenland ice sheet has indicated that folding instabilities may be a widespread feature of large-scale ice-sheet dynamics. The relationships between the properties of folding and the properties of the material is key to the geological technique of inferring the properties of the lower mantle from the geometry of folds, and is thus of central importance in structural geology. The classical analysis of the problem of folding has focused on the case of a strongly viscous or solid beam compressed or extended laterally in an infinite domain. Motivated particularly by the geometry of an ice sheet, this work addresses new effects induced by the presence of a horizontal rigid boundary, which is found to introduce new effects that can readily dominate the mechanics of folding.

2.8 Turbulence modelling in astrophysical turbulent mixing layers

JONATHAN DAVID FINN[†]

University of Leeds

The Rayleigh-Taylor, Richtmyer-Meshkov and Kelvin-Helmholtz mixing instabilities play an important role in describing astrophysical turbulent mixing layers. There are many astrophysical flows where these mixing instabilities arise such as, for example, the expansion of supernova remnants, the interaction of shocks with cool dense clouds embedded in the interstellar medium and in the deceleration of relativistic jets.

In studying these types of flows the large range of spatial and temporal scales often precludes the use of Direct Numerical Simulation and Large Eddy Simulation. An alternative approach is to solve for the ensemble averaged flow with closure approximations to model fully developed turbulence. The k - L and k - ϵ two equation turbulence models have been applied to astrophysical flows. At the University of Leeds a version of the k - ϵ turbulence model has been used to study shock-cloud interactions with single clouds in 2D and multiple cylindrical clouds in 2D [1,2]. Recently the k - L turbulence model was also implemented and used to study shock-cloud interactions.

The above types of models cannot address the problem of demixing of the fluids. To capture the relative motions of the fluids a multi-fluid approach is required. The two fluids are followed separately with mass, momentum and energy transfer terms coupling the fluids and the k - L equations to close the system [3]. Eventually, we plan to follow the turbulence variable fields for each fluid separately. These models are to be tested and compared through application to astrophysical flows and problems in the wider application domain.

References:

1. Pittard, J. M., Falle, S. A. E. G., Hartquist, T. W. and Dyson, J. E., 2009. The turbulent destruction of clouds—I. A k - ϵ treatment of turbulence in 2D models of adiabatic shock–cloud interactions. *Monthly Notices of the Royal Astronomical Society*, 394(3), pp.1351-1378.
2. Aluzas, R., Pittard, J. M., Hartquist, T. W., Falle, S. A. E. G. and Langton, R., 2012. Numerical simulations of shocks encountering clumpy regions. *Monthly Notices of the Royal Astronomical Society*, 425(3), pp.2212-2227.
3. Youngs, D. L., 1994. Numerical simulation of mixing by Rayleigh-Taylor and Richtmyer-Meshkov instabilities. *Laser and particle beams*, 12(4), pp.725-750.

2.9 Conventional and cryogenic coolants for machining applications

ELEANOR HARVEY
University of Leeds[†]

Coolants are frequently used in machining of hard-to-cut materials in order to combat the high thermo-mechanical loads experienced near the cutting edges of the tool. Managing the temperatures at the cutting edge has many benefits including an extended tool life and improved surface integrity of the workpiece. Conventional coolants employed in machining are oil-water emulsions however in recent decades as both the demand and costs of disposal have increased there have been investigations into alternative coolants. Cryogenic coolants are widely considered to be an environmentally friendly alternative to conventional coolants. The flow structures and heat transfer capabilities of cryogenic coolants in machining are not fully understood. In fact, the temperature management performance of cryogenic compared to conventional coolant is often inconsistent and seemingly highly dependent on the cutting conditions in each case.

This work's primary objective is to understand the flow structure and heat transfer involved when cooling with both conventional coolants and liquid CO₂ jets. Using OpenFOAM, the distribution of conventional coolant on both a machining tool and a simplified geometry is modelled and a study into the heat transfer for conventional coolant cases presented. Flow structures and phase compositions in more complex CO₂ jets are investigated using the software MG which is particularly suitable for modelling CO₂ thermodynamics.

2.10 Direct Numerical Simulation of an Oldroyd-B filament thinning

KONSTANTINOS ZINELIS[†], RICARDO CONSTANTE, LACHLAN MASON
& OMAR MATAR

Department of Chemical Engineering, Imperial College London

While both several experimental and numerical studies for Newtonian sprays have been conducted, the exploration of the non-Newtonian flows has received comparatively little attention. Achieving fundamental understanding of the physical phenomena governing spray formation of this type of flow remains a challenge. The present project aims to set the basis for the numerical examination of non-Newtonian atomisation and spray systems. To achieve this, a Direct Numerical Simulations (DNS) approach is followed where all the temporal and spatial scales are completely resolved. We begin with the simulation of the filament thinning of an Oldroyd-B viscoelastic fluid within a two-dimensional/axisymmetric framework, using the volume-of-fluid technique to track the interface and the log-conformation transformation for the solution of the viscoelastic constitutive equation. This permits the rapid exploration of parameter space, capturing the effect of the elastic, viscous and inertia forces (i.e. Deborah and Ohnesorge numbers), which characterise the internal relaxation and macroscopic time scales that viscoelasticity presents. This will serve as a departure point for further work involving three-dimensional simulations of an Oldroyd-B impulsive jet to explore the effect of viscoelasticity on the ejected droplet size. The numerical simulations of the spray formation of a viscoelastic fluid still offer substantial challenges, but it is reflective of industrial applications (i.e., spray-drying) and can lead to the optimisation of spray processes, containing fluids of a very complex behaviour.

2.11 Utilisation of instrumented particles for the study of incipient entrainment

KHALDOON ALOBAIDI[†], ATHANASIOS ALEXAKIS &
MANOUSOS VALYRAKIS

University of Glasgow

Sediment transport in rivers and estuaries environments represents one of the major challenges to engineers and researchers in the field of earth surface dynamics. Specifically, of interest for this study is to identify the flow events causing the entrainment of a coarse particle at low mobility conditions. In this work, the quadrant analysis technique is linked to the impulse criterion, a dynamic criterion in literature for defining incipient motion [1].

The goal of this work is to use the “smart sphere” developed by Valyrakis et al [2] and the 3D Acoustic Doppler Velocimetry (ADV) to assess the impulse criterion using different types of sensors for monitoring the hydrodynamic forces and relating the results to flow structures via linking particle and flow dynamics [3-4].

References:

1. M. Valyrakis, P. Diplas, C.L. Dancey, K. Greer, A.O. Celik, Role of instantaneous force magnitude and duration on particle entrainment, *J. Geophys. Res.* 115 (2010).
2. M. Valyrakis, A. Alexakis, E. Pavlovskis, “Smart pebble” designs for sediment transport monitoring, 17 (2015).
3. M. Valyrakis, P. Diplas, C. L. Dancey, Entrainment of coarse grains in turbulent flows: An extreme value theory approach, *Water Resour. Res.* 47 (2011) 1.
4. M. Valyrakis, P. Diplas, C.L. Dancey, Entrainment of coarse particles in turbulent flows: An energy approach, *J. Geophys. Res. Earth Surf.* 118 (2013) 42.
5. M. Valyrakis, P. Diplas, C.L. Dancey, Prediction of coarse particle movement with adaptive neuro-fuzzy inference systems, *Hydrol. Process.* 25, (2011) 3513-3524.

2.12 Hydrological Representations of Extreme Precipitation in East Africa under Climate Change using a Convection-Permitting ModelCLAIRE WEST[†]

University of Leeds

Climate change is projected to affect the global pattern of rainfall and increase climate induced hazards over the coming century. This is a particular concern for the African continent, where population increase and related infrastructure development are anticipated to grow at unprecedented levels, making local communities vulnerable to extremes. Currently, there is only sparse rain gauge data for many countries within East Africa, often making infrastructure projects challenging and limiting effective disaster risk management. This project aims to quantify how extreme precipitation events are characterised in parametrised and convection-permitting models, with the emphasis on using hydrological representations for long-term estimates of precipitation. Using the first pan-African convection-permitting model (CP4-A), a recently completed ten-year simulation, the opportunity to consider extreme events at a high (4.4km grid) resolution for current and future climate scenarios is now possible at a convection-permitting scale. Analysing this simulation and other parametrised model data, the intensity, frequency and duration of extreme precipitation events under climate change are identified using a selection of long-term return periods. Specifically, these are represented such that the information can be utilised to locally inform urban planning and improve water management and flood prevention for locations in East Africa prone to impacts of climate change.

2.13 Modelling the motion of the vitreous humour: A boundary integral approach

LAURA BEVIS[†]

Imperial College London

The eye is a highly complex system that is difficult to investigate both in vivo, due to its delicate nature, and ex vivo due to the degradation rates of its components. Mechanical modelling is therefore important to investigate proposed mechanisms of ophthalmological damage in order to highlight trends and significant parameters that may be used to improve diagnosis and surgical methods.

Here we use fluid models to consider the motion of the vitreous humour in the back of the eye and its effect on the retina, where light is detected. Little is known about how damage occurs to the retina, but it is thought that the stress as a result of this fluid motion is a key mechanism for its detachment. We consider a specific condition known as vitreoschisis, which results in retinal holes at the macula in about half of cases, and investigate the resultant stress on the retina [1].

We consider the regime where $Re \ll 1$, $\beta = \frac{L^2}{\nu T} \approx 1$, and therefore solve the unsteady (or linearised) Stokes equations. These hold for small amplitude oscillations such as reading, as well as for sudden motion, for example due to a car crash. Specifically, we consider the flow due to small amplitude oscillations of the eye, and construct a flat, two-dimensional model of vitreoschisis. We use boundary distributions of unsteady Stokeslets and boundary integral techniques to solve for the resultant velocity field and imposed stress on the retina, which can be compared to previous slip models and clinical observations. The results should provide insight into whether the stress on the retina is indeed a key mechanism for detachment, and highlight cases that would be more likely to require preventative treatment.

References:

1. Sebag, J., Gupta, P., Rosen, R. R., Garcia, P., & Sadun, A. A. (2007). Macular holes and macular pucker: the role of vitreoschisis as imaged by optical coherence tomography/scanning laser ophthalmoscopy. *Transactions of the American Ophthalmological Society*, **105**, 121.

2.14 Power spectrum and machine learning analysis applied to dried blood droplets [Talk]

L. HAMADEH, S. IMRAN, M. BENCSIK, G. SHARPE, M. JOHNSON
& D. J. FAIRHURST

Department of Physics and Mathematics,
Nottingham Trent University

One of the most interesting and everyday natural phenomenon is the formation of different patterns after the evaporation of colloidal droplets deposited on a solid surface. The analysis of dried patterns resulting from biological liquids, such as blood, has recently gained a lot of attention [1,2], experimentally and theoretically, due to its potential application in biomedicine and forensic science. This work presents an entirely novel approach to studying human blood droplet drying patterns that could be extended for use on any circular patterns. We took blood samples from 30 healthy young men before and after exhaustive exercise which is well known to cause large disturbances in blood chemistry. We objectively and quantitatively analysed 1800 dried blood droplet images by developing sophisticated image processing analysis routines and optimising a multivariate statistical machine learning algorithm. We look for statistically relevant correlations between the patterns and exercise-induced changes in blood chemistry. An analysis of various measured physiological parameters is also investigated. We use a machine learning algorithm, which is an optimisation to a statistical model that combines Principal Component Analysis (PCA) [3] and Linear Discriminant Analysis (LDA) [4] method. We apply this technique to the logarithmic power spectrum of the images, and are able to predict with up to 95% accuracy after physical exercise. Interestingly, we find that the predictive power is improved if we average over all the images taken per volunteer per condition.

Acknowledgements: The authors thank Nottingham Trent University for supporting this work.

References:

1. Deegan, R. D. and Bakajin, O. and Dupont, T. F. and Huber, G. and Nagel, S. R. and Witten, T. A. "Capillary Flow as the Cause of Ring Stains from Dried Liquid Drops". *Nature*, 1997, 389, 827–829.
2. Sobac, B. and Brutin, D. "Structural and evaporative evolutions in desiccating sessile drops of blood". *Phys. Rev. E*, 2011, 84, 011603.
3. Duda, R. O. and Hart, P.E. and Stork, D. G. "Pattern Classification, Second Edition: 1", A Wiley – Interscience Publication, 2000, 568.
4. Bishop, C. M. "Pattern recognition and machine learning", Springer, New York, 2006.

2.15 Flow analysis and fouling behaviour in 3-D printed wavy-patterned membranes [Talk]SAEED MAZINANI, ABOUTHER AL-SHIMMERY, Y. M. JOHN CHEW
& DAVIDE MATTIA

Department of Chemical Engineering, University of Bath

This study presents an innovative and systematic approach to design and fabricate fouling-resistant composite membranes by using a combination of computational modelling and 3D printing technology. Computational fluid dynamics (CFD) simulations coupled with extensive materials synthesis and characterisation were used to identify a set of optimal design parameters for the fabrication of 3D printed composite membranes with patterns that minimise the build-up of a common biological foulant, bovine serum albumin (BSA). CFD simulations were first carried out to identify the effect of the wavy pattern characteristics on the hydrodynamic profile of the feed solution. Membrane supports with different peak amplitudes and wavelengths were then printed by using an industrial Multi-jet 3D printer. Polyethersulfone (PES) selective layers were subsequently deposited onto these supports by vacuum filtration. The wavy 3D composite membranes were tested for multiple fouling and cleaning cycles in a cross-flow filtration setup. In comparison to the flat membrane, the wavy membrane showed superior performance in terms of pure water permeance (PWP) (10% higher) and permeance recovery ratio (87% versus 53%) after the first filtration cycle at $Re = 1000$. Prolong testing showed that the wavy membrane could retain approximately 87% of its initial PWP after 10 complete filtration cycles.

2.16 How Long To Reach Similarity? [Talk]

HERBERT HUPPERT, THOMASINA BALL & JOSEPH WEBBER
University of Cambridge

Many problems in fluid dynamics involve nonlinear partial differential equations with a range of specified initial conditions.

In general, this requires numerical integration to determine the solution.

However, frequently a similarity solution can be found, independent of the initial conditions.

How long after the initiation is the similarity solution within a required accuracy to the full solution?

How does this time depend on the initial conditions?

This presentation will set up a method to determine the answers and show how the relevant time can depend quite critically on the (neglected) initial condition.